Cosmological Perturbation Theory

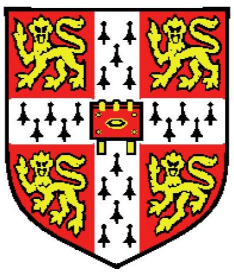

Sylvain D. Brechet

Astrophysics Group, Cavendish Laboratory

Robinson College, University of Cambridge

A dissertation submitted for the degree of

Doctor of Philosophy

in the University of Cambridge

May 2009

To my dearest beloved little Light...

Declaration

This dissertation is the result of work carried out in the Astrophysics Group of the Cavendish Laboratory, Cambridge, between October 2005 and May 2009. This dissertation is my own work and contains nothing which is the outcome of work done in collaboration except where specifically indicated in the text. Throughout this dissertation the plural pronoun 'we' is used for stylistic reasons and should be taken to refer to either the singular author, or to the author and his thesis advisors. No part of this dissertation has been submitted for a degree, diploma or other qualification at this or any other university. The total length of this dissertation does not exceed sixty thousand words.

Acknowledgements

A number of people have contributed both directly and indirectly to the completion of this thesis. Firstly, I would like to express my sincere appreciation and gratitude to my two supervisors Anthony Lasenby and Mike Hobson for their patience and support. With his integrity, outstanding scientific insight and innovative ideas, Anthony has been a great source of scientific wisdom and has provided much sound advice and guidance. With his enthusiasm, scientific expertise, and great efforts to explain things clearly and simply, Mike has been a continual source of inspiration and guidance. Their advice has been invaluable in deriving number of results presented in this thesis.

For financial support, I gratefully acknowledge the Institute of Astronomy who awarded me the Isaac Newton Studentship. I am also in debt towards the Swiss Federal Institutes of Technology for the Sunburst Studentship. I thank the Cavendish Laboratory for financial support, and Robinson College for a travel grant. This work would almost certainly not have been completed without the support of these bodies.

I am also very grateful to Anthony Challinor who has explained a number of theoretical issues, clearly and patiently. I am indebted to my office mates and student colleagues for providing a stimulating and lively environment in which to learn and grow. I would like to thank Jonathan Zwart, Farhan Feroz, Rebecca Johnnston, Daniel Berwick, Martin Huarte-Espinosa and Jeremy Taylor. Pierre Dechant deserves a special thanks for interesting and stimulating discussions on mathematics, physics, music, and for providing some much needed light relief over a coffee or a beer. I also thank him for his outstanding

vocal performance at my wedding. I thank especially Cédric Pahud for his friendship during our undergraduate and graduate years, sharing common passions for cosmology, gastronomy and snooker.

I also thank my family for their love and all what they have done for me. I thank especially my mother for her care and my father for having given me his copy of a 'Brief History of Time' stirring up in me the secret dream to come to Cambridge and study cosmology there. This thesis is the visible fulfillment of that dream.

Last but not least, a very special thank you goes to my dear wife Lucie for her love, her encouragement and support throughout the completion of this thesis. Without her, more than anyone else, this thesis would never have become what it is. Thanks especially for enduring my many overly enthusiastic scientific explanations and for always being there for me whenever I needed you most.

Abstract

Firstly, a dynamical analysis of adiabatic perturbations of a perfect fluid is performed to first-order about a general FLRW background using the $1+3$ covariant and gauge-invariant formalism. The $1+3$ covariant analog of the Mukhanov-Sasaki and Grishchuk variables needed to quantise the scalar and tensor perturbations respectively about a spatially-curved FLRW background space-time are identified. The dynamics of the vector perturbations is also discussed.

Secondly, a dynamical analysis of an inhomogeneous and anisotropic effective Weyssenhoff fluid, which is a perfect fluid with spin in the Einstein-Cartan theory, is performed by Brechet *et al.* (2007) in a gauge-invariant manner using the $1+3$ covariant and gauge-invariant approach. A verification of the dynamical equations is performed for the special case of irrotational flow with zero peculiar acceleration by evolving the constraints.

Thirdly, a dynamical analysis of an effective homogeneous and irrotational Weyssenhoff fluid in general relativity is performed by Brechet *et al.* (2008) using the $1+3$ covariant and gauge-invariant approach. The spin contributions to the field equations produce a bounce that averts an initial singularity, provided that the spin density exceeds the rate of shear. At later times, when the spin contribution can be neglected, a Weyssenhoff fluid reduces to a standard cosmological fluid in general relativity. Numerical solutions for the time evolution of the generalised scale factor $R(t)$ in spatially-curved models are presented, some of which exhibit eternal oscillatory behaviour without any singularities. In spatially-flat models, analytical solutions for particular values of the equation-of-state parameter are derived. Although the

scale factor of a Weyssenhoff fluid generically has a positive temporal curvature near a bounce (i.e. $\ddot{R}(t) > 0$), it requires unreasonable fine tuning of the equation-of-state parameter to produce a sufficiently extended period of inflation to fit the current observational data.

Fourthly, in order to determine numerically the background dynamics of general inflationary models, suitable classical initial conditions have to be found from which to start the integration of the equations of motion. The method proposed by Boyanovsky, de Vega and Sanchez assumes a spatially-flat model with an inflaton potential typical of new inflation and determines the initial conditions at a time when the inflaton field is at the local maximum of the potential by assuming equipartition of the kinetic and potential energies of the inflaton field. This leaves the normalisation of the solutions undetermined. The procedure followed by Lasenby and Doran assumes a spatially-closed model with a chaotic inflaton potential and determines the initial conditions as the model emerges from the initial singularity by performing a series expansion. We note that quite generically immediately after the initial singularity, the pre-inflationary dynamics of the universe is dominated by the kinetic energy of the inflaton, which naturally yields analytic solutions for any spatial curvature − provided there is no bounce − with no dependence on the potential. This therefore suggests a new generic way of setting initial conditions for inflation. Using this new procedure, we determine the initial conditions for chaotic and new inflation potentials and study both the subsequent background evolution and the spectrum of scalar perturbations produced in the spatially-flat case.

Contents

List of Figures

Chapter 1

Introduction

Cosmology is the study of the dynamics and content of the Universe as a whole. Until the dawn of the 20^{th} century, space and time were regarded as two distinct entities, and the universe was considered as static, infinite and eternal. Einstein (1905) overthrew the prevailing paradigm by showing that space and time are not independent notions but form a single four dimensional continuum called 'space-time'. In his theory of General Relativity, Einstein (1916) went even one step further by relating the dynamics of physical bodies to the geometry of space-time. The first cosmological model based on General Relativity that Einstein (1917) developed was a static model of the cosmos, which he studied for philosophical reasons but finally rejected after Hubble (1929) discovered that the observable universe was expanding. Friedman (1922) and Lemaitre (1927) independently showed how the expansion of the universe could be described by a spatially homogeneous and isotropic model obeying the field equations of General Relativity. The expansion pointed to an extremely hot origin of the Universe, called the "Big Bang", which was predicted by Alpher *et al.* (1948) to leave a thermal relic radiation. This prediction was confirmed by Penzias & Wilson (1970) with the discovery of the cosmic microwave background radiation (CMB), which established the hot Big Bang model as a cosmological paradigm.

On sufficiently large scales, the observable universe has been shown by Mather *et al.* (1992) to be almost homogeneous and isotropic based on observations of the CMB using the satellite COBE. Thus, to a very good approximation the geometry of the universe obeys the Cosmological Principle and can be described

by the homogeneous and isotropic Friedman (1924)-Lemaitre (1927)-Robertson (1935)-Walker (1937) or FLRW space-time metric, which is sometimes referred to as FRW or simply RW metric. The cosmological models based on an FLRW geometry are very successful in explaining the major features of the observed universe, but they fail to describe accurately the 'real' universe due to their highly idealised degree of symmetry, which does not correspond to the 'lumpy' real universe. Although these models can describe the 'smoothed-out' features of the observable universe on large scales, one needs to perturb them in order to get realistic 'almost-FLRW' universe models, which account for the presence of inhomogeneities and anisotropies arising during structure formation.

Cosmological perturbation theory about a FLRW background metric was initiated by Lifschitz (1947) and extended notably by Grishchuk (1974), Bardeen (1980), Mukhanov *et al.* (1992), and Kodama & Sasaki (1984). This is the standard approach to performing a perturbation analysis of general relativity in order to describe the 'realistic' dynamics of cosmological models. It has the disadvantage that truly physical results can be obtained only after completely specifying the correspondence between the 'real' perturbed space-time and a 'fictitious' unperturbed FLRW background space-time. Such a correspondence is not uniquely defined and changes under a gauge transformation. The degrees of freedom in the definition of the correspondence, or the gauge freedom, leave unphysical gauge modes in the dynamical equations describing the evolution of the perturbations as mentioned by Bruni *et al.* (1992a). This gauge problem described by Lifshitz & Khalatnikov (1963) and Sachs & Wolfe (1967) is inherent to such a 'background-based' perturbation approach. Indeed, the metric, and consequently the Einstein equations, have 10 degrees of freedom whereas the dynamics is determined by 6 parameters only. Therefore, the 4 remaining degrees of freedom are directly related to the gauge.

To solve this problem, Bardeen (1980) determined a set of gauge-invariant quantities to describe the perturbations and derived their dynamical equations. These quantities are mathematically well defined but do not have a transparent geometrical meaning since they are defined with respect to a particular coordinate system as mentioned by Stewart (1990), and their physical meaning is obscure as stated by Ellis *et al.* (1989).

An alternative way to circumvent the gauge problem is to follow the $1+3$-covariant approach, which was developed by Heckmann & Schücking (1955), Raychaudhuri (1957), and Ehlers (1961), and extended by Hawking (1966), Olson (1976) and Ellis & Bruni (1989). We shall pursue that approach in this dissertation.

1.1 1 + 3 covariant formalism

The aim of the $1+3$ covariant and gauge-invariant approach is to study the dynamics of real cosmological fluid models in a physically transparent manner. This formalism relies on covariantly defined variables, which are gauge-invariant by construction as explained by Bruni *et al.* (1992a), thus simplifying the methodology and clarifying the physical interpretation of the models. It also allows the metric to be arbitrary. The formalism uses the kinematic quantities, the energy-momentum tensor of the fluid, the 'electric' and 'magnetic' parts of the Weyl tensor, instead of the metric, which in itself does not provide a covariant description, as explained by Tsagas *et al.* (2008). The key equations are the Ricci and Bianchi identities, applied to the fluid 4-velocity vector, while Einsteins equations are incorporated via algebraic relations between the Ricci and the energy-momentum tensor. This approach admits a covariant and gauge-invariant linearisation that allows a first-order perturbation analysis to be performed in a direct manner, as mentioned by Challinor (2000) and explained in *Section* 1.1.3.

To introduce the $1+3$ covariant formalism, we follow the approach outlined by Ellis & van Elst (1999). For convenience, we follow Hawking (1966) and Ellis & Bruni (1989) by adopting the $(-,+,+,+)$ signature convention for the Lorentzian metric throughout this dissertation. This choice of signature is particularly appropriate for the $1+3$ covariant formalism. Indeed, using such a formalism, the dynamical equations are projected on the local spatial hypersurfaces, which are positively defined for our signature convention. The correspondence for dynamical quantities expressed in terms of the opposite signature convention used by Obukhov & Korotky (1987) and Brechet *et al.* (2007) can be found in *Appendix* A. For convenience, we use Planck or 'natural' units ($G = c = \hbar = 1$).

1.1.1 1 + 3 decomposition

The 1+3 covariant and gauge-invariant approach is based on a 1+3 decomposition of geometric quantities with respect to a fundamental 4-velocity u^a that uniquely determines the frame and the worldline of every infinitesimal volume element of fluid,

$$u^a = \frac{dx^a}{d\tau} \ , \qquad u_a u^a = -1 \ , \tag{1.1}$$

where x^a are arbitrary cosmic coordinates, and τ is the proper time measured along the worldlines. In the context of a general cosmological model, we require that the 4-velocity be chosen in a physical manner such that in the FLRW limit the dipole of the cosmic microwave background radiation vanishes. This condition is necessary to ensure the gauge-invariance of the approach.

The 4-velocity u^a defines locally two projection tensors in a unique fashion,

$$\begin{aligned} &U_{ab} = -u_a u_b \qquad \Rightarrow \quad U^a{}_c U^c{}_b = U^a{}_b \ , \quad U^a{}_a = 1 \ , \quad U_{ab}u^b = u_a \ , \\ &h_{ab} = g_{ab} + u_a u_b \quad \Rightarrow \quad h^a{}_c h^c{}_b = h^a{}_b \ , \quad h^a{}_a = 3 \ , \quad h_{ab}u^b = 0 \ . \end{aligned} \tag{1.2}$$

The first projects parallel to the 4-velocity vector u^a, and the second determines the (orthogonal) metric properties of the instantaneous rest-spaces of observers moving with 4-velocity u^a. The volume element for the rest-spaces is defined as

$$\varepsilon_{bcd} = u^a \eta_{abcd} \qquad \Rightarrow \qquad \varepsilon_{abc} = \varepsilon_{[abc]} \ , \quad \varepsilon_{abc}u^c = 0 \ , \tag{1.3}$$

where η_{abcd} is the totally antisymmetric pseudotensor and 4-dimensional volume element ($\eta_{abcd} = \eta_{[abcd]}$, $\eta_{0123} = \sqrt{-\det g_{ab}}$). Note that the contraction of the rest-space volume elements can be expressed in terms of the induced metric on these rest-spaces as,

$$\varepsilon_{abc}\varepsilon^{def} = 3! h^{[d}{}_a h^e{}_b h^{f]}{}_c = 3! h^d{}_{[a} h^e{}_b h^f{}_{c]} \ . \tag{1.4}$$

Moreover, we define two projected covariant derivatives which are the time projected covariant derivative along the worldline (denoted $\dot{}$) and the spatially projected covariant derivative (denoted D_a). For any quantity $Q^{a\ldots}{}_{b\ldots}$, these are respectively defined as

$$\begin{aligned} &\dot{Q}^{a\ldots}{}_{b\ldots} \equiv u^c \nabla_c Q^{a\ldots}{}_{b\ldots} \ , \\ &D_c Q^{a\ldots}{}_{b\ldots} \equiv h^f{}_c h^a{}_d \ldots h^e{}_b \ldots \nabla_f Q^{d\ldots}{}_{e\ldots} \ . \end{aligned} \tag{1.5}$$

Furthermore, the kinematics and the dynamics are determined by projected tensors that are orthogonal to u^a on every index. The angle brackets are used to denote respectively orthogonal projections of vectors V^a and the orthogonally projected symmetric trace-free part (PSTF) of rank-2 tensors T^{ab} according to,

$$\begin{aligned} V^{\langle a\rangle} &= h^a{}_b V^b \ , \\ T^{\langle ab\rangle} &= \left(h^{(a}{}_c h^{b)}{}_d - \tfrac{1}{3}h^{ab}h_{cd}\right) T^{cd} \ . \end{aligned} \tag{1.6}$$

For convenience, the angle brackets are also used to denote the orthogonal projections of covariant time derivatives of vectors and tensors along the worldline u^a as follows,

$$\begin{aligned} \dot{V}^{\langle a\rangle} &= h^a{}_b \dot{V}^b \ , \\ \dot{T}^{\langle ab\rangle} &= \left(h^{(a}{}_c h^{b)}{}_d - \tfrac{1}{3}h^{ab}h_{cd}\right) \dot{T}^{cd} \ . \end{aligned} \tag{1.7}$$

Note that, in general, the time derivative of vectors and tensors does not commute with the projection of these quantities on the spatial hypersurfaces according to,

$$\begin{aligned} \dot{V}^{\langle a\rangle} &\neq (V^{\langle a\rangle})^{\cdot} \ , \\ \dot{T}^{\langle ab\rangle} &\neq (T^{\langle ab\rangle})^{\cdot} \ . \end{aligned} \tag{1.8}$$

The projection of the covariant time derivative of a quantity $Q^{a\cdots}{}_{b\cdots}$ on the spatial hypersurfaces is defined as,

$${}^{(3)}(Q^{a\cdots}{}_{b\cdots})^{\cdot} \equiv h^a{}_c \ldots h^d{}_b \ldots u^e \nabla_e Q^{c\cdots}{}_{d\cdots} \ . \tag{1.9}$$

It is also useful to define the projected covariant curl as,

$$\operatorname{curl} Q_{a\ldots b} \equiv \varepsilon_{cd\langle a} D^c Q^d{}_{\ldots b\rangle} \ . \tag{1.10}$$

1.1.2 Kinematical quantities

Information relating to the kinematics is contained in the covariant derivative of u^a which can be split into irreducible parts, defined by their symmetry properties,

$$\nabla_a u_b = -u_a a_b + D_a u_b = -u_a a_b + \tfrac{1}{3}\Theta h_{ab} + \sigma_{ab} + \omega_{ab} \ , \tag{1.11}$$

where

- $a^a \equiv u^b \nabla_b u^a$ is the relativistic acceleration vector, representing the degree to which matter moves under forces other than gravity.
- $\Theta \equiv D_a u^a$ is the scalar describing the volume rate of expansion of the fluid (with $H = \frac{1}{3}\Theta$ the Hubble parameter).
- $\sigma_{ab} \equiv D_{\langle a} u_{b\rangle}$ is the trace-free rate-of-shear tensor describing the rate of distortion of the fluid flow.
- $\omega_{ab} \equiv D_{[a} u_{b]}$ is the antisymmetric vorticity tensor describing the rotation of the fluid relative to a non-rotating frame.

These kinematical quantities have the following properties,

$$\begin{aligned} &a_a u^a = 0 \ , \\ &\sigma_{ab} u^b = 0 \ , \quad \sigma_{ab} = \sigma_{(ab)} \ , \quad \sigma^a{}_a = 0 \ , \\ &\omega_{ab} u^b = 0 \ , \quad \omega_{ab} = \omega_{[ab]} \ , \quad \omega^a{}_a = 0 \ . \end{aligned} \tag{1.12}$$

It is useful to introduce a pseudovector ω^a defined as the dual of the vorticity tensor ω_{bc},

$$\omega^a \equiv \tfrac{1}{2}\varepsilon^{abc}\omega_{bc} \ , \tag{1.13}$$

and thus satisfying,

$$\omega_a u^a = 0 \ , \quad \omega_{ab}\omega^b = 0 \ . \tag{1.14}$$

Note that in presence of vorticity the spatially projected covariant derivatives do not commute, which implies that any scalar field S has to satisfy the non-commutation relation,

$$D_{[a} D_{b]} S = \omega_{ab} \dot{S} \ . \tag{1.15}$$

It is also of physical interest to introduce three further scalars, which are respectively the acceleration, the shear and the vorticity magnitudes squared and are defined as,

$$\begin{aligned} a^2 &= \frac{1}{2} a_b a^b \geq 0 \ , \\ \sigma^2 &= \frac{1}{2} \sigma_{ab}\sigma^{ab} \geq 0 \ , \\ \omega^2 &= \frac{1}{2} \omega_{ab}\omega^{ab} \geq 0 \ . \end{aligned} \tag{1.16}$$

1.1.3 Linearisation about a FLRW background

The basic philosophy of the perturbation theory based on the $1+3$ covariant formalism is different from the 'background-based' perturbation theory as explained by Ellis *et al.* (1990). Instead of starting with a background space-time and then perturbing it, the approach begins with an inhomogeneous and anisotropic 'real' space-time, which reduces to the background space-time on large scales. We will take the background to be an homogeneous and isotropic FLRW space-time, although this formalism allows in principle for more complicated backgrounds. Therefore, the 'real' space-time has been appropriately called by Ellis *et al.* (1989) an 'almost FLRW' space-time. In this perturbation theory, the approximation takes place by neglecting higher-order terms in the exact equations when the values of the kinematic and dynamic variables are close to those they would take in the background FLRW space-time. The analysis is performed in the real space-time and the dynamical equations are subsequently linearised. The background solution is simply the zero-order approximation of the exact solution of the dynamical equations.

To build a covariant linear perturbation theory, we will linearise the quantities of the $1+3$ covariant formalism about an FLRW background space-time. Gauge invariance of the perturbations is guaranteed by the Gauge Invariance Lemma established by Stewart & Walker (1974), which states if a quantity vanishes in the background space-time, then it is gauge invariant at first-order. The 4-velocity is uniquely defined in the 'almost FLRW' space-time, which ensures that the perturbations are also uniquely defined, as mentioned by Ellis & van Elst (1999).

The homogeneity of the background space-time implies that the acceleration a^a is a first-order variable, since it vanishes in the background space-time (i.e. at zeroth order). Similarly, the isotropy of the background space-time implies that rate of shear σ_{ab} is also a first-order variable. Finally, the existence of spatial hypersurfaces orthogonal to the worldline in the background space-time implies that vorticity tensor ω_{ab} and the vorticity covector ω_a are first-order variables. Therefore, the only zero-order kinematic quantity is the rate of expansion Θ.

In the background space-time, which means to zero-order in the dynamical

variables, the covariant derivative of the worldline thus becomes,

$$\nabla_a u_b = \tfrac{1}{3}\Theta h_{ab} \ . \tag{1.17}$$

It is also useful to define (up to some constant factor) a zero-order scale factor R such that,

$$\Theta = 3H \equiv \frac{\dot{R}}{R} \ , \tag{1.18}$$

where H is the cosmic Hubble scale factor. In the $1+3$ covariant approach, R is generally a locally defined variable. However, for the homogeneous FLRW background space-time, the symmetries allow R to be globally defined and interpreted as a cosmological scale factor.

Finally, to carry out a linear perturbation analysis, it is convenient to introduce the conformal time variable $\hat{\tau}$ satisfying the differential relation,

$$d\hat{\tau} \equiv \frac{d\tau}{R} \ , \tag{1.19}$$

which implies that the derivatives with respect to cosmic time τ and conformal time $\hat{\tau}$ of a quantity $Q^{a\cdots}{}_{b\cdots}$ are related by,

$$Q'^{a\cdots}{}_{b\cdots} = R\dot{Q}^{a\cdots}{}_{b\cdots} \ , \tag{1.20}$$

where a prime denotes a derivative with respect to conformal time $\hat{\tau}$. The conformal Hubble scale factor $\mathcal{H}$ is related to the cosmic scale factor H by $\mathcal{H} = RH$.

1.2 Outline

The remainder of this thesis is structured as follows.

In *Chapter* 2, we perform an analysis of first-order adiabatic perturbations of a perfect fluid about a general FLRW background using the $1+3$ covariant and gauge-invariant formalism.

In *Chapter* 3, Brechet *et al.* (2007) carry out a dynamical analysis of an inhomogeneous and anisotropic effective Weyssenhoff fluid in General Relativity using the $1+3$ covariant and gauge-invariant formalism.

In *Chapter* 4, Brechet *et al.* (2008) investigate the dynamics of an homogeneous and irrotational Weyssenhoff fluid in general relativity using the $1+3$

covariant and gauge-invariant approach. Under certain conditions, such a fluid gives rise to a Big Bounce cosmology.

In *Chapter* 5, we determine suitable classical initial conditions for the background evolution of general inflationary models and study both the subsequent background evolution and the spectrum of scalar perturbations produced in the spatially-flat case.

In *Chapter* 6, we present concluding remarks, summarising the work performed in this thesis and outlining promising avenues of future research.

Chapter 2

First-order adiabatic perturbations of a perfect fluid about a general FLRW background in the $1+3$ covariant approach

The perturbation theory based on the $1+3$ covariant formalism and gauge-invariant uses a 'real' unperturbed 'almost FLRW' space-time, which reduces to the background space-time on sufficiently large scales. The perturbation analysis consists in linearising the dynamical equations about an FLRW background space-time by neglecting second- or higher-order terms in the exact equations when the values of the kinematic and dynamic variables are close to those they would take in the background FLRW space-time. Note that the background FLRW space-time is simply the zero-order approximation of the exact solution of the dynamical equations. Although in the $1+3$ covariant formalism, the scalar, vector and tensor perturbations are handled in a unified way, as mentioned by Challinor (2000), they decouple to first-order and can be studied independently, as explained by Mukhanov *et al.* (1992). The first attempt to establish an explicit relation between the perturbation variables in the $1+3$ covariant formalism and the corresponding variables in the 'background-based' approach was

made by Goode (1989). For a perfect fluid in a spatially-curved case, the analog of the Bardeen variable for the scalar perturbations in the $1+3$ covariant approach was first identified by Woszczyna & Kulak (1989) and the analog of the curvature perturbation by Bruni *et al.* (1992a).

In the $1+3$ formalism, the time derivative of a physical quantity is defined usually as the projection of the covariant derivative of the quantity on the worldline as outlined in *Section* 1.1, but this is not the only way to define covariantly a time derivative as Thiffeault (2001) showed. As Langlois & Vernizzi (2005) suggested, the Lie derivative along the worldline of a fluid element is another possible definition. However, the Lie derivative of a scalar field along the worldline is identical to time derivative of the scalar field along the worldline. Since, in this dissertation, we aim to identify scalar quantities, which are respectively scalar perturbations and the scalar amplitude of vector and tensor perturbations, we will define the time derivative of physical quantities to be the projection of the covariant derivative of the quantity on the worldline.

It is worth mentioning that, recently, Pitrou & Uzan (2007) used Lie derivatives to recast the dynamical equations for the scalar and tensor perturbations in the $1+3$ covariant formalism in order to identify perturbation variables, which are similar to the Sasaki-Mukhanov variables in a spatially-flat case. In particular, they claim to identify the scalar and tensor variables that map to the Mukhanov-Sasaki variables when considering a spatially-flat almost FLRW universe, but this is not clear. Firstly, in the scalar case, the perturbation variable v_a that Pitrou and Uzan obtained is not a scalar but a covector. Secondly, for tensor perturbations in the spatially-flat case, Pitrou and Uzan obtained a wave equation in terms of Lie derivatives of tensor fields, which they identify as the Mukhanov-Sasaki variables. However, the scalar amplitudes of the tensor perturbations obtained by contracting the tensors do not map to the corresponding scalar Mukhanov-Sasaki variables obtained in the 'background-based' approach. Furthermore, Pitrou and Uzan did not consider a perfect fluid but instead restricted their analysis to a single scalar field.

This chapter is devoted to the identification, in the $1+3$ covariant approach, for adiabatic perturbations of a perfect fluid in spatially-curved FLRW models, of the analog of the Mukhanov-Sasaki and Grishchuk variables needed to quantise

the scalar and tensor perturbations respectively. The quantisation of fields in a spatially-curved space-time lies outside the scope of this dissertation. However, this topic has been addressed in detail by Birrell & Davies (1982) and Fulling (1989). Our approach broadens the scalar perturbations analysis performed by Woszczyna & Kulak (1989), Bruni *et al.* (1992a) and Lyth & Woszczyna (1995) in a spatially-curved case.

The structure of this chapter is as follows. In *Section* 2.1, we compare the Eulerian and Lagrangian fluid descriptions. In *Section* 2.2, we establish the first-order dynamical equations for adiabatic perturbations of a perfect fluid in the 1+3 covariant approach. In *Section* 2.4, we identify the analog of the Mukhanov-Sasaki variable for the scalar perturbations. In *Section* 2.5, we determine the dynamics of the scalar amplitude of the vector perturbations. In *Section* 2.6, we finally identify the analog of the Grishchuk variables for the tensor perturbations.

2.1 Lagrangian and Eulerian dynamical descriptions of fluid perturbations

It is useful to consider the two complementary ways of describing the non-relativistic dynamics of a perfect fluid. Firstly, the Lagrangian description identifies infinitesimal elements of fluid, which are sometimes referred to as "fluid particles", and follows them along their motion. Secondly, the Eulerian description does not identify infinitesimal elements of fluid but focuses instead on the fluid flow through the fixed infinitesimal spatial volume at rest in the coordinate system, as explained by Smirnov-Rueda (2005).

The main difference between Newtonian fluid dynamics and its relativistic counterpart is that, in the former, space and time are two distinct entities whereas, in the latter, they form a single four dimensional continuum. A dynamical description of a relativistic fluid requires unambiguous definitions of "rates-of-change" of dynamical quantities, which require in turn a clear distinction between space and time. Fortunately, the $1+3$ covariant formalism allows such a distinction, as mentioned by Andersson & Comer (2007), provided the fluid is irrotational with no acceleration, which ensures the existence of spatial hypersurfaces orthogonal

to the worldline and of a globally defined cosmic time t, as explained by Ellis & van Elst (1999). Since scalar perturbations are density perturbations, which generate accelerations, and vector perturbations are vorticity perturbations, as shown by Hawking (1966), a fluid model describing a (real) universe albeit based on an almost FLRW space-time does not allow "rates-of-change" of dynamical quantities to be unambiguously defined. The "rates-of-change" of such quantities can, however, be unambiguously defined in the FLRW background space-time and extended to the almost FLRW space-time, where the "rates-of-change" of the corresponding dynamical quantities are obtained by perturbation of the background quantities.

The $1+3$ covariant formalism is gauge-invariant but not frame-independent. To study the relativistic dynamics of the adiabatic perturbations of a perfect fluid, it is necessary to distinguish the background frame from the perturbation frame. As in the non-relativistic dynamics of a perfect fluid, there are two ways to describe the dynamics of adiabatic perturbations. Firstly, the Lagrangian description, identifies infinitesimal elements of the perturbed fluid and follows their motion along the worldlines. Secondly, the Eulerian description, identifies an infinitesimal tri-dimensional spatial volume in the background space-time, and describes the flow of the perturbed fluid through the infinitesimal spatial volume. Thus, the background frame is a relativistic generalisation of the rest frame of a Newtonian fluid. Note that, unlike the Newtonian rest frame, the background frame is not static, and therefore, the infinitesimal background volume element itself evolves along its own worldline. The background frame corresponds to the Eulerian frame and the perturbation frame to the Lagrangian frame of the fluid.

The unperturbed dynamical background quantities are all scalars, since the background FLRW space-time is isotropic and homogeneous, and thus does not admit any privileged point or direction in accordance with the Cosmological Principle. Hence, unlike the perturbations, the unperturbed quantities are defined in a frame-independent way. Therefore, the following discussion focuses only on perturbations.

In the $1+3$ covariant formalism, the dynamics of an infinitesimal fluid element is uniquely determined by the worldline. Similarly to the procedure followed by Ellis *et al.* (2001), we require the 4-velocity u^a of the fluid element in the

Lagrangian perturbation frame to have a non-relativistic spatial motion relative to 4-velocity $\bar{u}_a$ of the fluid element in the Eulerian background frame. The non-relativistic velocity composition relation is given by,

$$u^a = \bar{u}^a + v^a \ , \tag{2.1}$$

where v^a is the spatial velocity vector of the infinitesimal Laplacian displacement and satisfies $\bar{u}_a v^a = 0$. The velocity vectors contract as,

$$\bar{u}_a \bar{u}^a = -1 \ , \qquad v_a v^a = v^2 \ , \qquad u_a u^a = -1 + v^2 \ , \tag{2.2}$$

where the non-relativistic velocity composition relation (2.1) implies that $v^2 \ll 1$. Since the velocity v^a vanishes in the background, the velocity squared v^2 is a second-order perturbation variable, which can be safely neglected in a first-order perturbation analysis. Hence to first-order, the 4-velocities satisfy,

$$u_a u^a \simeq \bar{u}_a \bar{u}^a = -1 \ . \tag{2.3}$$

Using the time derivative (1.5) of a perturbation $Q^{a\cdots}{}_{b\cdots}$ and the velocity composition law (2.3), the "rates-of-change" of $Q^{a\cdots}{}_{b\cdots}$ evaluated respectively in the Eulerian background frame and in the Lagrangian perturbation frame are related by,

$$u^c \nabla_c Q^{a\cdots}{}_{b\cdots} = \bar{u}^c \nabla_c Q^{a\cdots}{}_{b\cdots} + v^c D_c Q^{a\cdots}{}_{b\cdots} \ , \tag{2.4}$$

where $u^c \nabla_c Q^{a\cdots}{}_{b\cdots}$ is the "rate-of-change" of $Q^{a\cdots}{}_{b\cdots}$ in the Lagrangian frame, $\bar{u}^c \nabla_c Q^{a\cdots}{}_{b\cdots}$ is the "rate-of-change" of $Q^{a\cdots}{}_{b\cdots}$ in the Eulerian frame and $v^c D_c Q^{a\cdots}{}_{b\cdots}$ is a convective term accounting for the "rate of change" of $Q^{a\cdots}{}_{b\cdots}$ due to the relative motion of the Lagrangian perturbation frame with respect to the Eulerian background frame. It is important to note that although the perturbation $Q^{a\cdots}{}_{b\cdots}$ vanishes in the background FLRW space-time, it does not vanish in the Eulerian background frame of an almost FLRW (real) space-time.

Since the peculiar velocity of the fluid element and the perturbation vanish in the background, they are first-order terms. Hence, the convective term $v^c D_c Q^{a\cdots}{}_{b\cdots}$ in (2.4) is a second-order term, since it is the product of two first-order terms. Thus, to first-order in the perturbation (which means neglecting second- and higher-order products of first-order variables) it follows from (2.4)

that the time derivative of the perturbation in the Eulerian background frame is equal to the time derivative of the perturbation in the Lagrangian perturbation frame, and (2.4) reduces to,

$$u^c\nabla_c Q^{a\cdots}{}_{b\cdots} = \bar{u}^c\nabla_c Q^{a\cdots}{}_{b\cdots} \ . \tag{2.5}$$

Hence, to first-order, the dynamical analysis of the adiabatic perturbations is frame-independent, since the choice of frame or worldline induces a second-order difference in the time derivative of a perturbation. However, to perform a second- or higher- order perturbation analysis, the Eulerian and Lagrangian frames have to distinguished. This lies beyond the scope of this dissertation.

It is worth mentioning that in the non-relativistic limit, the differential operators occurring in (2.4) reduce respectively to,

$$u^c\nabla_c = \frac{D}{Dt} \ , \qquad \bar{u}^c\nabla_c = \frac{\partial}{\partial t} \ , \qquad v^c D_c = \mathbf{v}\cdot\boldsymbol{\nabla} \ , \tag{2.6}$$

where $\frac{D}{Dt}$ is the Lagrangian total time differential operator, $\frac{\partial}{\partial t}$ the Eulerian partial time differential operator, $\mathbf{v}$ the spatial velocity vector and $\boldsymbol{\nabla}$ the spatial gradient. Thus, for a scalar perturbation S and a spatial vector perturbation $\mathbf{V}$ in the non-relativistic limit, (2.4) reduces respectively to the well-known non-relativistic fluid dynamical relations,

$$\begin{aligned} \frac{D}{Dt}S &= \frac{\partial}{\partial t}S + \mathbf{v}\cdot\boldsymbol{\nabla}S \ , \\ \frac{D}{Dt}\mathbf{V} &= \frac{\partial}{\partial t}\mathbf{V} + \mathbf{v}\cdot\boldsymbol{\nabla}\mathbf{V} \ . \end{aligned} \tag{2.7}$$

2.2 First-order adiabatic dynamics of a perfect fluid about an FLRW background

We will now use the 1+3 covariant formalism, outlined in *Section* 1.1, to describe the adiabatic dynamics of a perfect fluid to first-order in the dynamical variables, which means neglecting second and higher order products of first-order dynamical variables. We then perform a perturbation analysis of such a fluid about an FLRW background, which will be used in *Section* 2.4 - *Section* 2.6 to describe scalar, vector and tensor perturbations respectively.

2.3 Einstein field equations

The dynamics of a perfect fluid is described by the Einstein field equations, which read,

$$R_{ab} - \tfrac{1}{2} g_{ab} \mathcal{R} = \kappa T_{ab} \ , \tag{2.8}$$

where R_{ab} and $\mathcal{R}$ are respectively the Ricci tensor and scalar. The dynamical model is fully determined by the matter content and the curvature. The matter content is described by the stress-energy momentum tensor T_{ab}. For a perfect fluid, using the $1+3$ formalism, it can be recast as,

$$T_{ab} = \rho u_a u_b + p h_{ab} \ , \tag{2.9}$$

where ρ is the energy density and p the pressure of the fluid. We assume the fluid to be barotropic $\rho = \rho(p)$ and linear so that it satisfies the equation of state,

$$p = w\rho \ , \tag{2.10}$$

where w is the equation-of-state parameter. The energy density ρ and the pressure p are zero-order variables that do not vanish on the background.

For an adiabatic flow, the speed of sound is defined as

$$c_s^2 \equiv \frac{dp}{d\rho} \ , \tag{2.11}$$

and the time derivative of the equation-of-state parameter satisfies,

$$\dot{w} = -\Theta(c_s^2 - w)(1+w) \ , \tag{2.12}$$

where we used the energy conservation equation (2.50). Note that from (2.12), it follows that $c_s^2 = w$ if $\dot{w} = 0$.

The Ricci tensor R_{ab} is simply obtained by substituting the expression (2.9) for the stress energy momentum tensor into the Einstein field equations (2.8),

$$R_{ab} = \tfrac{\kappa}{2} (\rho + 3p) u_a u_b + \tfrac{\kappa}{2} (\rho - p) h_{ab} \ . \tag{2.13}$$

As shown by Hawking (1966), all the information related to the curvature is encoded in the Riemann tensor which can be decomposed as,

$$R^{ab}{}_{cd} = C^{ab}{}_{cd} + 2\delta^{[a}{}_{[c} R^{b]}{}_{d]} - \tfrac{1}{3} \mathcal{R} \delta^{a}{}_{[c} \delta^{b}{}_{d]} \ , \tag{2.14}$$

where $C^{ab}{}_{cd}$ is the Weyl tensor.

2.3.1 Weyl tensor

The Weyl tensor C_{abcd} is constructed to be the trace-free part of the Riemann tensor R_{abcd} and thus satisfies the identities,

$$\begin{aligned} C_{abcd} &= C_{[ab][cd]} \ , \\ C_{abcd} &= C_{cdab} \ , \\ C_{a[bcd]} &= 0 \ , \\ C_{abc}{}^{b} &= 0 \ , \end{aligned} \tag{2.15}$$

which implies that it also satisfies the duality identity

$$\eta_{abcd} C_{ef}{}^{cd} = \eta_{efcd} C_{ab}{}^{cd} \ . \tag{2.16}$$

By analogy to classical electrodynamics, the Weyl tensor can be split relative to u^a into an 'electric' and a 'magnetic' part, as mentioned by Hawking (1966), according to,

$$E_{ab} = C_{acbd} u^c u^d \ , \tag{2.17}$$

$$H_{ab} =^{*} C_{acbd} u^c u^d = \tfrac{1}{2} \varepsilon_{ade} C^{de}{}_{bc} u^c \ , \tag{2.18}$$

where ${}^{*}C_{acbd}$ is the dual of the Weyl tensor. These parts represent the 'free gravitational field', enabling gravitational action at a distance and describing tidal forces and gravitational waves. Their properties follow directly from the symmetries of the Weyl tensor (2.15) and (2.16),

$$\begin{aligned} E_{ab} u^b = 0 \ , \quad E_{ab} = E_{(ab)} \ , \quad E^a{}_a = 0 \ , \\ H_{ab} u^b = 0 \ , \quad H_{ab} = H_{(ab)} \ , \quad H^a{}_a = 0 \ . \end{aligned} \tag{2.19}$$

Finally, the Weyl tensor can be decomposed in terms of its two parts as,

$$C^{ab}{}_{cd} = 4 u^{[a} u_{[c} E^{b]}{}_{d]} + 4 h^{[a}{}_{[c} E^{b]}{}_{d]} + 2 \varepsilon^{abe} u_{[c} H_{d]e} + 2 \varepsilon_{cde} u^{[a} H^{b]e} \ . \tag{2.20}$$

2.3.2 Riemann tensor decomposition

The Riemann tensor R_{abcd} can now be recast in terms of the Ricci tensor (2.13), the electric (2.17) and magnetic (2.18) parts of the Weyl tensor according to the

decomposition (2.14) in the following way,

$$\begin{aligned} R^{ab}{}_{cd} &= \tfrac{2}{3}\kappa\left(\rho+3p\right)u^{[a}u_{[c}h^{b]}{}_{d]} + \tfrac{2}{3}\kappa\rho h^{a}{}_{[c}h^{b}{}_{d]} \\ &\quad + 4u^{[a}u_{[c}E^{b]}{}_{d]} + 4h^{[a}{}_{[c}E^{b]}{}_{d]} + 2\varepsilon^{abe}u_{[c}H_{d]e} + 2\varepsilon_{cde}u^{[a}H^{b]e} \ . \end{aligned} \tag{2.21}$$

The Riemann tensor restricted to the spatial hypersurface, ${}^{(3)}R^{ab}{}_{cd}$, is related to the Riemann tensor defined on the whole space-time, $R^{ab}{}_{cd}$, by

$${}^{(3)}R^{ab}{}_{cd} = h^{a}{}_{e}h^{b}{}_{f}h^{g}{}_{c}h^{h}{}_{d}R^{ef}{}_{gh} - 2v^{a}{}_{[c}v^{b}{}_{d]} \ . \tag{2.22}$$

where the tensor v_{ab} is defined as,

$$v_{ab} \equiv D_{a}u_{b} \ . \tag{2.23}$$

For a perfect fluid, using the decomposition (2.21), the spatial Riemann tensor (2.22) becomes,

$${}^{(3)}R^{ab}{}_{cd} = \tfrac{2}{3}\kappa\rho h^{a}{}_{[c}h^{b}{}_{d]} + 4h^{a}{}_{[c}E^{b}{}_{d]} - 2v^{a}{}_{[c}v^{b}{}_{d]} \ . \tag{2.24}$$

To zero-order, the decomposition of the spatially projected Riemann tensor (2.22) reduces to,

$${}^{(3)}R^{ab}{}_{cd} = \frac{2K}{R^{2}}h^{a}{}_{[c}h^{b}{}_{d]} \ . \tag{2.25}$$

where K is the curvature parameter, which is related to the Gaussian curvature $\mathcal{K}$ by,

$${}^{(3)}R = \mathcal{K} = \frac{6K}{R^{2}} \ , \tag{2.26}$$

where ${}^{(3)}\mathcal{R}$ is the spatial curvature scalar, which is obtained by twice contracting the spatially projected Riemann tensor (2.22).

In general, there are three sets of dynamical equations for a perfect fluid. These sets are derived, respectively, from the Ricci identities, the Bianchi identities, once- and twice-contracted. We present now each set in turn and expand the dynamical equations to first-order about an FLRW background space-time.

2.3.3 Ricci identities

The first set of dynamical equations arises from the Ricci identities. These identities can firstly be applied to the whole space-time and secondly to the spatial hypersurfaces according to,

$$\nabla_{[a}\nabla_{b]}u_c = \tfrac{1}{2}R_{abcd}u^d \ , \tag{2.27}$$

$$D_{[a}D_{b]}v_c = \tfrac{1}{2}{}^{(3)}R_{abcd}v^d \ , \tag{2.28}$$

where the spatial vectors v^a are orthogonal to the worldline, i.e. $v^a u_a = 0$.

The information contained in the Ricci identities (2.27)-(2.28) can be extracted by projecting them on different hypersurfaces using the decomposition of the corresponding Riemann tensors (2.21)-(2.24) and following the same procedure as Brechet *et al.* (2007).

To first-order, the Ricci identities applied to the whole space-time (2.27) yield three propagation equations, which are respectively the Raychaudhuri equation, the rate of shear propagation equation and the vorticity propagation equation,

$$\dot{\Theta} = -\tfrac{1}{3}\Theta^2 - \tfrac{\kappa}{2}(\rho + 3p) + D^b a_b \ , \tag{2.29}$$

$$\dot{\omega}_{\langle a\rangle} = -\tfrac{2}{3}\Theta\,\omega_a + \tfrac{1}{2}\,\mathrm{curl}\,a_a \ , \tag{2.30}$$

$$\dot{\sigma}_{\langle ab\rangle} = -\tfrac{2}{3}\Theta\,\sigma_{ab} - E_{ab} + D_{\langle a}a_{b\rangle} \ , \tag{2.31}$$

and three constraint equations,

$$D^a\omega_a = 0 \ , \tag{2.32}$$

$$D^b\sigma_{ab} = \tfrac{2}{3}D_a\Theta - \,\mathrm{curl}\,\omega_a \ , \tag{2.33}$$

$$H_{ab} = \,\mathrm{curl}\,\sigma_{ab} - D_{\langle a}\omega_{b\rangle} \ . \tag{2.34}$$

The Ricci identities applied to the spatial hypersurfaces express the spatial curvature. Their contractions yield the spatial Ricci tensor ${}^{(3)}R_{ab}$ and scalar ${}^{(3)}\mathcal{R}$ respectively, which to first-order are given by,

$${}^{(3)}R_{ab} = \tfrac{1}{3}{}^{(3)}\mathcal{R}h_{ab} - \tfrac{1}{3}\Theta\,(\sigma_{ab} - \omega_{ab}) + E_{ab} \ , \tag{2.35}$$

$$\mathcal{K} = -\tfrac{2}{3}\Theta^2 + 2\kappa\rho \ . \tag{2.36}$$

To zero-order, using the expression for the Gaussian curvature (2.26), the contractions of the spatial Ricci identities (2.35) and (2.36) reduce respectively to,

$$ {}^{(3)}R_{ab} = \tfrac{1}{3}\,{}^{(3)}\mathcal{R}h_{ab} \ , \tag{2.37} $$

$$ \frac{1}{9}\Theta^2 = \frac{\kappa}{3}\rho - \frac{K}{R^2} \ . \tag{2.38} $$

Note that the above expression (2.38) is the Friedmann equation. It is useful to recast the Friedmann (2.38) and Raychaudhuri (2.29) equations in terms of conformal time. To zero-order, these equations are respectively given by,

$$ \mathcal{H}^2 = \tfrac{\kappa}{3}\rho R^2 - K \ , \tag{2.39} $$

$$ \mathcal{H}' = -\tfrac{\kappa}{6}\rho R^2(1+3w) \ . \tag{2.40} $$

Finally, it is convenient to recast them as,

$$ \mathcal{H}^2 - \mathcal{H}' + K = \tfrac{\kappa}{2}\rho R^2\,(1+w) \ , \tag{2.41} $$

$$ \mathcal{H}' = -\tfrac{\kappa}{2}\,(1+3w)\,(\mathcal{H}^2+K) \ . \tag{2.42} $$

2.3.4 Once-contracted Bianchi identities

The second and third set of dynamical equations are contained in the Bianchi identities. The Riemann tensor satisfies the Bianchi identities as follows,

$$ \nabla^{[e}R^{ab]}{}_{cd} = 0 \ . \tag{2.43} $$

By substituting the expression for the Riemann tensor decomposition (2.14) and the effective Einstein field equations (2.8) into the Bianchi identities (2.43) and contracting two indices ($d = e$), the once-contracted Bianchi identities are found to be,

$$ \nabla^d C^{ab}{}_{cd} + \nabla^{[a}R^{b]}{}_c + \tfrac{1}{6}\delta_c{}^{[a}\nabla^{b]}\mathcal{R} = 0 \ . \tag{2.44} $$

In a similar manner to the Ricci identities, the information stored in the once-contracted Bianchi identities has to be projected along the worldlines u^a and on the spatial hypersurfaces $h^a{}_b$.

To first order, the once-contracted Bianchi identities (2.44) yield two propagation equations, which are respectively the electric and magnetic propagation equations,

$$\dot{E}_{\langle ab\rangle} = -\Theta E_{ab} + \operatorname{curl} H_{ab} - \tfrac{\kappa}{2}(\rho + p)\,\sigma_{ab} \ , \tag{2.45}$$

$$\dot{H}_{\langle ab\rangle} = -\Theta H_{ab} - \operatorname{curl} E_{ab} \ , \tag{2.46}$$

and two constraint equations,

$$D^b E_{ab} = \tfrac{\kappa}{3} D_a \rho \ , \tag{2.47}$$

$$D^b H_{ab} = -\kappa\,(\rho + p)\,\omega_a \ . \tag{2.48}$$

2.3.5 Twice-contracted Bianchi identities

The third set of equations is given by the twice-contracted Bianchi identities which represent the conservation of the effective stress energy momentum tensor. They are obtained by performing a second contraction ($b = c$) on the once-contracted Bianchi identities (2.44),

$$\nabla^b \left(R_{ab} + \tfrac{1}{2} g_{ab} \mathcal{R}\right) = \kappa \nabla^b T_{ab} = 0 \ . \tag{2.49}$$

To first order, the twice-contracted Bianchi identities (2.49) yield one propagation equations, which is the energy conservation equation,

$$\dot{\rho} = -\Theta\ (\rho + p) \ , \tag{2.50}$$

and one constraint equation, which is the momentum conservation equation,

$$D_a p = -a_a\,(\rho + p) \ . \tag{2.51}$$

2.4 Scalar perturbations

2.4.1 Bardeen equation

Physically, scalar perturbations represent spatial variations of zero-order scalar quantities. Thus, spatial Laplacians of zero-order scalars are natural candidates

to describe such perturbations. Since we are interested in determining the time evolution of scalar perturbations in a comoving frame, we choose comoving spatial Laplacians of zero-order scalars as scalar perturbations variables. For the linearised dynamics of a perfect fluid about a homogeneous and isotropic background, there are only four zero-order scalars, the energy density ρ, the pressure p, the expansion rate Θ and the Gaussian curvature $\mathcal{K}$. For an adiabatic flow, the pressure is a function of the energy density (2.10). Thus, to describe the dynamics of adiabatic scalar perturbations, we define three scalar perturbation variables, which are respectively the comoving spatial Laplacian of the energy density Φ, the comoving spatial Laplacian of the expansion rate Ψ and the comoving spatial Laplacian of the Gaussian curvature χ,

$$\Phi \equiv R\kappa\Delta\rho \ , \tag{2.52}$$

$$\Psi \equiv R\Delta\Theta \ , \tag{2.53}$$

$$\chi \equiv \tfrac{1}{2}R\Delta\mathcal{K} \ , \tag{2.54}$$

where the comoving spatial Laplacian Δ is related to the cosmic spatial Laplacian D^2 by,

$$\Delta = R^2D^2 = R^2D^aD_a \ , \tag{2.55}$$

and the factor of a half in (2.54) is included to be consistent with the usual definition of the corresponding variable in the 'background-based' approach developed by Mukhanov *et al.* (1992). Similar definitions for the comoving spatial Laplacian of the energy density and the comoving spatial Laplacian of the Gaussian curvature were used respectively by Woszczyna & Kulak (1989) and Bruni *et al.* (1992a). For a vanishing background curvature, it is worth mentioning that the curvature perturbation does not vanish, since it is a first-order variable. The dynamics of the scalar perturbations is obtained by taking the comoving spatial Laplacian of the scalar propagation equations (2.50), (2.29), (2.36) and the spatial gradient of the constraint (2.51) in order to express the constraint in terms of a comoving spacial Laplacian of a zero-order scalar. The dynamical equations of the scalar perturbations are respectively the comoving spatial Laplacian of the energy conservation equation (2.50), the comoving spatial Laplacian of the Raychaudhuri equation (2.29), the comoving spatial Laplacian of the Gauss-Codacci

equation (2.36) and the spatial gradient of the momentum conservation equation, which to first-order reduce to,

$$\Delta\dot{\rho} + \Theta\Delta(\rho + p) + (\rho + p)\Delta\Theta = 0 \ , \tag{2.56}$$

$$\Delta\dot{\Theta} + \tfrac{2}{3}\Theta\Delta\Theta + \tfrac{\kappa}{2}\Delta(\rho + 3p) - \Delta\left(D^b a_b\right) = 0 \ , \tag{2.57}$$

$$\Delta\mathcal{K} + \tfrac{4}{3}\Theta\Delta\Theta - 2\kappa\Delta\rho = 0 \ , \tag{2.58}$$

$$\Delta p + R^2\left(\rho + p\right) D^b a_b = 0 \ . \tag{2.59}$$

In order to reverse the order of the comoving spatial Laplacian and the time derivative of a scalar field S in the propagation equations (2.56) and (2.57), it is useful to introduce the first-order scalar identity,

$$\Delta\dot{S} = (\Delta S)^{\cdot} - \tfrac{1}{3}\Theta\Delta S - R^2\dot{S}D^b a_b \ . \tag{2.60}$$

The dynamical equations (2.56), (2.57), and (2.58) are recast in terms of the comoving spatial Laplacian (2.52), (2.53) and (2.54) using the the scalar identity (2.60), the gradient of the momentum conservation equation (2.59), the Friedmann equation (2.38), the Raychaudhuri equation (2.29) and the energy conservation equation (2.50). To first-order, in a comoving frame, the dynamical equations reduce to,

$$\dot{\Phi} + \tfrac{1}{3}\Theta\Phi + \kappa\rho(1 + w)\Psi = 0 \ , \tag{2.61}$$

$$\dot{\Psi} + \left(\frac{1}{2} + \frac{3Kc_s^2}{R^2\kappa\rho(1 + w)}\right)\Phi + \frac{c_s^2}{R^2\kappa\rho(1 + w)}\Delta\Phi = 0 \ , \tag{2.62}$$

$$\chi + \tfrac{2}{3}\Theta\Psi - \Phi = 0 \ . \tag{2.63}$$

In order to determine the dynamics of the scalar perturbations, it is useful to express the dynamical equations (2.61), (2.62) and (2.63) in terms of conformal time according to,

$$\Phi' + \mathcal{H}\Phi + R\kappa\rho(1 + w)\Psi = 0 \ , \tag{2.64}$$

$$\Psi' + \left(\frac{R}{2} + \frac{3Kc_s^2}{R\kappa\rho(1 + w)}\right)\Phi + \frac{c_s^2}{R\kappa\rho(1 + w)}\Delta\Phi = 0 \ , \tag{2.65}$$

$$\chi + \frac{2\mathcal{H}}{R}\Psi - \Phi = 0 \ . \tag{2.66}$$

In order to determine the conformal time evolution of the density perturbation variable Φ, the dynamics has to be recast in terms of a second-order differential equation for Φ. By differentiating the Φ-propagation equation (2.64) with respect to conformal time, using the Ψ-propagation equation (2.65) to substitute Φ for Ψ and the zero-order relations (2.41) and (2.42), a second-order differential equation for Φ is obtained according to,

$$\Phi'' + 3\mathcal{H}\left(1 + c_s^2\right)\Phi' + \left[(1 + 3c_s^2)(\mathcal{H}^2 - K) + 2\mathcal{H}'\right]\Phi - c_s^2\Delta\Phi = 0 \ , \qquad (2.67)$$

which is the Bardeen (1980) equation (denoted [4.9]) and identified by Woszczyna & Kulak (1989) in the $1+3$ covariant formalism.

We now formally relate the energy density perturbation variable Φ used in the $1+3$ covariant approach to the Bardeen variables Φ_A and Φ_H used in the 'background-based' approach. By taking the comoving spatial Laplacian of the divergence of the electric part of the Weyl tensor E_{ab} (2.47), the energy density perturbation Φ is found to be related to E_{ab} according to,

$$\Phi = 3R^3 D^a D^b E_{ab} \ . \qquad (2.68)$$

The expression of the electric part of the Weyl tensor E_{ab} in terms of the Bardeen variables Φ_A and Φ_H was first established by Bruni *et al.* (1992a) in equations [113-114]. For a perfect fluid (i.e. in absence of anisotropic stress), the Bardeen variables have the same norm but opposite signs (i.e. $\Phi_H = -\Phi_A$). Substituting the relations [113-114] derived by Bruni *et al.* (1992a) into (2.68), the energy density perturbation Φ is found to be the fourth-order derivative of the Bardeen variable Φ_A according to,

$$\Phi = 3\Box\Phi_A \ , \qquad (2.69)$$

where,

$$\Box \equiv 3D^a D^b D_{\langle a} D_{b\rangle} \ . \qquad (2.70)$$

Note that by taking spatial derivatives of the electric part of the Weyl tensor, the vector and tensor perturbation terms contained in equations [113-114] vanish. To first-order, the conformal time derivative and the comoving spatial Laplacian

commute with the spatial differential operator $\Box$,

$$\Phi' = \Box\Phi'_A \ , \tag{2.71}$$

$$\Delta\Phi = \Box\Delta\Phi_A \ . \tag{2.72}$$

Thus, to first-order, the dynamics of the energy density perturbation Φ is identical to the dynamics of the Bardeen variable Φ_A since the Bardeen equation (2.67) is entirely described by conformal time derivatives and spatial Laplacians of Φ. Therefore, in the $1+3$ covariant formalism, Φ is the analog of Φ_A.

2.4.2 Mukhanov-Sasaki equation

The Bardeen equation describes the time evolution of the density perturbation variable Φ. Similarly, the Mukhanov-Sasaki equation describes the time evolution of the curvature perturbation variable, which in the spatially-curved case we will denote by ζ, and which reduces to χ defined in (2.54) in the spatially-flat case ($K = 0$), as we will now show.

To make contact with the standard definition of the curvature perturbation in the 'background-based' approach, it is useful to express χ in terms of Φ only. By substituting (2.64) into (2.66), using the Friedmann equation (2.39), the expression for χ to first-order becomes,

$$\chi = \frac{2}{3(1+w)}\left(1+\frac{K}{\mathcal{H}^2}\right)^{-1}\left(\Phi+\frac{\Phi'}{\mathcal{H}}\right)+\Phi \ , \tag{2.73}$$

which, for a spatially-flat background space-time ($K = 0$), reduces to,

$$\chi = \frac{2}{3(1+w)}\left(\Phi+\frac{\Phi'}{\mathcal{H}}\right)+\Phi \ , \tag{2.74}$$

which is the standard definition of the curvature perturbation (see Mukhanov (2005), Durrer (2008)). In the spatially-flat case, the conformal time derivative of the curvature perturbation χ is given by,

$$\chi' = \frac{2c_s^2}{3\mathcal{H}(1+w)}\Delta\Phi \ , \tag{2.75}$$

which shows that the curvature perturbation χ is a conserved quantity on large scales. To show this explicitly a Fourier transform has to be performed (see Durrer

(2008)). However, we note that on large scales the comoving spatial Laplacian of the analog of Bardeen variable is negligible compared to the comoving scale $\mathcal{H}$, thus satisfying $\Delta\Phi \ll \mathcal{H}$. Nonetheless, the curvature perturbation is not conserved on super-Hubble scales for a spatially-curved background space-time as explained by Bruni *et al.* (1992a).

In the spatially-curved case, Bruni *et al.* (1992a) mention that there is a generalised curvature perturbation $\tilde{C}$, which is conserved on large scales and defined up to a constant amplitude. Thus, we define the generalised curvature variable ζ as

$$\zeta \equiv \frac{R}{2}\left(\Delta\mathcal{K} - \frac{4K}{R^2(1+w)}\frac{\Delta\rho}{\rho}\right) , \tag{2.76}$$

where $\zeta \equiv \frac{1}{2}\tilde{C}$ in order for ζ to reduce to χ in the spatially-flat case ($K = 0$). The generalised curvature perturbation variable ζ in the spatially-curved case is related to the curvature perturbation χ in the spatially-flat case by,

$$\zeta = \chi - \frac{2K}{3\mathcal{H}^2\,(1+w)}\left(1 + \frac{K}{\mathcal{H}^2}\right)^{-1}\Phi \, . \tag{2.77}$$

We now briefly show that ζ is conserved on large scales. By substituting (2.73) into (2.77), the generalised curvature perturbation ζ is recast in terms of the analog of the Bardeen variable Φ only according to,

$$\zeta = \frac{2}{3(1+w)}\left(1 + \frac{K}{\mathcal{H}^2}\right)^{-1}\left[\left(1 - \frac{K}{\mathcal{H}^2}\right)\Phi + \frac{\Phi'}{\mathcal{H}}\right] + \Phi \, . \tag{2.78}$$

For a spatially-curved case, by differentiating (2.78) and substituting the Bardeen equation (2.67), the conformal time derivative of the generalised curvature perturbation ζ' is found to be,

$$\zeta' = \frac{2c_s^2}{3\mathcal{H}(1+w)}\left(1 + \frac{K}{\mathcal{H}^2}\right)^{-1}\Delta\Phi \, , \tag{2.79}$$

which means that the generalised curvature perturbation ζ is a conserved quantity on super-Hubble scales. To show this explicitly a harmonic decomposition has to be performed. However, similarly to the spatially-flat case, we note that on large scale the comoving spacial Laplacian of the analog of the Bardeen variable is negligible compared to the comoving scale $\mathcal{H}$, thus satisfying $\Delta\Phi \ll \mathcal{H}$.

In order to determine the conformal time evolution of the curvature perturbation variable ζ, the dynamics has to be recast in terms of a second-order differential equation for ζ. By differentiating the ζ-propagation equation (2.79) with respect to time and using the comoving Laplacian of the generalised curvature perturbation ζ (2.78) to substitute ζ for Φ, a second order differential equation for ζ is obtained according to,

$$\zeta'' + 2\left(\frac{\mathcal{H}}{2}\left(1 - 3c_s^2\right) - \frac{\mathcal{H}'}{\mathcal{H}}\right)\zeta' - c_s^2\Delta\zeta = 0 \ . \tag{2.80}$$

It is convenient to introduce a new variable z,

$$z \equiv \frac{R^2}{c_s\mathcal{H}}\left(\frac{\kappa}{3}\rho(1+w)\right)^{1/2} \ , \tag{2.81}$$

which allows the ζ-propagation equation (2.80) to be recast in a more convenient form as,

$$\zeta'' + 2\frac{z'}{z}\zeta' - c_s^2\Delta\zeta = 0 \ . \tag{2.82}$$

Note that using the dynamical equation (2.41), z is rewritten as,

$$z = \frac{R^2}{c_s\mathcal{H}}\left(\mathcal{H}^2 - \mathcal{H}' + K\right)^{1/2} \ , \tag{2.83}$$

which corresponds to the variable defined by Mukhanov *et al.* (1992) in equation [10.43b].

It is also useful to define another variable,

$$v \equiv z\zeta \ , \tag{2.84}$$

which is the analog of the variable v defined by Mukhanov *et al.* (1992) in equation [10.61]. Using v, the dynamics of the second-order dynamical equation (2.82) is explicitly recast in terms of a wave equation given by,

$$v'' - \left(c_s^2\Delta + \frac{z''}{z}\right)v = 0 \ . \tag{2.85}$$

This wave equation is the Mukhanov-Sasaki equation in a spatially-curved FLRW background space-time denoted [11.7] by Mukhanov *et al.* (1992).

2.4.3 Mukhanov-Sasaki variable

The scalar variable $v = z\zeta$ is hence the $1+3$ covariant analog of the Mukhanov-Sasaki variable associated to the scalar perturbations (note that in a spatially-flat case, the analog of the Mukhanov-Sasaki variable reduces to $v = z\chi$). In the general case, the homogeneity and isotropy of the spatial hypersurfaces enable us to perform a harmonic decomposition of the scalar perturbation variable v, where v is decomposed into components that transform irreducibly under translations and rotations, and evolve independently, as explained by Durrer (2008). The harmonic analysis of the scalar perturbation v consists of a decomposition into eigenfunctions of the comoving spatial Laplacian of v according to,

$$\Delta v_k = -k^2 v_k \ , \tag{2.86}$$

where k is the eigenvalue of the associated harmonic mode and the k-index denotes the eigenvector of the mode. The comoving wavenumber ν of the scalar mode is defined as,

$$\nu^2 = k^2 + K \ , \tag{2.87}$$

where $K = \{-1, 0, 1\}$ is normalised. The comoving wavenumber ν takes continuous values when $K = \{-1, 0\}$ and discrete ones for $K = 1$. In particular, the regular normalisable eigenmodes have $\nu \geq 0$ for flat and hyperbolic spatial hypersurfaces, and an integer satisfying $\nu \geq 1$ for spheric hypersurfaces as explained by Lyth & Woszczyna (1995) and Tsagas *et al.* (2008).

To first order, the dynamics of the scalar perturbations can be rewritten as a series of decoupled harmonic oscillators. Using the harmonic decomposition (2.86) in terms of k, the Mukhanov-Sasaki wave equation (2.85) in the k-mode is given by,

$$v_k{}'' + \left(c_s^2 k^2 - \frac{z''}{z}\right) v_k = 0 \ . \tag{2.88}$$

Note that (2.88) corresponds to a simple damped harmonic oscillator in the k-mode,

$$v_k{}'' + \omega_k^2 v_k = 0 \ , \tag{2.89}$$

where the conformal time dependent frequency $\omega_k(\hat{\tau})$ is given by,

$$\omega_k = \left(c_s^2 k^2 - \frac{z''}{z}\right)^{1/2} \ . \tag{2.90}$$

2.4.4 Comparison with scalar perturbations of a scalar field in the 'background-based' approach

The dynamics of the early universe is believed to undergo an inflation phase described by a scalar field as shown by Guth (1981) and Linde (1982). In a 'background-based' approach, the scalar field ϕ in the 'real' space-time is decomposed into a background component ϕ_0 and a gauge-dependent perturbation $\delta\phi$ according to,

$$\phi(t, \mathbf{x}) = \phi_0(t) + \delta\phi(t, \mathbf{x}) \ . \tag{2.91}$$

According to Weinberg (2008), the energy-momentum tensor of an unperturbed scalar field takes the perfect fluid form with an energy density and pressure respectively given by,

$$\begin{aligned} \rho_0 &= \tfrac{1}{2}\dot{\phi}_0^2 + V(\phi_0) \ , \\ p_0 &= \tfrac{1}{2}\dot{\phi}_0^2 - V(\phi_0) \ , \end{aligned} \tag{2.92}$$

where $V(\phi_0)$ is an arbitrary real potential. The initial conditions for inflation needed to perform the quantisation are set as the model emerges from the Big Bang, where the scalar field dynamics is dominated by the kinetic term and satisfies $\dot{\phi}_0 \gg V(\phi_0)$. Therefore, at very early times, the scalar field behaves like stiff matter and the equation of state parameter w is related to the speed of sound by $w = c_s^2 = 1$ as mentioned by Durrer (2008). The dynamics of scalar perturbations of a scalar field in a $1+3$ covariant approach was first investigated by Bruni *et al.* (1992b). Langlois & Vernizzi (2007) later generalised the $1+3$ covariant approach to multi-scalar fields.

To first order, the dynamical equation for the Bardeen variable is given by,

$$\dot{\Phi}_A + H\Phi_A = \tfrac{\kappa}{2}\dot{\phi}_0\delta\phi \ , \tag{2.93}$$

which corresponds to equation [10.1.12] presented by Weinberg (2008). By comparing this dynamical relation with the corresponding result (2.64) found in the $1+3$ covariant approach using the zero-order expression for the energy density and pressure of a scalar field (2.92) and by using the correspondence relation (2.69),

the $1+3$ covariant perturbation variable Ψ is found to be related to the scalar field perturbation $\delta\phi$ by,

$$\Psi = -\Box\left(\frac{\delta\phi}{2\dot{\phi}_0}\right) \ . \tag{2.94}$$

The curvature perturbation variables in the flat case χ and the curved case ζ can be recast in terms of the Bardeen variable Φ_A and the scalar field perturbation variable $\delta\phi$ according to,

$$\begin{aligned} \chi &= \Box\left(\Phi_A + \mathcal{H}\frac{\delta\phi}{\phi_0'}\right) \ , \\ \zeta &= \Box\left(\left[1 - \frac{K}{3\mathcal{H}^2}\left(1+\frac{K}{\mathcal{H}^2}\right)^{-1}\right]\Phi_A + \mathcal{H}\frac{\delta\phi}{\phi_0'}\right) \ . \end{aligned} \tag{2.95}$$

The quantisation variable z can also be expressed in terms of the scalar field perturbation according to,

$$z = \left(\frac{\kappa}{3}\right)^{1/2}\frac{R\phi_0'}{\mathcal{H}} \ . \tag{2.96}$$

Finally, for a scalar field behaving like a stiff fluid (i.e. $c_s = 1$), the Mukhanov-Sasaki wave equation in the k-mode (2.88) reduces to,

$$v_k{}'' + \left(k^2 - \frac{z''}{z}\right)v_k = 0 \ . \tag{2.97}$$

Thereby, with the identities presented above, we formally related the first-order scalar perturbation variables in the 1+3 covariant formalism to the corresponding variables in the 'background-based' approach.

2.5 Vector perturbations

Vector perturbations are described by spatially projected and divergence-free vectors as explained by Tsagas *et al.* (2008). The only dynamical variable which satisfies these constraints to first-order is the vorticity pseudo-vector ω^a. The vanishing divergence of ω^a to first-order can be deduced from (2.32).

The dynamics of the vorticity covector ω_a is determined by the vorticity propagation equation (2.30). To obtain an explicit evolution equation in terms of the

vorticity covector only, the term involving the acceleration has to be recast in terms of the vorticity. Using the momentum conservation equation (2.51) and the kinetic non-commutation identity (1.15), we find to first-order,

$$\mathrm{curl}\, a_a = 2c_s^2 \Theta \omega_a \ . \tag{2.98}$$

Thus, to first-order, the vorticity propagation equation (2.30) can be recast as,

$$\dot{\omega}_{\langle a\rangle} + \tfrac{2}{3}\Theta\left(1 - \tfrac{3}{2}c_s^2\right)\omega_a = 0 \ , \tag{2.99}$$

as shown by Hawking (1966). It is convenient to express this dynamical equation in a comoving frame according to,

$$\omega'_{\langle a\rangle} + 2\mathcal{H}\left(1 - \tfrac{3}{2}c_s^2\right)\omega_a = 0 \ . \tag{2.100}$$

Using the vorticity contraction identity,

$$w^{2'} = 2\omega'_{\langle a\rangle}\omega^a \ , \tag{2.101}$$

a first-order propagation equation for the vorticity scalar w is obtained,

$$\omega' = -2\mathcal{H}\left(1 - \tfrac{3}{2}c_s^2\right)\omega \ , \tag{2.102}$$

and implies that the vorticity scalar scales as,

$$\omega \propto R^{-2+3c_s^2} \ , \tag{2.103}$$

which is in agreement with the result obtained by Hawking (1966) and mentioned by Tsagas *et al.* (2008).

The scaling relation (2.103) implies that during the expansion phase ($R' > 0$), the scalar amplitude of the vorticity ω decays if $c_s^2 < \frac{2}{3}$. The inflationary scenario is the simplest known generating mechanism for the initial density fluctuations. For an inflaton field in slow-roll ($w = -1$), the vorticity scalar scales as $\omega \propto R^{-5}$. Hence, the value of the vorticity scalar at the end of slow-roll inflation ω_f is related to the value of the vorticity scalar at the onset of the slow-roll inflation ω_i by,

$$\frac{\omega_f}{\omega_i} = \exp\left(-5N\right) \ , \tag{2.104}$$

where N is the number of e-fold during the slow-roll phase. Hence, if the vector perturbations were initially significant, they have decayed by a factor $\exp(5N)$ during slow-roll inflation (2.104) and can safely be neglected in a subsequent quantitative perturbation analysis.

2.6 Tensor perturbations

Tensor perturbations are described by spatially projected, symmetric, trace-free and transverse second rank tensors, as explained by Tsagas *et al.* (2008). To find a suitable tensor to describe such perturbations, it is useful to split the magnetic part of the Weyl tensor H_{ab} into a transverse part denoted $H^{(T)}_{ab}$ and a non-transverse part denoted $H^{(V)}_{ab}$ according to,

$$H_{ab} = H^{(T)}_{ab} + H^{(V)}_{ab} \ . \tag{2.105}$$

where the $^{(T)}$ and $^{(V)}$ indices refer respectively to tensorial and vectorial degrees of freedom. By construction, $H^{(T)}_{ab}$ is divergence-free and satisfies the requirements for a tensor perturbation. For convenience, in this section, we will not use explicitly the $^{(T)}$ index to refer to the transverse part of the magnetic part of the Weyl tensor, since we are only considering tensorial degrees of freedom. Note that in the irrotational case, the magnetic part of the Weyl tensor is divergence-free to first-order − this can be deduced from the constraint (2.48). Thus, in that case, the analysis is restricted to the tensorial degrees of freedom only and $H_{ab} = H^{(T)}_{ab}$. It is also worth mentioning that the electric part of the Weyl cannot qualify as a tensor perturbation, since it is not divergence-free in presence of matter − this can be inferred from the constraint (2.47).

2.6.1 Grishchuk equation

In order to obtain a second-order differential equation in terms of H_{ab}, it is useful to introduce linearised identities mentioned by Challinor (2000). Using the Ricci identities (2.27)-(2.28), the expression for the Riemann tensor to zero-order (2.25) and the definition of a curl (1.10), a symmetric and spatially projected tensor $T_{\langle ab\rangle}$ to first-order has to satisfy the geometric linearised identity,

$$^{(3)}(\operatorname{curl} T_{ab})^{\cdot} = \operatorname{curl} \dot{T}_{\langle ab\rangle} - \tfrac{1}{3}\Theta \operatorname{curl} T_{ab} \ , \tag{2.106}$$

and if T_{ab} is transverse to first-order,

$$D^b T_{ab} = 0 \ , \tag{2.107}$$

then it also satisfies the identity,

$$\mathrm{curl}\,(\,\mathrm{curl}\,T_{ab}) = -D^2 T_{ab} + \frac{3K}{R^2} T_{ab}\ . \tag{2.108}$$

By differentiating the magnetic propagation equation (2.46), substituting the electric propagation equation (2.45) and using the linearised identities (2.106) and (2.108), the dynamical equation for H_{ab} to first order reduces to,

$$\ddot{H}_{\langle ab\rangle} + \frac{7}{3}\Theta\dot{H}_{\langle ab\rangle} + 2\left((1-w)\kappa\rho - \frac{3K}{R^2}\right) H_{ab} - D^2 H_{ab} = 0\ , \tag{2.109}$$

which has been established by Challinor (2000). Using the zero-order dynamical relations (2.39) and (2.40), it is convenient to recast the dynamics of H_{ab} (2.109) in terms of conformal time $\hat{\tau}$ according to,

$$H''_{\langle ab\rangle} + 6\mathcal{H}H'_{\langle ab\rangle} - \left(\Delta - 2K - 8\mathcal{H}^2 - 4\mathcal{H}'\right) H_{ab} = 0\ . \tag{2.110}$$

In order to eliminate the second term on the LHS of (2.110) and find a suitable wave equation for the gravitational waves, it is useful to introduce the rescaled magnetic part of the Weyl tensor $\tilde{H}_{ab}$ defined as

$$\tilde{H}_{ab} \equiv R^3 H_{ab}\ . \tag{2.111}$$

The propagation equation of the tensor perturbations (2.110) can be now elegantly reformulated to first-order in terms of $\tilde{H}_{ab}$ and yields,

$$\tilde{H}''_{\langle ab\rangle} - \left(\Delta - 2K + \frac{R''}{R}\right) \tilde{H}_{ab} = 0\ , \tag{2.112}$$

which is the Grishchuk equation Grishchuk (1974) describing the dynamics of primordial gravitational waves in a spatially-curved case.

2.6.2 Tensor decomposition of $\tilde{H}_{ab}$

In order to determine the scalar Grishchuk variables associated to the tensor perturbations, which are the scalar amplitudes of the tensor perturbations, a tensor decomposition of $\tilde{H}_{ab}$ has to be performed. From the properties of the magnetic part of the Weyl tensor H_{ab}, we deduce that the key tensor $\tilde{H}_{ab}$ is

symmetric, trace-free and transverse to first-order. The transversality of $\tilde{H}_{ab}$ can be expressed as,

$$D^b\tilde{H}_{ab} = k^b\tilde{H}_{ab} = 0 \ , \tag{2.113}$$

where k^b is the spatial wavevector of the transverse gravitational waves satisfying $u^b k_b = 0$. For convenience, we now define two vectors $e^{(1)a}$ and $e^{(2)a}$ that provide an orthonormal basis for the two-dimensional spatial hypersurface orthogonal to the propagation direction k^a of the gravitational waves, and thus satisfy the following constraints,

$$\begin{aligned} &u^a e^{(1)}_a = u^a e^{(2)}_a = k^a e^{(1)}_a = k^a e^{(2)}_a = 0 \ , \\ &e^{(1)a} e^{(1)}_a = e^{(2)a} e^{(2)}_a = 1 \ , \\ &e^{(1)a} e^{(2)}_a = 0 \ . \end{aligned} \tag{2.114}$$

Note that these two vectors are not uniquely defined, which does not hinder our perturbation analysis since any orthonormal vector basis of the two dimensional hypersurface can be rotated to recover our vector basis $\{e^{(1)a}, e^{(2)a}\}$.

For an irrotational fluid, the Fermi-Walker transport of the basis vectors $e^{(1)}_a$ and $e^{(2)}_a$ vanishes as mentioned by Weinberg (1972),

$$\begin{aligned} u^b\nabla_b e^{(1)}_a - u_a a^b e^{(1)}_b = 0 \ , \\ u^b\nabla_b e^{(2)}_a - u_a a^b e^{(2)}_b = 0 \ . \end{aligned} \tag{2.115}$$

Projecting the Fermi-Walker transported basis vectors (2.115) on the spatial hypersurface yields,

$$e^{(1)\prime}_{\langle a\rangle} = e^{(2)\prime}_{\langle a\rangle} = 0 \ . \tag{2.116}$$

Taking the comoving spatial Laplacian of the constraints (2.114), we deduce the following identities,

$$\begin{aligned} e^{(1)a}\Delta e^{(1)}_a = e^{(2)a}\Delta e^{(2)}_a = 0 \ , \\ e^{(1)a}\Delta e^{(2)}_a = -e^{(2)a}\Delta e^{(1)}_a \ . \end{aligned} \tag{2.117}$$

In order to decompose the tensor perturbation tensor $\tilde{H}_{ab}$ into two polarisation modes, we define two covariant, trace-free and linearly independent polarisation

tensors,

$$\begin{aligned} e^{+}_{ab} &= \tfrac{1}{2}\left(e^{(1)}_{a}e^{(1)}_{b} - e^{(2)}_{a}e^{(2)}_{b}\right) \ , \\ e^{\times}_{ab} &= \tfrac{1}{2}\left(e^{(1)}_{a}e^{(2)}_{b} + e^{(2)}_{a}e^{(1)}_{b}\right) \ , \end{aligned} \tag{2.118}$$

which satisfy the orthonormality conditions,

$$\begin{aligned} e^{+}_{ab}e^{+ab} &= e^{\times}_{ab}e^{\times ab} = 1 \ , \\ e^{+}_{ab}e^{\times ab} &= 0 \ , \end{aligned} \tag{2.119}$$

and thus form an orthonormal tensor basis for the polarisation modes as shown by Durrer (2008). From the identities (2.116), we deduce that the spatially projected time derivatives of the polarisation tensors vanish,

$$e^{+\prime}_{\langle ab\rangle} = e^{\times\prime}_{\langle ab\rangle} = 0 \ . \tag{2.120}$$

Taking the comoving Laplacian of the orthonormality conditions (2.119) and using the identities (2.117), we deduce the following constraints,

$$\begin{aligned} e^{+}_{ab}\Delta e^{+ab} &= e^{\times}_{ab}\Delta e^{\times ab} = 0 \ , \\ e^{+}_{ab}\Delta e^{\times ab} &= e^{\times}_{ab}\Delta e^{+ab} = 0 \ . \end{aligned} \tag{2.121}$$

The tensor perturbation variable $\tilde{H}_{ab}$ is spatially projected, transverse, traceless, and therefore can be decomposed into two polarisation modes $\{+,\times\}$ according to,

$$\tilde{H}_{ab} = h^{+}e^{+}_{ab} + h^{\times}e^{\times}_{ab} \ , \tag{2.122}$$

where

$$\begin{aligned} h^{+} &= \tilde{H}^{ab}e^{+}_{ab} \ , \\ h^{\times} &= \tilde{H}^{ab}e^{\times}_{ab} \ , \end{aligned}$$

are the scalar amplitudes of the tensor perturbations. The corresponding decomposition in the 'background-based' approach is mentioned by Durrer (2008). The linear independence of the polarisation tensors in the first-order perturbation analysis allows us to study separately the dynamics of the two decoupled polarisation modes. To keep the notation compact, we introduce the polarisation mode superscript $\lambda = \{+,\times\}$.

2.6.3 Grishchuk variables

Contracting the Grishchuk equation (2.112) with the polarisation basis tensors e^{λ}_{ab} and using the identities (2.120) and (2.121), we obtain the Grishchuk equation for the scalar amplitude of the tensor perturbations associated to the polarisation mode λ,

$$h^{\lambda\prime\prime} - \left(\Delta - 2K + \frac{R''}{R}\right) h^{\lambda} = 0 \ . \tag{2.123}$$

where h^{λ} is the Grishchuk variable, which describes the scalar amplitude of the tensor perturbations in the polarisation mode λ. There are two Grishchuk variables $\{h^{+}, h^{\times}\}$ associated to the polarisation modes of the tensor perturbations.

In a similar manner than for the scalar perturbations, we perform a harmonic decomposition of the tensors perturbations. The harmonics analysis of the tensor perturbations consists in a decomposition into eigenfunctions of the comoving spatial Laplacian of the scalar amplitude of the tensor perturbation variable h^{λ} according to,

$$\Delta h^{\lambda}_{k} = -k^2 h^{\lambda}_{k} \ , \tag{2.124}$$

where k is the eigenvalue of the associated harmonic mode and the suffix k denotes the eigenvector of the mode.

Finally, to first-order, the dynamics of the tensor perturbations for each polarisation mode λ can be rewritten as a serie of decoupled harmonic oscillators. Using the harmonic decomposition of the scalar amplitudes in terms of k (2.124), the evolution equation for the scalar amplitude of the tensor perturbations (2.123) in the k-mode satisfies,

$$h^{\lambda\prime\prime}_{k} + \left(k^2 + 2K - \frac{R''}{R}\right) h^{\lambda}_{k} = 0 \ , \tag{2.125}$$

for each polarisation $\lambda = \{+, \times\}$. The tensor perturbation amplitudes variables h^{λ} are identified as the two scalar Grishchuk variables associated to the tensor perturbations. Note that (2.125) corresponds to a simple harmonic oscillator with a polarisation λ in the k-mode,

$$h^{\lambda\prime\prime}_{k} + {\omega^{\lambda}_{k}}^{2} h^{\lambda}_{k} = 0 \ , \tag{2.126}$$

where the conformal time dependent frequency $\omega_k^\lambda(\hat{\tau})$ is given by,

$$\omega_k^\lambda = \left(k^2 + 2K - \frac{R''}{R}\right)^{1/2} . \tag{2.127}$$

Chapter 3

Effective Weyssenhoff fluid dynamics in the $1+3$ covariant approach

Gravitation, the first fundamental force known to modern physics seems also to be the least understood. Even though the validity of Einstein's theory of general relativity has been very well tested on a macroscopic scale, it is known to present great theoretical challenges on a microscopic scale. General relativity was originally formulated as a classical field theory valid for mass distributions in a macrophysical realm. To extend general relativity to the microphysical realm, the spin of matter has to be considered. Macroscopic matter is made of elementary particles of mass m and spin s, whose dynamics can be locally described by quantum field theory and special relativity. As a result, these particles can be classified using unitary representations of the Poincare group, where the mass m is connected with the translational part of the group and the spin s is related to the rotational part as mentioned by Hehl *et al.* (1976). Mass and spin are two elementary and complementary microscopic notions which, once averaged on a macroscopic scale, have a distinctive behaviour. The mass acts like a monopole and adds up because of its scalar nature whereas the spin behaves like a dipole and can average out because of its vectorial nature.

The vanishing expectation value of the spin seems to allow a macroscopic description of a continuous distribution of matter in terms of the mass alone.

This is precisely the case in general relativity where the energy-momentum tensor of matter is the only source of the gravitational field. In that case, the dynamics can be entirely expressed in terms of the metric, which locally accounts for the curvature of space-time. Even though for a macroscopic random distribution of elementary particles with spin, the expectation value of the spin vanishes, the variance does not vanish. To take into account all the local degrees of freedom of the Poincare gauge, there has to be a spin source of the gravitational field. The hypothesis made by Sciama (1962) is the existence of a spin density tensor acting as a material source of the rotational field. The rotational field can be entirely expressed in terms of the antisymmetric part of the connection called torsion, which is independent of the metric.

The EC theory extends Einstein's theory of GR in a natural way by including the spin properties of matter and their influence on the geometrical structure of space-time, which could be summarised as follows: "mass bends space-time and spin twists it". By removing the symmetry requirement on the two lower indices of the connection, Cartan (1922) showed that the dynamics is no longer entirely determined by the metric; the antisymmetric part of the connection called torsion became an independent dynamical variable. Besides the energy-momentum of the matter content sourcing curvature, its spin was later postulated by Sciama (1962) to be the source of torsion. As mentioned by Hehl *et al.* (1976), the EC theory locally satisfies the Poincaré symmetry accounting for rotational degrees of freedom associated with curvature and translational degrees of freedom linked to torsion.

Weyssenhoff & Raabe (1947) initiated a careful study of the behaviour of perfect fluids with spin. In order to build cosmological models based on the EC theory, Obukhov & Korotky (1987) extended their work. They showed, in particular, that by assuming the Frenkel condition the model reduces to the description of an effective fluid in GR where the effective stress-energy momentum tensor contains some additional spin squared terms. Note that the Frenkel condition arises naturally when performing a rigorous variation of the action. It simply means that the spin pseudovector is spacelike in the fluid rest frame.

As Puetzfeld & Chen (2004) point out, there are an increasing number of theoretical reasons for studying cosmological models based on a non-Riemannian

geometry, as some key features of the current concordance model such as dark matter, dark energy and in particular inflation still need to be explained. The Weyssenhoff fluid, for example, seems a promising candidate to describe cosmological inflation in a geometrical manner without using scalar fields, which have not yet been observed. This promising behaviour may arise from the spin density squared terms contained within the effective stress energy momentum tensor derived by Obukhov & Korotky (1987), since these spin contributions dominate the dynamics at early times. Although the Weyssenhoff fluid is expected to leave the late time dynamics unchanged, making it an unsuitable candidate to describe dark energy, it may still therefore significantly affect the early time evolution of the fluid.

In this chapter, we restricted our study to the formal derivation of the dynamical relations for an effective Weyssenhoff fluid. A detailed study of the large scales dynamics of such a fluid in an attempt to get a spin based inflation will be pursued in *Chapter* 4. To remain as general as possible we chose not to perform in this dissertation a first- or second-order perturbation analysis for a particular class of models, although it would be interesting to pursue such a study in further work. The dynamics of such a fluid in a $1+3$ covariant approach has been studied previously in a cosmological context by Palle (1999). However, the use of effective GR relations in conjunction with EC identities is rather opaque in this work, and also certain length scales are excluded from the analysis making a new study, which considers all length scales, appropriate.

In the standard GR theory, the $1+3$ covariant approach leads to six propagation equations and six constraint equations. These give respectively the time and spatial covariant derivatives of the set of dynamical variables, which are the energy density ρ, the expansion rate Θ, the shear density σ, the vorticity density ω, the 'electric' part of the Weyl tensor E and the 'magnetic' part of the Weyl tensor H. The Weyssenhoff fluid is described by an effective GR theory, where the additional degrees of freedom due to torsion are entirely determined by the spin density S. Therefore, in addition to the spin density modifying the dynamical equations for the six standard variables, we also expect to find additional dynamical relations.

The structure of this chapter is as follows. In *Section* 3.1, we introduce the notion of torsion and interpret it geometrically. In *Section* 3.2, we briefly outline the EC theory. In *Section* 3.3, we show how the EC theory can be recast as an effective GR theory. In *Section* 3.4 we give a concise description of a Weyssenhoff fluid. *Section* 3.5 is devoted to the Weyssenhoff fluid dynamical analysis using the $1+3$ covariant and gauge-invariant formalism outlined in *Section* 1.1. The consistency of the particular case with zero vorticity and peculiar acceleration ($\omega = a = 0$) is established by evolving the constraints in *Section* 3.6. The last section draws a comparison with Palle's results.

3.1 Torsion

The effect of the spin density tensor is to locally induce torsion in the structure of space-time. The torsion tensor $T^a{}_{bc}$ is defined as the antisymmetric part of the affine connection $\tilde{\Gamma}^a{}_{bc}$,

$$T^a{}_{bc} = \tilde{\Gamma}^a{}_{[bc]} = \frac{1}{2}\left(\tilde{\Gamma}^a{}_{bc} - \tilde{\Gamma}^a{}_{cb}\right) \ , \tag{3.1}$$

which vanishes in GR since the connection is assumed to be symmetric in its two lower indices. Note that the tilde denotes an EC geometrical object to distinguish it from an effective GR object. In a non-Riemanian manifold, the connection is not symmetric with respect to its lower indices. For such a manifold, the analytic expression for the EC connection $\tilde{\Gamma}^a{}_{bc}$ follows from the definition of the infinitesimal parallel transport of a vector V^a along a curve with a tangent vector t^c,

$$t^c \tilde{\nabla}_c V^a = t^c \left(\partial_c V^a + \tilde{\Gamma}^a{}_{bc} V^b\right) = 0 \ , \tag{3.2}$$

where we adopt the same convention as Obukhov & Korotky (1987). In order to recover the other convention adopted by Schouten (1954), the indices b and c have to be permuted in the definition of the connection (3.2). Note that for a Riemanian manifold both conventions are strictly equivalent since the connection is symmetric with respect to its lower indices.

To get some new insight into the geometrical significance of torsion we now interpret the torsion tensor in geometrical terms following the approach of Hammond (2002). We consider transporting the infinitesimal vector χ^a along ζ^a, and

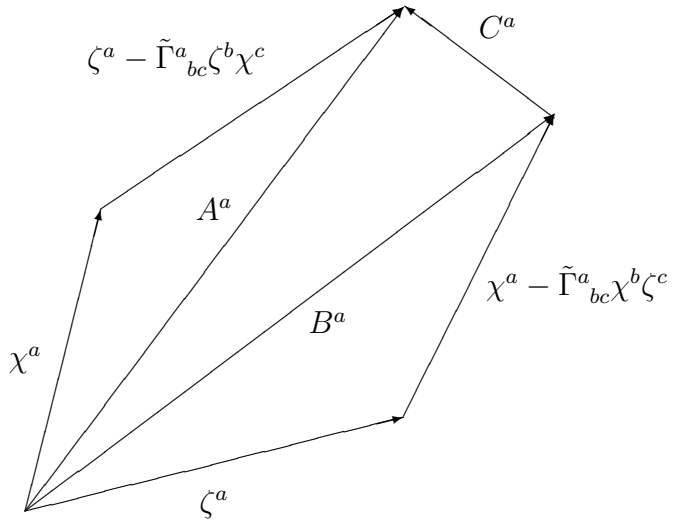

Figure 3.1: Parallel transport of ζ^a along χ^a and vice versa. The non-closure C^a is proportional to the torsion $T^a{}_{bc}\chi^b\zeta^c$.

compare that to transporting ζ^a along χ^a. Suppose we define A^a to be the vector resulting from parallel transporting ζ^a along χ^a, and B^a the one resulting from parallel transporting χ^a along ζ^a, using (3.2), we obtain

$$\begin{aligned} A^a &= \chi^a + \zeta^a - \tilde{\Gamma}^a{}_{bc}\zeta^b\chi^c \\ B^a &= \zeta^a + \chi^a - \tilde{\Gamma}^a{}_{bc}\chi^b\zeta^c \ . \end{aligned} \tag{3.3}$$

The difference between these infinitesimal parallel transported vectors C^a is proportional to the contracted torsion tensor (3.1),

$$C^a = A^a - B^a = 2T^a{}_{bc}\chi^b\zeta^c. \tag{3.4}$$

From a geometrical point of view, torsion twists space-time such that parallelograms do not close any more as shown in *Figure* 3.1.

The EC theory can be extended to include non-metricity since the covariant derivative of the metric does not necessarily vanish according to,

$$\tilde{\nabla}_a g_{bc} \equiv M_{abc} \ , \tag{3.5}$$

where M_{abc} is the non-metricity tensor. The four dimensional manifold X_4 includes non-metricity, torsion and curvature. For a vanishing nonmetricity, X_4 reduces to the Weitzenboeck manifold U_4. In absence of either torsion or curvature, the resulting manifolds are respectively the Riemannian manifold V_4 and the Teleparallel manifold T_4. In absence of curvature and torsion, the Minkowski manifold M_4 is recovered.

Even if non-metricity seems an interesting mathematical generalisation for a gravitation theory, it is not compatible with local Poincaré invariance. In order for lengths and angles to be invariant under parallel transport, the non-metricity has to vanish, as mentioned by Hehl *et al.* (1976). Therefore, we impose the metricity condition,

$$\tilde{\nabla}_a g_{bc} = 0 \ , \tag{3.6}$$

which leaves us with torsion and curvature.

The effects of torsion are not able to affect significantly the physics of the observable universe. In fact, the densities required for spin density to dominate the dynamics can only be reached in the very early universe so that cosmology is the only viable approach to test torsion as explained by Capozziello & Stornaiolo (1998).

3.2 Einstein-Cartan theory

In order to find a proper description of a Weyssenhoff fluid, we first have to determine the EC field equations. The gauge group associated with the EC theory is the Poincaré group as mentioned by Hehl *et al.* (1976). This is easy to understand as the asymmetry of the connection requires an affine generalisation of the Lorentz group which is precisely the Poincaré group. Under a Poincaré transformation, a contravariant vector x^a transforms as,

$$x'^a = \Lambda^a{}_b x^b + a^b \ , \tag{3.7}$$

where $\Lambda^a{}_b$ is an infinitesimal Lorentz transformation and a^a an arbitrary contravariant vector. In the following, lower case indices refer to a holonomic coordinate basis, while capital indices denote an arbitrary non-holonomic orthonormal basis.

The gauge theory approach has an intrinsic elegance since it can not only be applied to gravity but also to quantum field theory and is therefore a promising framework for the unification of the physical laws. In the Poincaré gauge theory of gravity, the gravitational field is described by the tetrad field ${e_a}^A$ and the local spin connection $\tilde{\omega}^{AB}{}_a$. The spin connection is antisymmetric in its capital case indices, $\tilde{\omega}^{AB}{}_a = -\tilde{\omega}^{BA}{}_a$, and the inverse of the tetrad is given by $e^a{}_A$, such that $e^a{}_A {e_a}^B = \delta^B_A$ and $e^a{}_A {e_b}^A = \delta^a_b$. The geometrical structure of U_4 – i.e. the metric g_{ab} and the EC connection $\tilde{\Gamma}^a{}_{bc}$ – is completely determined by the tetrad (translational field) and the spin connection (rotational field) according to,

$$g_{ab} = {e_a}^A {e_b}^B \eta_{AB} \ , \tag{3.8}$$

$$\tilde{\Gamma}^a{}_{bc} = e^a{}_A \tilde{\omega}^A{}_{Bc} {e_b}^B + e^a{}_A \partial_c {e_b}^A \ . \tag{3.9}$$

Using the gauge relations (3.8) and (3.9), the torsion tensor (3.1) can be rewritten in terms of the translational and rotational fields,

$$Q^A{}_{ab} = {e_c}^A \tilde{\Gamma}^c{}_{[ab]} = -\tfrac{1}{2}\left(\partial_a {e_b}^A - \partial_b {e_a}^A + \tilde{\omega}^A{}_{Ba} {e_b}^B - \tilde{\omega}^A{}_{Bb} {e_a}^B\right) \ . \tag{3.10}$$

The metric and the connection are assumed to be compatible, which means that the non-metricity vanishes (3.6) and implies that the EC connection $\tilde{\Gamma}^a{}_{bc}$ can be decomposed in terms of the Levi-Civita connection $\Gamma^a{}_{bc}$ and the contortion tensor $K^a{}_{bc}$ as,

$$\tilde{\Gamma}^a{}_{bc} = \Gamma^a{}_{bc} - K^a{}_{bc} \ , \tag{3.11}$$

where,

$$\Gamma^a{}_{bc} = \tfrac{1}{2} g^{ad}(\partial_b g_{dc} + \partial_c g_{bd} - \partial_d g_{bc}) \ ,$$
$$K^a{}_{bc} = -T^a{}_{bc} - T_{bc}{}^a - T_{cb}{}^a \ .$$

The curvature is described by the Riemann-Cartan tensor and its contractions, i.e. the Ricci-Cartan tensor and the Ricci-Cartan scalar,

$$\tilde{R}^A{}_{Bab} = \partial_a \tilde{\omega}^A{}_{Bb} - \partial_b \tilde{\omega}^A{}_{Ba} + \tilde{\omega}^C{}_{Bb} \tilde{\omega}^A{}_{Ca} - \tilde{\omega}^C{}_{Ba} \tilde{\omega}^A{}_{Cb} \ , \tag{3.12}$$

$$\tilde{R}_{ab} = \tilde{R}^c{}_{acb} = e^c{}_A {e_a}^B \tilde{R}^A{}_{Bcb} \ , \tag{3.13}$$

$$\tilde{\mathcal{R}} = \tilde{R}^{cb}{}_{cb} = e^c{}_A e^b{}_C \eta^{CB} \tilde{R}^A{}_{Bcb} \ . \tag{3.14}$$

where we used the same conventions as Obukhov & Korotky (1987). The field equations of the EC theory are derived from the action S defined on a space-time manifold $\mathcal{M}$ as,

$$S = \int_{\mathcal{M}} d^4x \left[\frac{e}{2\kappa} \left(\tilde{\mathcal{R}} - 2\Lambda \right) + \mathcal{L}_m \right], \tag{3.15}$$

where $\kappa = 8\pi G/c^4$, $e = \det(e_a{}^A)$, Λ is the cosmological constant and $\mathcal{L}_m = \mathcal{L}_m(e_a{}^A, \tilde{\omega}^{AB}{}_a, \phi_m)$ is the Lagrangian density of the matter fields ϕ_m. Varying the action (3.15) independently for $e_a{}^A$ and $\tilde{\omega}^{AB}{}_a$, the field equations are respectively found to be,

$$\tilde{R}^a{}_A - \tfrac{1}{2} e^a{}_A \tilde{\mathcal{R}} + e^a{}_A \Lambda = \kappa \tilde{T}^a{}_A \ , \tag{3.16}$$

$$T^a{}_{AB} + 2e^a{}_{[A} T_{B]} = \kappa S^a{}_{AB} \ , \tag{3.17}$$

where $T_B = T^a{}_{Ba}$ is the torsion trace, and the material sources of the gravitational field are respectively the energy-momentum and the spin density tensors defined as,

$$\tilde{T}^a{}_A \equiv \frac{1}{e} \frac{\delta \mathcal{L}_m}{\delta e_a{}^A} \ , \tag{3.18}$$

$$S^a{}_{AB} \equiv \frac{1}{e} \frac{\delta \mathcal{L}_m}{\delta \tilde{\omega}^{AB}{}_a} \ . \tag{3.19}$$

These source terms are the functional tensors of the EC classical field theory obtained by variation of the action S. They should not be confused with the corresponding canonical tensors derived from Noether's theorem since these two kinds of tensors may differ in an EC framework.

It is important to mention that Cartan (1922) initially postulated the orbital angular momentum tensor to be the source of torsion. After the successful introduction of the spin as an intrinsic angular momentum tensor by Uhlenbeck & Goudsmit (1925), Sciama (1962) extended Cartan's ideas by assuming the spin density tensor to be the source of torsion. Although Sciama's postulate became the new paradigm of the Einstein-Cartan theory, there is no theoretical reason to discard Cartan's initial insight. Since the source of curvature is the energy-momentum tensor, which is a function of the rest energy and the translational kinetic energy, it seems conceptually appealing to postulate, by analogy with the

translational case, the total angular momentum, which is a function of the intrinsic angular momentum and the orbital angular momentum, as the source of torsion. It would be interesting to pursue such an idea, but we will not do so in this dissertation. Instead, we will restrict our analysis to Sciama's postulate.

The translational field equation (3.16) can be recast in terms of purely holonomic coordinates and decomposed into symmetric and anti-symmetric parts,

$$\tilde{R}_{(ab)} - \tfrac{1}{2} g_{ab} \tilde{\mathcal{R}} + g_{ab}\Lambda = \kappa \tilde{T}_{(ab)} \ , \tag{3.20}$$

$$\tilde{R}_{[ab]} = \kappa \tilde{T}_{[ab]} \ . \tag{3.21}$$

In is useful to established geometrical identities for the Riemann and Ricci tensor. Using the definition of the Riemann tensor (3.12), the Riemann cyclic identity is found to be,

$$\tilde{R}^{a}{}_{[bcd]} = 2\tilde{\nabla}_{[b} T^{a}{}_{cd]} + 4T^{e}{}_{[bc} T^{a}{}_{d]e} \ . \tag{3.22}$$

Contracting the cyclic identity with respect to a and c yields the antisymmetric part of the Ricci tensor,

$$\tilde{R}_{[ab]} = \left(\tilde{\nabla}_{c} - 2T_{c}\right)\left(T^{c}{}_{ab} + 2\delta^{c}{}_{[a} T_{b]}\right) \ . \tag{3.23}$$

3.3 EC theory as an effective GR theory

Given that the EC rotational field equation (3.17) is an algebraic coupling between the torsion tensor and its material source (i.e. the spin density tensor), the torsion tensor $T^{a}{}_{bc}$ can be recast entirely in terms of the spin density tensor $S^{a}{}_{bc}$ and its trace $\mathcal{S}_{c}$ according to,

$$T^{a}{}_{bc} = \kappa \left(S^{a}{}_{bc} + \delta^{a}{}_{[b}\mathcal{S}_{c]}\right) \ , \tag{3.24}$$

where $\mathcal{S}_{c} = S^{a}{}_{ca}$ and $\mathcal{S}_{c} = -2\kappa T_{c}$. Using the rotational field equation (3.24), the expression (3.11) for the EC connection $\tilde{\Gamma}^{a}{}_{bc}$ can be recast in terms of the GR Levi-Civita connection $\Gamma^{a}{}_{bc}$ with additional spin density terms,

$$\tilde{\Gamma}^{a}{}_{bc} = \Gamma^{a}{}_{bc} + \kappa \left(S^{a}{}_{bc} + S_{bc}{}^{a} + S_{cb}{}^{a} - \delta^{a}{}_{c}\mathcal{S}_{b} + g_{bc}\mathcal{S}^{a}\right) \ . \tag{3.25}$$

Since the EC curvature tensors are entirely described by the EC connection, they can be decomposed into the corresponding GR tensors with additional spin

terms. Using the EC connection (3.25), the LHS of the symmetric translational field equation (3.20) reduces to,

$$\begin{aligned}\tilde{R}_{(ab)} - \frac{1}{2}g_{ab}\tilde{\mathcal{R}} = R_{ab} - \frac{1}{2}g_{ab}\mathcal{R} + 2\kappa\nabla_c S_{(ab)}{}^c \\ + 2\kappa^2\left(S_{(ab)}{}^c\mathcal{S}_c + S_{(a}{}^{cd}S_{|dc|b)} + \frac{1}{2}S_{(a}{}^{cd}S_{b)cd}\right) \\ + g_{ab}\kappa^2\left(\mathcal{S}_c\mathcal{S}^c - S_{cde}S^{edc} - \frac{1}{2}S_{cde}S^{cde}\right) .\end{aligned} \tag{3.26}$$

Similarly, using the contracted cyclic identity (3.23), the rotational field equation (3.24) and the EC connection (3.25), the LHS of the antisymmetric translational field equation (3.21) becomes,

$$\tilde{R}_{[ab]} = \kappa\nabla_c S^c{}_{ab} + 2\kappa^2\left(S_{[a}{}^{cd}S_{|cd|b]} + S^c{}_{ab}\mathcal{S}_c - \frac{1}{2}S_{[ab]}{}^c\mathcal{S}_c\right) . \tag{3.27}$$

The EC stress-energy momentum tensor $\tilde{T}_{ab}$ can also formally be decomposed into the sum of its GR analog T_{ab} and an effective tensor τ_{ab} according to,

$$\tilde{T}_{ab} = T_{ab} + \tau_{ab} , \tag{3.28}$$

where τ_{ab} is a function of the spin density tensor $S^c{}_{ab}$, which depends on the fluid model.

Having decomposed the geometric and material parts of the EC field equation into GR tensors with additional spin density tensorial terms (3.26), the symmetric EC field equation (3.20) is recast now as an effective GR field equation,

$$R_{ab} - \frac{1}{2}g_{ab}\mathcal{R} = \kappa T^s_{ab} ,$$

where the effective stress-energy momentum tensor T^s_{ab} contains the spin terms and is related to the GR stress-energy momentum tensor T_{ab} by,

$$\begin{aligned}T^s_{ab} = T_{ab} + \tau_{(ab)} - 2\nabla_c S_{(ab)}{}^c - 2\kappa\left(S_{(ab)}{}^c\mathcal{S}_c + S_{(a}{}^{cd}S_{|dc|b)} + \frac{1}{2}S_{(a}{}^{cd}S_{b)cd}\right) \\ - g_{ab}\kappa\left(\mathcal{S}_c\mathcal{S}^c - S_{cde}S^{edc} - \frac{1}{2}S_{cde}S^{cde}\right) .\end{aligned} \tag{3.29}$$

The antisymmetric EC field equation (3.21) has no GR equivalent. Using the decomposition (3.27), it can be recast in terms of the GR covariant derivative

as a GR spin field equation describing the time evolution of the material spin density source according to,

$$\tau_{[ab]} = \nabla_c S^c{}_{ab} + 2\kappa \left(S_{[a}{}^{cd} S_{|cd|b]} + S^c{}_{ab} \mathcal{S}_c - \frac{1}{2} S_{[ab]}{}^c \mathcal{S}_c \right) \ . \tag{3.30}$$

3.3.1 Perfect fluid with spin

In order to determine the dynamics of a model in an effective GR framework, we need to specify the nature of the matter content. We consider the particular case of a perfect fluid with spin, which is the EC generalisation of a perfect fluid in GR. By analogy with a perfect fluid in GR, following the approach of Obukhov & Korotky (1987), we postulate the EC stress-energy momentum tensor of a perfect fluid with spin to be defined as,

$$\tilde{T}_{ab} \equiv u_a \tilde{P}_b + p \left(g_{ab} + u_a u_b \right) \ , \tag{3.31}$$

where u^a is the 4-velocity of the fluid, p is the pressure of the fluid and $\tilde{P}_a$ is the EC 4-momentum, which is related to the GR 4-momentum P_a by,

$$u_a \tilde{P}^a = u_a P^a = -\rho \ , \tag{3.32}$$

where ρ is the energy density of the fluid.

The antisymmetric part of the EC energy-momentum tensor τ_{ab} represents the angular momentum tensor, which is recast in terms of the EC 4-momentum $\tilde{P}_b$ as,

$$\tau_{[ab]} = u_{[a} \tilde{P}_{b]} \ . \tag{3.33}$$

By contracting the angular momentum conservation equation (3.30) with the 4-velocity u^a and using the angular momentum identity (3.33) and the contraction relation (3.32), the EC 4-momentum $\tilde{P}_b$ is found to be,

$$\tilde{P}_b = \rho u_b - 2u^a \left[\nabla_c S^c{}_{ab} + 2\kappa \left(S_{[a}{}^{cd} S_{|cd|b]} + S^c{}_{ab} \mathcal{S}_c - \frac{1}{2} S_{[ab]}{}^c \mathcal{S}_c \right) \right] \ . \tag{3.34}$$

The EC stress energy momentum tensor of a perfect fluid with spin $\tilde{T}_{ab}$ is obtained by substituting the EC 4-momentum $\tilde{P}_b$ into (3.31) according to,

$$\begin{aligned} \tilde{T}_{ab} = {} & \rho u_a u_b + p \left(g_{ab} + u_a u_b \right) \\ & - 2u_a u^d \left[\nabla_c S^c{}_{db} + 2\kappa \left(S_{[d}{}^{ce} S_{|ce|b]} + S^c{}_{db} \mathcal{S}_c - \frac{1}{2} S_{[db]}{}^c \mathcal{S}_c \right) \right] \ . \end{aligned} \tag{3.35}$$

From the effective decomposition (3.28) and the GR stress energy momentum tensor T_{ab} of a perfect fluid (2.9), it follows that the effective tensor τ_{ab} yields,

$$\tau_{ab} = -2u_a u^d \left[\nabla_c S^c{}_{db} + 2\kappa \left(S_{[d}{}^{ce} S_{|ce|b]} + S^c{}_{db} \mathcal{S}_c - \frac{1}{2} S_{[db]}{}^c \mathcal{S}_c \right) \right] . \tag{3.36}$$

3.4 Weyssenhoff fluid description

The Weyssenhoff fluid is a continuous macroscopic medium, which is characterized on microscopic scales by the spin of the matter fields. The spin density of matter is described by an antisymmetric tensor,

$$S_{ab} = -S_{ba} , \tag{3.37}$$

and has been postulated by Obukhov & Korotky (1987) to be related to the source of torsion according to,

$$S^a{}_{bc} = u^a S_{bc} . \tag{3.38}$$

The Frenkel condition requires the intrinsic spin of a matter field to be spacelike in the rest frame of the fluid,

$$S_{ab} u^b = 0 . \tag{3.39}$$

This condition arises naturally from a rigorous variation of the matter Lagrangian $\mathcal{L}_m$ as shown by Obukhov & Korotky (1987).

The Frenkel condition implies that the spin density trace vanishes,

$$\mathcal{S}_a = 0 , \tag{3.40}$$

and therefore the algebraic coupling (3.24) reduces to,

$$T^a{}_{bc} = \kappa u^a S_{bc} . \tag{3.41}$$

The Weyssenhoff fluid is an EC perfect fluid with spin, as mentioned by Obukhov & Korotky (1987), which can be recast as an effective GR perfect fluid with spin, as shown in *Section* 3.3. Using the Frenkel condition, the analytical expression for the effective GR field equation (3.29) and the spin field equation (3.30) are considerably reduced. In order to simplify the notation and

clarify the physical interpretation of the dynamics, it is useful to introduce a spin density pseudovector S^a and a spin density scalar S defined respectively as,

$$S^a = \tfrac{1}{2}\varepsilon^{abc}S_{bc} \ , \tag{3.42}$$

$$S^2 = \tfrac{1}{2}S_{ab}S^{ab} \geq 0 \ , \ . \tag{3.43}$$

Substituting the GR stress energy momentum tensor T_{ab} of a perfect fluid (2.9) and the symmetric part of the effective tensor τ_{ab} (3.36) into the effective GR field equation (3.29), and using the Weyssenhoff spin density tensor decomposition (3.38) and the Frenkel condition (3.39), the effective GR field equation of a Weyssenhoff fluid is found to be,

$$R_{ab} - \tfrac{1}{2}g_{ab}\mathcal{R} = \kappa T^s_{ab} \ ,$$

where the effective stress energy momentum tensor of the fluid is given by,

$$T^s_{ab} = (\rho_s + p_s)u_a u_b + p_s g_{ab} - 2\left(g^{cd} - u^c u^d\right)\nabla_c\left[u_{(a}S_{b)d}\right] \ , \tag{3.44}$$

with effective energy density and pressure of the form,

$$\rho_s = \rho - \kappa S^2 + \kappa^{-1}\Lambda \ , \qquad p_s = p - \kappa S^2 - \kappa^{-1}\Lambda \ , \tag{3.45}$$

satisfying the physical equation-of-state,

$$p = w\rho \ , \tag{3.46}$$

where w is the equation-of-state parameter. Note that the sign differences with Obukhov & Korotky (1987) in the analytical expression for the effective field equation (3.44) are due to an opposite choice of metric signature.

Similarly, by substituting the antisymmetric part of the effective tensor τ_{ab} (3.36) into the spin field equation (3.30), and using the Weyssenhoff spin density tensor decomposition (3.38) and the Frenkel condition (3.39), the spin field equation of a Weyssenhoff fluid is found to be,

$$\nabla_a\left(u^a S_{bc}\right) = -2u^d u_{[b}\nabla_{|a}\left(u^a S_{d|c]}\right) \ . \tag{3.47}$$

3.5 Weyssenhoff fluid dynamics using a 1+3 covariant approach

We will now use the $1+3$ covariant approach to describe accurately the dynamics of a Weyssenhoff fluid in GR on all scales and in a non-perturbative way. Once the dynamical evolution is entirely determined, a perturbation analysis can be performed for any given class of models according to their symmetries. We will not perform a perturbation analysis of a Weyssenhoff fluid in this dissertation, but such an analysis would be a natural and interesting extension of our study. In a cosmological context, we would require the cosmological fluid to be highly symmetric on large scales but allow for generic inhomogeneities on small scales. This is necessary to provide an accurate enough description of the observable universe accounting for its homogeneity and isotropy on large scales as well as for all the complicated structures it contains on small scales.

In GR, the Weyssenhoff fluid dynamics is actually a generalisation of the dynamics of a perfect fluid, where the effective energy density ρ_s and pressure p_s contain a spin density squared S^2 correction term, and the stress energy momentum tensor T^s_{ab} incorporates an additional spin divergence term. The new contribution to the effective dynamics comes from the spin field equation (3.47). Thus, the dynamics of a perfect fluid is recovered for a vanishing spin density.

The dynamical model of a perfect fluid with spin is fully determined by its matter content − including the spin properties of the particles − and its curvature. The matter content of the Weyssenhoff fluid is described by the effective stress-energy momentum tensor (3.44). Using the $1+3$ formalism, it can be recast as,

$$T^s_{ab} = (\rho_s + 4\omega^c S_c)\, u_a u_b + p_s h_{ab} - 2u_{(a} D^c S_{b)c} - 4u_{(a} a^c S_{b)c} - 2\sigma_{(a}{}^c S_{b)c} + 2\omega_{(a}{}^c S_{b)c} \,. \tag{3.48}$$

The physical interpretation of the Weyssenhoff fluid now becomes more transparent. The terms containing the effective energy density ρ_s and pressure p_s represent the behaviour of an effective perfect fluid, where ρ_s and p_s account for the spin contributions. The other terms describe how the peculiar acceleration of the fluid a_b and the fluid anisotropies − described by the rate-of-shear σ_{ab} and

the vorticity ω_{ab} respectively − couple to the spin density S_{ab} and contribute to the effective energy density of the fluid.

The Ricci tensor R_{ab} is simply obtained by substituting the expression (3.48) for the effective stress energy momentum tensor T^{s}_{ab} into the Einstein field equations (3.44),

$$\begin{aligned} R_{ab} = {} & \tfrac{\kappa}{2}\left(\rho_s + 3p_s + 8\omega^c S_c\right) u_a u_b + \tfrac{\kappa}{2}\left(\rho_s - p_s\right) h_{ab} \\ & - 2\kappa u_{(a} D^c S_{b)c} - 4\kappa u_{(a} a^c S_{b)c} - 2\kappa \sigma_{(a}{}^c S_{b)c} + 2\kappa \omega_{(a}{}^c S_{b)c} \ . \end{aligned} \tag{3.49}$$

3.5.1 Riemann tensor decomposition

The Riemann tensor $R^{ab}{}_{cd}$ can be fully split in a 1+3 manner according to (2.14) by using the expression (3.49) for the Ricci tensor R_{ab} and the decomposition of the Weyl tensor $C^{ab}{}_{cd}$ into its electric E_{ab} and magnetic H_{ab} parts. For convenience, the tensor is split into three parts: the spinning perfect fluid part (P), the electric part of the Weyl tensor (E) and the magnetic part of the Weyl tensor (H). The decomposition yields,

$$R^{ab}{}_{cd} = R^{ab}_{P\,cd} + R^{ab}_{E\,cd} + R^{ab}_{H\,cd} \ , \tag{3.50}$$

where

$$\begin{aligned} R^{ab}_{P\,cd} = {} & \tfrac{2}{3}\kappa\left(\rho_s + 3p_s + 12\omega^e S_e\right) u^{[a} u_{[c} h^{b]}{}_{d]} + \tfrac{2}{3}\kappa\rho_s h^{[a}{}_{[c} h^{b]}{}_{d]} \\ & - 2\kappa\left(h^{[a}{}_{[c} + u^{[a} u_{[c}\right)\left[u^{b]} D^e S_{d]e} + u_{d]} D_e S^{b]e} + 2u^{b]} a^e S_{d]e} + 2u_{d]} a_e S^{b]e}\right. \\ & \left. + \sigma^{b]e} S_{d]e} + \sigma_{d]e} S^{b]e} - \omega^{b]e} S_{d]e} - \omega_{d]e} S^{b]e}\right] \ , \\ R^{ab}_{E\,cd} = {} & C^{ab}_{E\,cd} = 4u^{[a} u_{[c} E^{b]}{}_{d]} + 4h^{[a}{}_{[c} E^{b]}{}_{d]} \ , \\ R^{ab}_{H\,cd} = {} & C^{ab}_{H\,cd} = 2\varepsilon^{abe} u_{[c} H_{d]e} + 2\varepsilon_{cde} u^{[a} H^{b]e} \ . \end{aligned}$$

Note that for a vanishing spin density (i.e. in absence of torsion), we recover the results of *Chapter* 2. This is also the case for every propagation and constraint equation describing the dynamics of the Weyssenhoff fluid because these expressions are projections of effective GR identities which are based on the Riemann tensor and its contractions.

We now derive the dynamical equations obtained by projection of the Ricci identities, the Bianchi identities, once- and twice-contracted, and the spin field equation. We discuss each set of identities in turn.

3.5.2 Ricci identities

The first set of dynamical equations arises from the Ricci identities (2.27). To extract the physical information stored in the Ricci identities, the latter have to be projected along the worldlines u^a and on the orthogonal spatial hypersurfaces $h^a{}_b$. The non-vanishing projections yield the propagation equations and the constraint equations respectively,

$$u^a h^b{}_e h^c{}_f \left(\nabla_{[a}\nabla_{b]}u_c - \tfrac{1}{2}R_{[ab]cd}u^d\right) = 0 \ , \tag{3.51}$$

$$\varepsilon^{ab}{}_e h^c{}_f \left(\nabla_{[a}\nabla_{b]}u_c - \tfrac{1}{2}R_{[ab]cd}u^d\right) = 0 \ , \tag{3.52}$$

where the latter have been expressed in terms of rank-2 tensors by duality ($\varepsilon^{ab}{}_e$) without loss of information.

The Ricci identities can be further split by separating the propagation and constraint equations into their trace part (T), symmetric trace-free part (STF) and antisymmetric trace-free part (ATF). The sets of equations are explicitly determined by the kinematics of the $1+3$ covariant formalism (1.11) and by substituting the Riemann tensor decomposition (3.50) into the projections yielding the propagation (3.51) and constraint (3.52) equations respectively before splitting them into parts.

The propagation equations are found to be as follows.

- The Raychaudhuri equation (T),

$$\dot{\Theta} = -\tfrac{1}{3}\Theta^2 + D_b a^b + 2\left(a^2 - \sigma^2 + \omega^2\right) - \tfrac{\kappa}{2}\left(\rho_s + 3p_s + 8\omega^b S_b\right) \ , \tag{3.53}$$

  which is the basic dynamical equation of a perfect fluid with spin in this system. The last term on the RHS describes how the interaction between the spin density and the vorticity density affects the large scale dynamics. The physical meaning of this term is clear: the energy required to align the spin with the vorticity will act like a brake on the expansion, leading to the presence of this damping term in the Raychaudhuri equation.

- The vorticity propagation equation (ATF),

$$\dot{\omega}_{\langle a\rangle} = -\tfrac{2}{3}\Theta\,\omega_a + \tfrac{1}{2}\operatorname{curl} a_a + \sigma_a{}^b\omega_b \ , \tag{3.54}$$

which shows how vorticity conservation follows for a perfect fluid. Note that there is no spin contribution, which means that torsion does not explicitly affect the vorticity evolution, although the effect of spin on the other dynamical variables must be taken into account.

- The shear propagation equation (STF),

$$\begin{aligned}\dot{\sigma}_{\langle ab\rangle} = &-\tfrac{2}{3}\Theta\,\sigma_{ab} + D_{\langle a}a_{b\rangle} + a_{\langle a}a_{b\rangle} - \sigma_{\langle a}{}^{c}\sigma_{b\rangle c} - \omega_{\langle a}\omega_{b\rangle} - E_{ab} \\ &- \kappa\left(\sigma_{\langle a}{}^{c}S_{b\rangle c} + \omega_{\langle a}S_{b\rangle}\right) \ ,\end{aligned} \tag{3.55}$$

which shows how the tidal gravitational field E_{ab} and the spin density S_{ab} induce shear. The coupling between the spin density, the shear density and the vorticity contributes to the fluid anisotropies by increasing the rate of shear.

The constraint equations are given by the following relations.

- The vorticity divergence constraint (T),

$$D_b\omega^b = a_b\omega^b \ . \tag{3.56}$$

This constraint simply expresses the fact that, in presence of a peculiar acceleration induced by a non-gravitational force due to the fluid dynamics, the spatial variation of vorticity is proportional to the vorticity.

- The shear and spin divergence constraint (ATF),

$$D_b\left(\sigma_a{}^b + \omega_a{}^b - \kappa S_a{}^b\right) - \tfrac{2}{3}D_a\Theta = -2a_b\left(\omega_a{}^b - \kappa S_a{}^b\right) \ . \tag{3.57}$$

Using the vorticity constraint (3.56), the shear and spin density constraint (3.57) can be recast as,

$$D_b\left(\sigma_a{}^b - \kappa S_a{}^b\right) - \tfrac{2}{3}D_a\Theta = -a_b\left(3\omega_a{}^b - 2\kappa S_a{}^b\right) \ . \tag{3.58}$$

This expression relates the spatial variation of physical quantities, such as the spin density, the rate of shear and the expansion rate on the LHS, to the coupling between the acceleration due to the fluid dynamics and the fluid anisotropies on the RHS.

- The magnetic constraint (STF),

$$H_{ab} = -D_{\langle a}\omega_{b\rangle} - 2a_{\langle a}\omega_{b\rangle} + \operatorname{curl}\sigma_{ab} \ . \tag{3.59}$$

Using the vorticity constraint (3.56), the magnetic constraint (3.59) reduces to,

$$H_{ab} = -3a_{\langle a}\omega_{b\rangle} + \operatorname{curl}\sigma_{ab} \ . \tag{3.60}$$

This constraint shows that the magnetic part of the Weyl tensor is induced by the curl of the shear and the coupling between the acceleration due to the fluid dynamics and the vorticity.

3.5.3 Once-contracted Bianchi identities

The second and third set of dynamical equations are contained in the Bianchi identities (2.43). In a similar manner to the Ricci identities, the information stored in the once-contracted Bianchi identities (2.44) has to be projected on the different hypersurfaces. The projections yield respectively two propagation and two constraint equations,

$$h_{a\langle e}h^{c}{}_{f\rangle}u_b\left(\nabla^d C^{ab}{}_{cd} + \nabla^{[a}R^{b]}{}_{c} + \tfrac{1}{6}\delta_c{}^{[a}\nabla^{b]}\mathcal{R}\right) = 0 \ , \tag{3.61}$$

$$\varepsilon_{ab\langle e}h^{c}{}_{f\rangle}\left(\nabla^d C^{ab}{}_{cd} + \nabla^{[a}R^{b]}{}_{c} + \tfrac{1}{6}\delta_c{}^{[a}\nabla^{b]}\mathcal{R}\right) = 0 \ , \tag{3.62}$$

$$h_{ae}h^{c}{}_{b}\left(\nabla^d C^{ab}{}_{cd} + \nabla^{[a}R^{b]}{}_{c} + \tfrac{1}{6}\delta_c{}^{[a}\nabla^{b]}\mathcal{R}\right) = 0 \ , \tag{3.63}$$

$$\varepsilon_{eab}u^{c}\left(\nabla^d C^{ab}{}_{cd} + \nabla^{[a}R^{b]}{}_{c} + \tfrac{1}{6}\delta_c{}^{[a}\nabla^{b]}\mathcal{R}\right) = 0 \ . \tag{3.64}$$

The sets of equations are explicitly determined by substituting the expression for the Weyl tensor splitting (3.50) and the Ricci tensor (3.49) into the projections of the once-contracted Bianchi identities (3.61)-(3.64).

The propagation equations are found to be as follows.

- The electric propagation equation,

$$\begin{aligned}\dot{E}_{\langle ab\rangle} = \ & -\Theta\, E_{ab} + \operatorname{curl} H_{ab} - \tfrac{\kappa}{2}(\rho_s + p_s)\,\sigma_{ab} \\ & + 3\sigma_{\langle a}{}^{c}E_{b\rangle c} - \omega_{\langle a}{}^{c}E_{b\rangle c} + 2\varepsilon_{cd\langle a}a^{c}H_{b\rangle}{}^{d} + \kappa\,(S_{\dot{E}})_{\langle ab\rangle} \ ,\end{aligned} \tag{3.65}$$

where

$$(S_{\dot{E}})_{\langle ab\rangle} = {}^{(3)}\!\left(\sigma_{\langle a}{}^{c}S_{b\rangle c} + \omega_{\langle a}S_{b\rangle}\right)^{\cdot} + \tfrac{1}{3}\,\Theta\left(\sigma_{\langle a}{}^{c}S_{b\rangle c} + \omega_{\langle a}S_{b\rangle}\right) + \tfrac{1}{2}\sigma_{cd}\left(\sigma_{\langle a}{}^{c}S_{b\rangle}{}^{d} - \omega_{\langle a}{}^{c}S_{b\rangle}{}^{d}\right) + \tfrac{1}{2}\left(D_{\langle a} + 2a_{\langle a}\right)\left(D^{c}S_{b\rangle c} + 2a^{c}S_{b\rangle c}\right) \ .$$

This equation is similar in form to Maxwell's electric propagation equation in an expanding universe. The $(S_{\dot{E}})_{\langle ab\rangle}$ term on the RHS of relation (3.65) describes how the coupling between the spin density and the fluid anisotropies contributes to the gravitational tidal field E_{ab}.

- The magnetic propagation equation,

$$\dot{H}_{\langle ab\rangle} = -\Theta\, H_{ab} - \operatorname{curl} E_{ab} + 3\sigma_{\langle a}{}^{c}H_{b\rangle c} - \omega_{\langle a}{}^{c}H_{b\rangle c} - 2\varepsilon_{cd\langle a}a^{c}E_{b\rangle}{}^{d} + \kappa\,(S_{\dot{H}})_{\langle ab\rangle} \ , \tag{3.66}$$

where

$$(S_{\dot{H}})_{\langle ab\rangle} = -\tfrac{1}{2}\varepsilon_{cd\langle a}[D^{c}\{(\sigma^{de} - \omega^{de})S_{b\rangle e} + S^{de}(\sigma_{b\rangle e} - \omega_{b\rangle c})\} - (\sigma_{b\rangle}{}^{d} - \omega_{b\rangle}{}^{d})(D_{e}S^{de} + 2a_{e}S^{de}) - \omega^{cd}(D^{e}S_{b\rangle e} + 2a^{e}S_{b\rangle e})] \ .$$

This expression is analogous to Maxwell's magnetic propagation equation in an expanding universe. The $(S_{\dot{H}})_{\langle ab\rangle}$ term on the RHS of this relation (3.66) describe how the coupling between the spin density and the fluid anisotropies contributes to the gravitational tidal field H_{ab}.

In a similar manner to that in which Maxwell's equations describe electrodynamics in an expanding universe, the coupling between the electric (3.65) and magnetic (3.66) propagation equations gives rise to gravitational waves damped by the expansion of the universe.

The constraint equations are given by the following relations.

- The electric constraint equation,

$$D^{b}E_{ab} = \tfrac{\kappa}{3}D_{a}\rho_{s} + 3\omega^{b}H_{ab} + \varepsilon_{abc}\sigma^{b}{}_{d}H^{cd} + \kappa\,(S_{\mathrm{div}E})_{a} \ , \tag{3.67}$$

where

$$(S_{\mathrm{div}E})_{a} = -D_{a}[(\sigma^{bc} - \omega^{bc})S_{bc}] + D^{b}[(\sigma_{\langle a}{}^{c} - \omega_{\langle a}{}^{c})S_{b\rangle c}] + \tfrac{1}{3}\Theta\left(D^{b}S_{ab} + 2a^{b}S_{ab}\right) - \tfrac{1}{2}\sigma_{ab}\left(D_{c}S^{bc} + 2a_{c}S^{bc}\right) \ .$$

This constraint is a vector analogue of the Newtonian Poisson equation. It is similar in form to Maxwell's electric divergence equation. For this gravitational field equation, the source is not the electric charge density but the energy density. The $(S_{\mathrm{div}E})_a$ term on the RHS of expression (3.67) describes how the coupling between the spin density and the fluid anisotropies acts like an effective electric divergence source.

- The magnetic constraint equation,

$$D^b H_{ab} = \kappa\left(\rho_s + p_s\right)\omega_a - 3\omega^b E_{ab} - \varepsilon_{abc}\sigma^b{}_d E^{cd} + \kappa\left(S_{\mathrm{div}H}\right)_a \ , \tag{3.68}$$

where

$$\left(S_{\mathrm{div}H}\right)_a = -\tfrac{1}{2}\varepsilon_{abc}D^b\left(D_e S^{ce} + 2a_e S^{ce}\right) \ .$$

This constraint is analogous to Maxwell's magnetic divergence equation. Unlike for Maxwell's equation, this gravitational field equation has a source term which is the fluid vorticity. The $(S_{\mathrm{div}H})_a$ term on the RHS of expression (3.68) describes how the coupling between the spin density and the fluid anisotropies acts like an effective magnetic divergence source.

3.5.4 Twice-contracted Bianchi identities

The third set of equations is given by the twice-contracted Bianchi identities which represent the conservation of the effective stress energy momentum tensor. They are obtained by performing a second contraction on the once-contracted Bianchi identities (2.44). There are only two possible projections to extract the information stored in the twice-contracted Bianchi identities,

$$u^a\nabla^b T^s_{ab} = 0 \ , \tag{3.69}$$

$$h_c{}^a\nabla^b T^s_{ab} = 0 \ . \tag{3.70}$$

The propagation and constraint equations are explicitly determined by substituting the reduced expression for the stress-energy momentum tensor (3.48) into the two projections of the twice-contracted Bianchi identities (3.69) and (3.70) respectively.

The propagation equation is found to be as follows.

- The effective energy conservation equation,

$$\dot{\rho_s} = -\Theta\ (\rho_s + p_s)\ . \tag{3.71}$$

  Note that for a vanishing spin density this relation reduces to the well-known energy conservation equation determining the evolution of the physical energy density ρ and pressure p.

The constraint equation is given by the following relation.

- The momentum conservation equation,

$$D_a p_s = -\left(\rho_s + p_s\right) a_a + \left(S_p\right)_a\ , \tag{3.72}$$

  where

$$\begin{aligned}\left(S_p\right)_a = {} & 2\left(D^b + a^b\right)\left(\sigma_{(a}{}^c S_{b)c} - \omega_{(a}{}^c S_{b)c}\right) + {}^{(3)}\left(D^c S_{ac} + 2a^c S_{ac}\right)^{\cdot} \\ & + \tfrac{4}{3}\Theta\left(D^c S_{ac} + 2a^c S_{ac}\right) + \left(\sigma_a{}^b - \omega_a{}^b\right)\left(D^c S_{bc} + 2a^c S_{bc}\right)\ .\end{aligned}$$

  The term $\left(S_p\right)_a$ describes how the coupling between the spin density and the fluid anisotropies contributes to the total angular momentum.

3.5.5 Spin dynamics

The last dynamical equation for the evolution of the Weyssenhoff fluid is the spin field equation (3.47). To extract the spin propagation equation, the field equation has to be twice projected on the hypersurface orthogonal to the worldline. By duality, we can write it in terms of the spin density pseudovector S^a without loss of information (3.42), and we obtain:

- The spin propagation equation,

$$\dot{S}_{\langle a\rangle} = -\Theta\, S_a\ . \tag{3.73}$$

  This expression (3.73) can be recast in terms of the spin-density scalar S^2 (3.43) defined as,

$$S^2 = S_a S^a\ . \tag{3.74}$$

It is then simply given by,

$$\dot{S} = -\Theta\, S \ . \tag{3.75}$$

This relation shows that the evolution of the spin density is the same on all scales because it is entirely determined by the volume rate of expansion of the fluid. For consistency, note that this expression implies that the spin density is inversely proportional to the volume of the fluid.

The effective energy conservation equation (3.71) can now be recast in terms of the true (i.e. not effective) energy density and pressure of the fluid by substituting the spin propagation equation (3.75),

$$\dot{\rho} = -\Theta\ (\rho + p)\ \ . \tag{3.76}$$

The effective energy density ρ_s and pressure p_s contain spin density squared S^2 correction terms (3.45). Thus, the spin propagation equation (3.75) and the energy conservation equation (3.76) imply that the spin density will rule entirely the dynamics of the fluid at early times ($\kappa S^2 \gg \rho, p$), whereas, at late times, the spin contribution can safely be neglected ($\kappa S^2 \ll \rho, p$).

In a cosmological context, the spin dominated era might lead to an inflationary behaviour. This promising prospect will be analysed in detail in the next chapter. Given that the matter dominated era is not affected by the spin contribution, the cosmological model thus reduces to the dynamical behaviour of a perfect fluid in GR. Hence, the spin density contribution from the Weyssenhoff fluid is expected to affect significantly the early time evolution of the fluid leaving the late time dynamics unchanged. Therefore, it is not currently promising as a candidate to describe dark energy.

3.6 Consistency of the dynamics for an irrotational Weyssenhoff fluid with no peculiar acceleration

The consistency of the propagation and constraint equations can be verified by evolving the constraints. This is a tedious but straightforward task. To make the

problem tractable, we chose to restrict our attention to the class of models for which the fluid dynamics is described by an irrotational flow (i.e. $\omega_{ab} = 0$) with no peculiar acceleration (i.e. $a^b = 0$). This ensures a hypersurface-orthogonal flow and the existence of a globally defined cosmic time. If the flow is initially irrotational, it will remain so at later times as mentioned by Ellis & van Elst (1999) and as it follows directly from (3.54) in the $a^b = 0$ case.

For each space-time slicing, we can now define the curvature tensors entirely in terms of the spatial hypersurface orthogonal to the worldline. For this purpose, let us define a vector v^a, which is orthogonal to the worldline, and an expansion tensor Θ_{ab} according to,

$$v^a u_a = 0 \ , \qquad \Theta_{ab} = v_{(ab)} = \tfrac{1}{3}\Theta\, h_{ab} + \sigma_{ab} \ . \tag{3.77}$$

The spatial Riemann tensor ${}^{(3)}R_{abcd}$ is related to the Riemann tensor R_{abcd} by

$${}^{(3)}R_{abcd} = h_a{}^e h_b{}^f h_c{}^g h_d{}^h R_{efgh} - \Theta_{ac}\Theta_{bd} + \Theta_{ad}\Theta_{bc} \ . \tag{3.78}$$

The spatial Ricci tensor and scalar can be obtained by contracting the spatial Riemann tensor with the induced spatial metric $h_{\mu\nu}$,

$${}^{(3)}R_{ab} = h^{cd}\,{}^{(3)}R_{acbd} \ , \tag{3.79}$$

$${}^{(3)}\mathcal{R} = h^{ab}h^{cd}\,{}^{(3)}R_{acbd} \ . \tag{3.80}$$

Using (1.11), (3.50), (3.55) and (3.78), these 3-space curvature quantities can be recast respectively as,

$$\begin{aligned} {}^{(3)}R^{ab}{}_{cd} &= \tfrac{2}{3}\kappa h^a{}_{[c}h^b{}_{d]}\rho_s + 4h^a{}_{[c}E^b{}_{d]} - 2\Theta^a{}_{[c}\Theta^b{}_{d]} \\ &\quad - 2\kappa h^{[a}{}_{[c}\left(\Theta_{d]e}S^{b]e} + \Theta^{b]e}S_{d]e}\right) \ , \end{aligned} \tag{3.81}$$

$${}^{(3)}R_{ab} = -\dot{\sigma}_{\langle ab\rangle} - \Theta\,\sigma_{ab} - \kappa\sigma_{\langle a}{}^c S_{b\rangle c} + \tfrac{1}{3}h_{ab}\left(2\kappa\rho_s - \tfrac{2}{3}\Theta^2 + 2\sigma^2\right) \ , \tag{3.82}$$

$${}^{(3)}\mathcal{R} = -\tfrac{2}{3}\Theta^2 + 2\kappa\rho_s + 2\sigma^2 \ . \tag{3.83}$$

3.6.1 Evolution of the constraints

To determine the time evolution of the constraint equations, we shall follow Maartens (1997) and generalise his results to include the presence of spin. For

an irrotational Weyssenhoff fluid in absence of any peculiar acceleration, the propagation equations (3.53), (3.55), (3.65), (3.66), (3.75) and (3.76), denoted by $\mathcal{P}^A = 0$ where $A = \mathbf{0}, \ldots, \mathbf{5}$, reduce to

$$\mathcal{P}^{\mathbf{0}} = \dot{S} + \Theta S \ , \tag{3.84}$$

$$\mathcal{P}^{\mathbf{1}} = \dot{\rho} + \Theta\,(\rho + p) \ , \tag{3.85}$$

$$\mathcal{P}^{\mathbf{2}} = \dot{\Theta} + \tfrac{1}{3}\Theta^2 + 2\sigma^2 + \tfrac{\kappa}{2}\,(\rho_s + 3p_s) \ , \tag{3.86}$$

$$\mathcal{P}^{\mathbf{3}}{}_{ab} = \dot{\sigma}_{\langle ab\rangle} + \tfrac{2}{3}\Theta\,\sigma_{ab} + \sigma_{\langle a}{}^{c}\sigma_{b\rangle c} + E_{ab} + \kappa\sigma_{\langle a}{}^{c}S_{b\rangle c} \ , \tag{3.87}$$

$$\begin{aligned}\mathcal{P}^{\mathbf{4}}{}_{ab} = {} & \dot{E}_{\langle ab\rangle} + \Theta\,E_{ab} - \operatorname{curl} H_{ab} + \tfrac{\kappa}{2}\,(\rho_s + p_s)\,\sigma_{ab} - 3\sigma_{\langle a}{}^{c}E_{b\rangle c} \\ & - \kappa^{(3)}\big(\sigma_{\langle a}{}^{c}S_{b\rangle c}\big)^{\cdot} - \tfrac{\kappa}{3}\,\Theta\sigma_{\langle a}{}^{c}S_{b\rangle c} - \tfrac{\kappa}{2}\sigma_{cd}\sigma_{\langle a}{}^{c}S_{b\rangle}{}^{d} - \tfrac{\kappa}{2}D_{\langle a}D^{c}S_{b\rangle d} \ ,\end{aligned} \tag{3.88}$$

$$\begin{aligned}\mathcal{P}^{\mathbf{5}}{}_{ab} = {} & \dot{H}_{\langle ab\rangle} + \Theta\,H_{ab} + \operatorname{curl} E_{ab} - 3\sigma_{\langle a}{}^{c}H_{b\rangle c} \\ & + \tfrac{\kappa}{2}\varepsilon_{cd\langle a}D^{c}\left(\sigma^{de}S_{b\rangle e} + \sigma_{b\rangle e}S^{\rho de}\right) - \tfrac{\kappa}{2}\varepsilon_{cd\langle a}\sigma_{b\rangle}{}^{c}D_{e}S^{de} \ ,\end{aligned} \tag{3.89}$$

and the constraint equations (3.58), (3.60), (3.67), (3.68), and (3.72), denoted by $\mathcal{C}^A = 0$ where $A = \mathbf{0}, \ldots, \mathbf{4}$, become

$$\begin{aligned}\mathcal{C}^{\mathbf{0}}{}_{a} = {} & D_a p_s - 2D^b\left(\sigma_{(a}{}^{c}S_{b)c}\right) + \sigma_b{}^{c}D^{b}S_{ac} - \sigma_a{}^{b}D^{c}S_{bc} \\ & + S_a{}^{b}D_b\Theta - \tfrac{1}{2}S_a{}^{b}D^{c}S_{bc} + \varepsilon_{abc}S^{b}{}_{d}H^{cd} \ ,\end{aligned} \tag{3.90}$$

$$\mathcal{C}^{\mathbf{1}}{}_{a} = D^b\sigma_{ab} - \kappa D^b S_{ab} - \tfrac{2}{3}D_a\Theta \ , \tag{3.91}$$

$$\mathcal{C}^{\mathbf{2}}{}_{ab} = \operatorname{curl}\sigma_{ab} - H_{ab} \ , \tag{3.92}$$

$$\begin{aligned}\mathcal{C}^{\mathbf{3}}{}_{a} = {} & D^b E_{ab} - \tfrac{\kappa}{3}D_a\rho_s - \varepsilon_{abc}\sigma^{b}{}_{d}H^{cd} \\ & - \kappa D^b\left(\sigma_{(a}{}^{c}S_{b)c}\right) - \tfrac{\kappa}{3}\Theta D^b S_{ab} + \tfrac{\kappa}{2}\sigma_{ab}D_c S^{bc} \ ,\end{aligned} \tag{3.93}$$

$$\mathcal{C}^{\mathbf{4}}{}_{a} = D^b H_{ab} + \varepsilon_{abc}\sigma^{b}{}_{d}E^{cd} + \tfrac{\kappa}{2}\varepsilon_{abc}D^b D_d S^{cd} \ . \tag{3.94}$$

The evolution of the constraints $\mathcal{C}^A$ along the worldlines u^a leads to a system of equations $\dot{\mathcal{C}}^A = \mathcal{F}^A(\mathcal{C}^B)$, where $\mathcal{F}^A$ do not contain time derivatives, since these are eliminated via the propagation equations $\mathcal{P}^A$ and suitable identities. The covariant analysis of propagation and constraint equations involves frequent use of a number of algebraic and differential identities governing the kinematical and dynamical quantities. In particular, one requires commutation rules for spatial and time derivatives. The necessary identities are collected for convenience in *Appendix* B. After lengthy calculations the explicit time evolution of

the constraints (3.91), (3.92), and (3.94) is found to be,

$$^{(3)}(\mathcal{C}^{\mathbf{1}}{}_{a})^{\cdot} = -\Theta\mathcal{C}^{\mathbf{1}}{}_{a} + 2\varepsilon_{a}{}^{bc}\sigma_{b}{}^{d}\mathcal{C}^{\mathbf{2}}{}_{cd} - \mathcal{C}^{\mathbf{3}}{}_{a} + \kappa\mathcal{C}^{\mathbf{0}}{}_{a} \ , \tag{3.95}$$

$$^{(3)}(\mathcal{C}^{\mathbf{2}}{}_{ab})^{\cdot} = -\Theta\mathcal{C}^{\mathbf{2}}{}_{ab} - \varepsilon^{cd}{}_{(a}\sigma_{b)c}\mathcal{C}^{\mathbf{1}}{}_{d} \ , \tag{3.96}$$

$$^{(3)}(\mathcal{C}^{\mathbf{4}}{}_{a})^{\cdot} = -\tfrac{4}{3}\Theta\mathcal{C}^{\mathbf{4}}{}_{a} + \tfrac{1}{2}\sigma_{a}{}^{b}\mathcal{C}^{\mathbf{4}}{}_{b} + \tfrac{3}{2}H_{a}{}^{b}\mathcal{C}^{\mathbf{1}}{}_{b} - \varepsilon_{a}{}^{bc}H_{b}{}^{d}\mathcal{C}^{\mathbf{2}}{}_{cd} - \tfrac{1}{2}\,\mathrm{curl}\,\mathcal{C}^{\mathbf{3}}{}_{a} \ . \tag{3.97}$$

The constraints are preserved under evolution as we now briefly explain. Suppose that the constraints are satisfied on an initial spatial hypersurface $\{t = t_0\}$, i.e. $\mathcal{C}^{A}|_{t_0} = 0$, where t is the proper time along the worldlines. Since $\mathcal{C}^{A} = 0$ is a solution for the initial data, it then follows from (3.95)-(3.97) that the constraints are satisfied for all time.

The time evolution of $\mathcal{C}^{\mathbf{0}}{}_{a}$ was not explicitly established because the equation of state needs to be specified for this endeavour. Neither was the expression for the time evolution of $\mathcal{C}^{\mathbf{3}}{}_{a}$ explicitly determined due to the overwhelming algebraic complexity of that particular computation. However, it is plausible that the dynamics is consistent since the three time evolution equations for the constraints (3.95), (3.96) and (3.97) involve all the constraint and propagation equations. This is true with the exception of $\mathcal{P}^{\mathbf{1}}$. As we discuss in detail below, $\mathcal{P}^{\mathbf{1}}$ is not involved in the time evolution of (3.95), (3.96) and (3.97). However, Obukhov & Korotky (1987) have shown, using the Frenkel condition, that any perfect fluid with spin in the EC theory has an energy conservation equation of the form $\mathcal{P}^{\mathbf{1}}$. This is sufficient to show independently the consistency of $\mathcal{P}^{\mathbf{1}}$.

The time evolution of $\mathcal{C}^{\mathbf{1}}{}_{a}$, (3.95), involves the propagation equations $\mathcal{P}^{\mathbf{0}}$, $\mathcal{P}^{\mathbf{2}}$, $\mathcal{P}^{\mathbf{3}}{}_{ab}$ and the constraint equations $\mathcal{C}^{\mathbf{0}}{}_{a}$, $\mathcal{C}^{\mathbf{1}}{}_{a}$, $\mathcal{C}^{\mathbf{2}}{}_{ab}$. It has been determined by using the covariant identities (B.4) and (B.8).

The time evolution of $\mathcal{C}^{\mathbf{2}}{}_{ab}$, (3.96), involves the propagation equations $\mathcal{P}^{\mathbf{3}}{}_{ab}$, $\mathcal{P}^{\mathbf{5}}{}_{ab}$ and the constraint equations $\mathcal{C}^{\mathbf{1}}{}_{a}$, $\mathcal{C}^{\mathbf{2}}{}_{ab}$. It has been determined by using the covariant identities (B.7) and (B.11).

The time evolution of $\mathcal{C}^{\mathbf{4}}{}_{a}$, (3.97), involves the propagation equations $\mathcal{P}^{\mathbf{0}}$, $\mathcal{P}^{\mathbf{3}}{}_{ab}$, $\mathcal{P}^{\mathbf{4}}{}_{ab}$, $\mathcal{P}^{\mathbf{5}}{}_{ab}$ and the constraint equations $\mathcal{C}^{\mathbf{1}}{}_{a}$, $\mathcal{C}^{\mathbf{2}}{}_{ab}$, $\mathcal{C}^{\mathbf{3}}{}_{a}$, $\mathcal{C}^{\mathbf{4}}{}_{a}$. It has been determined by using the covariant identities (B.3), (B.5), (B.8), (B.9) and (B.10).

The constraint equations are not linearly independent given that they satisfy,

$$\mathcal{C}^{\mathbf{4}}{}_{a} = \tfrac{1}{2}\,\mathrm{curl}\,\mathcal{C}^{\mathbf{1}}{}_{a} - D^{b}\mathcal{C}^{\mathbf{2}}{}_{ab} \ . \tag{3.98}$$

The consistency of the constraint equations can be explicitly inferred from relation (3.98) as mentioned by Maartens (1997) and explained below. For any given spatial hypersurface, i.e. $\{t = \text{const}\}$, the linear dependence (3.98) of the constraint equations implies the constraint $\mathcal{C}^{\mathbf{4}}{}_a$ is satisfied provided that the constraints $\mathcal{C}^{\mathbf{1}}{}_a$ and $\mathcal{C}^{\mathbf{2}}{}_{ab}$ are also satisfied. Moreover, the time evolution of $\mathcal{C}^{\mathbf{1}}{}_a$ and $\mathcal{C}^{\mathbf{2}}{}_{ab}$, described by (3.95) and (3.96) respectively, depends explicitly on $\mathcal{C}^{\mathbf{0}}{}_a$ and $\mathcal{C}^{\mathbf{3}}{}_a$. Hence, if we take $\mathcal{C}^{\mathbf{0}}{}_a$ as determining $D^b S_{ab}$, $\mathcal{C}^{\mathbf{1}}{}_a$ as defining $D_a\Theta$, $\mathcal{C}^{\mathbf{2}}{}_{ab}$ as establishing H_{ab} and $\mathcal{C}^{\mathbf{3}}{}_a$ as setting $D_a\rho_s$, the constraint equations are consistent with each other because $\mathcal{C}^{\mathbf{4}}{}_a$ then follows.

The consistency of the constraints for a perfect fluid in GR with non vanishing vorticity and peculiar acceleration has been established by van Elst (1996). Thus, having shown that the dynamics of an irrotational Weyssenhoff fluid in absence of any peculiar acceleration ($\omega = a = 0$) is consistent, it is very plausible − although not proven − that this will remain the case in the general case when the vorticity and the peculiar acceleration are considered. Hence, in that case, to establish explicitly the consistency of the constraints for such a fluid, the coherence of the terms involving the coupling between the spin density, the vorticity density and the peculiar acceleration would have to be shown respectively. This would be a extremely laborious algebraic task, but it is, in fact, quite likely to be true since the consistency of two different particular cases has already been established.

3.7 Comparison with previous results obtained by Palle

A first attempt to study the dynamics of a Weyssenhoff fluid in a $1+3$ covariant approach was initiated by Palle (1999). The results we find in this thesis disagree, however, with the majority of the results derived by Palle, as we now briefly explain.

In a similar way to our own procedure, Palle based his analysis on the effective Einstein field equations for a Weyssenhoff fluid obtained by Obukhov & Korotky (1987), which are outlined in relation $\{1\}$ of his publication. As explicitly stated in his work, Palle projects the EC version of the Ricci identities determined

by Hehl (1974),

$$\tilde{\nabla}_{[a}\tilde{\nabla}_{b]}u_c = \tfrac{1}{2}\tilde{R}_{cdab}u^d + Q^d{}_{ab}\tilde{\nabla}_d u_c, \tag{3.99}$$

which are given in relation {4} of his paper to find the corresponding propagation and constraint equations. This stands in direct contradiction with the fact that the $1+3$ covariant approach used is based on effective GR field equations.

Moreover, in Palle's work, there is no mention of the antisymmetric part of the EC field equations which lead to the spin field equation. It seems unfeasible to provide an accurate description of a cosmological fluid with spin without describing the spin dynamics.

Furthermore, Palle chose to neglect the contributions due to the electric and magnetic part of the Weyl tensor but did not provide any explanation for this. Indeed, the relation {7} he obtained for the shear propagation equation has no tidal gravitational field E_{ab} contribution, and there is no magnetic constraint equation. To describe the late time cosmological evolution, it seems indeed reasonable to neglect the contributions due to the primordial free propagating gravitational fields which have been damped by the cosmological expansion. However, these fields do significantly affect the early dynamics and have to be taken into account in a general description of cosmological models.

Finally, Palle does not determine the cosmological relations derived from the Bianchi identities. Again, these would be very useful to understand the dynamics of the early time evolution of cosmological models.

Palle (2007) has recently clarified certain points relating to the approach he followed in analysing the cosmological implications of a Weyssenhoff fluid. Several issues still, however, remain a concern, as outlined below.

It is perfectly legitimate to analyse the Weyssenhoff fluid dynamics within an EC framework without resorting to an effective GR framework. In such a case, the appropriate way to determine the large scale propagation and constraint equations is indeed to project the EC Ricci identites (3.99) on the relevant hypersurfaces, which is what Palle seems to have done. To achieve this, the EC Ricci identities have to be explicitly determined using the effective EC field equations. Our contention is that the only effective field equations {1} mentioned by Palle (1999), and used to perform the calculations, are the effective GR field equations obtained

by Obukhov & Korotky. We believe that the GR field equations are incompatible with EC Ricci identities, which would thus invalidate the analysis.

The physical motivation for using GR field equations is that it provides a more natural generalisation for the dynamics of a perfect fluid within GR. Although Palle's procedure seems inconsistent, we have nevertheless translated his results within a GR framework to be able to compare them. To compare explicitly our results with those obtained by Palle, note that the torsion scalar Q^2 he uses is related − due to the algebraic coupling between spin and torsion − to our definition of the spin density scalar S^2 by,

$$Q^2 = -\kappa^2 S^2 \ . \tag{3.100}$$

It is now straightforward to see that neither the propagation equations $\{5-7\}$ nor the constraint equations $\{8-9\}$ he found agree with our own corresponding results. The detailed comparision and analysis is given in *Section* 3.7.1. We hope that it might clarify this particular issue.

With regard to the scope of Palle's paper, on large scales, the contribution of the tidal forces to dynamics of the Weyssenhoff fluid can indeed be neglected in dynamical analysis of the background evolution. Hence, the Weyl tensor can safely be ignored in his approach, but it was not stated by Palle that only the dynamics on large scales were under consideration. It was important to clarify this issue because we have considered the dynamical evolution of Weyssenhoff fluid on all scales.

Finally, let us just mention that, as suggested by Palle (2007), it might indeed be more appropriate to consider an N-body simulation to determine the large scale and late time dynamics of a Weyssenhoff fluid in a cosmological context. However, this seems to us to lie outside our study, as we simply considered the evolution of such a fluid on all scales and for all times.

3.7.1 Explicit comparison with Palle's results

To compare our results (BHL) explicitly with the corresponding results obtained by Palle, we reexpressed his EC propagation and constraint equations − presumably obtained within an EC framework − into a GR framework using the relations

given in *Appendix* B. The correspondence between the EC and GR connections is given by,

$$\tilde{\Gamma}^{a}{}_{bc} = \Gamma^{a}{}_{bc} + \kappa \left(u^{a} S_{bc} + u_{a} S_{b}{}^{c} + u_{b} S_{a}{}^{c} \right) \ , \tag{3.101}$$

and necessary to recast the EC covariant derivative $\tilde{\nabla}_a$ in terms of its GR counterpart ∇_a. To be consistent with Palle's procedure, we only considered the dynamics on large scales, hence neglecting the contribution due to the tidal forces ($E_{ab} = H_{ab} = 0$).

The propagation equations are respectively found to be (where we highlight in bold face the terms that differ):

$$\text{(Palle)}: \quad \dot{\Theta} = -\tfrac{1}{3}\Theta^2 + D_b a^b + 2\left(a^2 - \sigma^2 + \omega^2\right) - \tfrac{\kappa}{2}\left(\rho_s + 3p_s\right) \ , \tag{3.102}$$

$$\text{(BHL)}: \quad \dot{\Theta} = -\tfrac{1}{3}\Theta^2 + D_b a^b + 2\left(a^2 - \sigma^2 + \omega^2\right) - \tfrac{\kappa}{2}\left(\rho_s + 3p_s + \boldsymbol{8\omega^b S_b}\right) \ , \tag{3.103}$$

$$\text{(Palle)}: \quad \dot{\omega}_{\langle a\rangle} = -\tfrac{2}{3}\Theta\,\omega_a + \tfrac{1}{2}\,\mathrm{curl}\, a_a + \left(\sigma_a{}^b - \boldsymbol{\kappa S_a{}^b}\right)\omega_b \ , \tag{3.104}$$

$$\text{(BHL)}: \quad \dot{\omega}_{\langle a\rangle} = -\tfrac{2}{3}\Theta\,\omega_a + \tfrac{1}{2}\,\mathrm{curl}\, a_a + \sigma^b_a\omega_b \ , \tag{3.105}$$

$$\begin{aligned}\text{(Palle)}: \quad \dot{\sigma}_{\langle ab\rangle} &= -\tfrac{2}{3}\Theta\,\sigma_{ab} - D_{\langle a}a_{b\rangle} + a_{\langle a}a_{b\rangle} - \sigma_{\langle a}{}^{c}\sigma_{b\rangle c} - \omega_{\langle a}\omega_{b\rangle} \\ &\quad - \boldsymbol{2\kappa\sigma_{\langle a}{}^{c}S_{b\rangle c}} + \boldsymbol{\tfrac{1}{3}h_{ab}\left(\Theta + 2D_c a^c - 2a^2 + 2\kappa^2 S^2\right)} \ ,\end{aligned} \tag{3.106}$$

$$\begin{aligned}\text{(BHL)}: \quad \dot{\sigma}_{\langle ab\rangle} &= -\tfrac{2}{3}\Theta\,\sigma_{ab} - D_{\langle a}a_{b\rangle} + a_{\langle a}a_{b\rangle} - \sigma_{\langle a}{}^{c}\sigma_{b\rangle c} - \omega_{\langle a}\omega_{b\rangle} \\ &\quad - \boldsymbol{\kappa\left(\sigma_{\langle a}{}^{c}S_{b\rangle c} + \omega_{\langle a}S_{b\rangle}\right)} \ .\end{aligned} \tag{3.107}$$

The constraint equations respectively yield (where we highlight in bold face the terms that differ):

$$\text{(Palle)}: \quad D_b\left(\omega^b - \boldsymbol{\kappa S^b}\right) = -a_b\left(\omega^b - \boldsymbol{\kappa S^b}\right) \ , \tag{3.108}$$

$$\text{(BHL)}: \quad D_b\omega^b = -a_b\omega^b \ , \tag{3.109}$$

$$\text{(Palle)}: \quad D_b\left(\sigma_a{}^b + \omega_a{}^b\right) - \tfrac{2}{3}D_a\Theta = 2a_b\omega_a{}^b \ , \tag{3.110}$$

$$\text{(BHL)}: \quad D_b\left(\sigma_a{}^b + \omega_a{}^b - \boldsymbol{\kappa S_a{}^b}\right) - \tfrac{2}{3}D_b\Theta = 2a_a\left(\omega_a{}^b - \boldsymbol{\kappa S_a{}^b}\right) \ . \tag{3.111}$$

Note that the shear propagation equation is by definition trace free. This result is recovered by BHL but not by Palle. Furthermore, in absence of torsion − i.e. for a vanishing spin contribution − the shear evolution equation obtained by

Palle does not reduce to Hawking and Ellis' result whereas the relation obtained by BHL does.

We could not rigorously verify Palle's result by evolving the constraints because the spin contribution to the Bianchi identities are needed for that purpose as shown in *Section* 3.6. However, it would be of considerable interest if Palle could emulate BHL and demonstrate that his set of equations also reduce to Hawking and Ellis' results in absence of torsion, and that the consistency of his equations could be established in the absence of vorticity and of any peculiar acceleration.

Chapter 4

Classical big-bounce cosmology: dynamical analysis of a homogeneous and irrotational Weyssenhoff fluid

In *Chapter* 3, we performed a formal derivation of the dynamical relations for an effective Weyssenhoff fluid. In this chapter, we restrict our analysis to the dynamics of such a fluid on large scales. We focus in particular on the cosmological application of Weyssenhoff fluid. Firstly, we wish to investigate the possibility that the spin contributions for a Weyssenhoff fluid may avert an initial singularity, as first suggested by Trautman (1973). Secondly, since the inflation scenario is the simplest known generating mechanism for the initial density fluctuations, it is also of particular interest to see if the spin contributions are able to generate a dynamical model endowed with an early inflationary era, as first suggested by Gasperini (1986). Scalars fields can generate inflation, but they have not yet been observed. Therefore, it is of interest to examine possible alternatives, such as a Weyssenhoff fluid. In contrast to the approaches of Trautman (1973) and Gasperini (1986), our use of the $1+3$ covariant formalism enables us to determine the dynamics of a Weyssenhoff fluid without assuming any particular form for the space-time metric.

The study of the dynamics of a Weyssenhoff fluid in a $1+3$ covariant approach

was initiated by Palle (1999). His work has been revised and extended by Brechet *et al.* (2007). This chapter extends the work carried out first by Trautman (1973) in an isotropic space-time, and Kopczynski (1973) and Stewart & Hájiček (1973) in an anisotropic space-time. It also generalises the analysis of the inflationary behaviour of Weyssenhoff fluid models made by Gasperini (1986) to anisotropic space-times.

In our dynamical analysis, we choose to restrict our study to a spatially homogeneous and irrotational Weyssenhoff fluid. This particular choice, which implies a vanishing vorticity and peculiar acceleration, has been motivated by underlying fundamental physical reasons. For a vanishing vorticity, the fluid flow is hypersurface-orthogonal, which means that the instantaneous rest spaces defined at each space-time point should mesh together to form a set of 3-surfaces in space-time as explained by Ellis (1971). These hypersurfaces, which are surfaces of simultaneity for all the fluid observers, define a global cosmic time coordinate determined by the fluid flow. Moreover, by assuming that any peculiar acceleration vanishes, the cosmic time is then uniquely defined. It is worth mentioning that the absence of vorticity is an involutive property, which means that if it is true initially then it will remain so at later times as shown by Ellis & van Elst (1999). Finally, the assumption that there is no vorticity on all scales implies that the fluid has no global rotation. This is in line with recent Bayesian MCMC analysis of WMAP data performed by Bridges *et al.* (2006). Their work confirms that a physical Bianchi $\mathrm{VII_h}$ model, which has a non-vanishing vorticity, is statistically disfavored by the data.

It is worth pointing out that Szydłowski & Krawiec (2004) have considered an isotropic and homogeneous cosmological model in which a Weyssenhoff fluid is proposed as a potential candidate to describe dark energy at late times. In a subsequent publication, Krawiec *et al.* (2005) showed that it is not disfavoured by SNIa data, but it may be in conflict with CMB and BBN observational constraints. By contrast, in this dissertation, we consider the full evolutionary history of an, in general, anisotropic universe with a Weyssenhoff fluid as its matter source, concentrating in particular on the 'early universe' behaviour when the spin terms are significant. Indeed, at late times, when the spin contributions can be neglected, the Weyssenhoff fluid reduces to a standard cosmological fluid. We

thus allow for the presence of a non-zero cosmological constant, in accord with current observational constraints.

In *Section* 4.1, we discuss how to apply the spatial symmetries and macroscopic spin averaging procedure to a Weyssenhoff fluid. In *Section* 4.2, we establish the relevant dynamical relations for a homogeneous and irrotational Weyssenhoff fluid. In *Section* 4.3, we perform a geodesic singularity analysis for such a fluid. *Section* 4.4 is devoted to the fluid dynamics. The behaviour of the generalised scale factor $R(t)$ of such a fluid in a spatially-curved models is discussed in *Section* 4.5 and explicit analytical solutions in spatially-flat models are given in *Section* 4.6.

4.1 Spatial symmetries and macroscopic spin averaging

Although much of our following discussion will concern cosmological models that are anisotropic, it is of interest to consider the status of a Weyssenhoff fluid as a matter source for homogeneous and isotropic models.

4.1.1 Spatial symmetries

To be a suitable candidate for the matter content of such a cosmological model, a Weyssenhoff fluid has to be compatible with the Cosmological Principle. In mathematical terms, a four-dimensional space-time manifold satisfying this principle is foliated by three dimensional spatial hypersurfaces, which are maximally symmetric and thus invariant under the action of translations and rotations.

Although a Weyssenhoff fluid can be expressed as an effective GR fluid, the dynamical nature of such a fluid is rooted in the EC theory. Thus, the dynamics of such a fluid is determined by the translational and the rotational fields, which are respectively the metric g_{ab} and the torsion $T^{c}{}_{ab}$. The symmetries require the dynamical fields to be invariant under the action of an infinitesimal isometry.

Hence, the Lie derivatives of the dynamical fields have to vanish according to,

$$\mathcal{L}_\xi g_{ab} = 0 \ , \tag{4.1}$$

$$\mathcal{L}_\xi T^c{}_{ab} = 0 \ . \tag{4.2}$$

where ξ^c are the Killing vectors generating the spatial isometries. A maximally symmetric spatial hypersurface admits 6 Killings vectors as mentioned by Weinberg (1972). The 3 Killing vectors ξ^a generating the infinitesimal translations are related to homogeneity and the 3 Killing pseudo-vectors χ^a generating the infinitesimal rotations are related to isotropy. They satisfy,

$$\xi^a = h^a{}_b \xi^b \ , \tag{4.3}$$

$$\chi^a = \varepsilon^{abc} \tilde{D}_{[b} \xi_{c]} \ , \tag{4.4}$$

where ε^{abc} is three-dimensional Levi-Civita tensor.

For a cosmological fluid based on the EC theory, such as a Weyssenhoff fluid, we can consider two different forms of the Cosmological Principle:

1. the Strong Cosmological Principle (SCP), where the Lie derivatives of the metric (4.1) and of the torsion (4.2) have to vanish; and

2. the Weak Cosmological Principle (WCP), where only the Lie derivatives of the metric (4.1) have to vanish and no restriction is imposed on the torsion.

The translational Killing equation resulting from the symmetries imposed on the metric (4.1) yields,

$$\tilde{D}_{(a} \xi_{b)} = D_{(a} \xi_{b)} = 0 \ , \tag{4.5}$$

which is a well-know result obtained in GR. Hence, the WCP is identical to the GR Cosmological Principle, which implies that the space-time geometry is described in terms of an FLRW metric.

Using the translational Killing equation (4.5), the rotational Killing equation resulting from the symmetries imposed on the metric (4.2) is found to be,

$$(\tilde{D}_d T^c{}_{ab}) \xi^d = \left(h^{ce} T^d{}_{ab} + h^e{}_a T^{cd}{}_b + h^e{}_b T_a{}^{cd} \right) \tilde{D}_{[d} \xi_{e]} \ . \tag{4.6}$$

For any maximally symmetric space as mentioned by Weinberg (1972), we can choose respectively a Killing vector ξ^a to vanish at a given point P, and

independently, a Killing pseudo-vector χ^a to vanish at a given point Q according to,

$$\xi^a(P) = 0 \ , \tag{4.7}$$

$$\chi^a(Q) = 0 \ . \tag{4.8}$$

Hence, homogeneity and isotropy can be considered separately.

By imposing the homogeneity condition (4.8) on the rotational Killing equation (4.6), the spatial covariant derivative of the torsion tensor has to vanish according to,

$$\tilde{D}_d T_{abc} = 0 \ . \tag{4.9}$$

Hence, torsion can only be a function of cosmic time t,

$$T_{abc} \equiv T_{abc}(t) \ . \tag{4.10}$$

By imposing the isotropy condition (4.7) on the rotational Killing equation (4.6), the torsion tensor has to satisfy the constraint,

$$h^{[a}{}_c h^{b]}{}_d T^c{}_{ef} + h^{[a}{}_c h^{b]}{}_e T^c{}_{df} + h^{[a}{}_c h^{b]}{}_e T_{df}{}^c = 0 \ . \tag{4.11}$$

As shown explicitly in a theorem established by Tsamparlis (1979) and mentioned subsequently by Boehmer & Bronowski (2006), the homogeneity (4.10) and isotropy (4.11) constraints taken together put severe restrictions on the torsion tensor. The only non-vanishing components are found to be,

$$T_{abc} = h_a{}^d h_b{}^e h_c{}^f T_{[def]} = f(t)\epsilon_{abc} \ , \tag{4.12}$$

$$T^b{}_{ab} = u_a u^b h_c{}^d h_d{}^e T^c{}_{be} = \tfrac{1}{3} u_a u^{b\,(3)}T_b \ , \tag{4.13}$$

where $f(t)$ is a scalar function of cosmic time t, a is a fixed index and ${}^{(3)}T_b$ is the spatial trace of the torsion tensor defined as

$${}^{(3)}T_b \equiv h^{ac} T_{abc} \ . \tag{4.14}$$

We now discuss the application of this general framework to a Weyssenhoff fluid.

4.1.2 Weyssenhoff fluid with macroscopic spin averaging

The algebraic coupling between the spin density and torsion tensors (3.41) shows that the spin density S_{ab} of a Weyssenhoff fluid can be related to the torsion as,

$$S_{ab} = u^c h_a{}^d h_b{}^e \kappa^{-1} T_{cde} \ . \tag{4.15}$$

By substituting the non-vanishing components of the torsion (4.12) and (4.13) satisfying the SCP into the expression for the spin density of a Weyssenhoff fluid (4.15), it is straightforward to show that the spin density tensor has to vanish,

$$S_{ab} = 0 \ . \tag{4.16}$$

Thus, Tsamparlis (1979) claims that a Weyssenhoff fluid is incompatible with the SCP. This conclusion would hold if all the dynamical contributions of the spin density were second rank tensors of the form S_{ab}. However, this is not the case since the dynamics contains spin density squared scalar terms. These scalar terms are invariant under spatial isometries like rotations and translations. Hence, they do satisfy the SCP.

In order for the Weyssenhoff fluid to be compatible with the SCP, the spin density tensorial terms have to vanish leaving the scalar terms unaffected. This can be achieved by making the reasonable physical assumption that, locally, macroscopic spin averaging leads to a vanishing expectation value for the spin density tensor according to,

$$\langle S_{ab} \rangle = 0 \ . \tag{4.17}$$

However, this macroscopic spin averaging does not lead to a vanishing expectation value for the spin density squared scalar since this term is a variance term,

$$\left\langle S^2 \right\rangle = \tfrac{1}{2} \left\langle S_{ab} S^{ab} \right\rangle \neq 0 \ . \tag{4.18}$$

The macroscopic spatial averaging of the spin density was performed in an isotropic case by Gasperini (1986). It can be extended to an anisotropic case provided that on small macroscopic scales the spin density pseudo-vectors are assumed to be randomly oriented.

By considering a Weyssenhoff fluid in the absence of any peculiar acceleration and by performing a macroscopic spin averaging, we indirectly require the fluid to be homogeneous. This follows from the fact that, in this case, the conservation law of momentum leads to a vanishing spatial derivative of the pressure and energy density. This will be explicitly shown in *Section* 4.2.1.

Note that even in the absence of a macroscopic spin averaging, the Weyssenhoff fluid is still compatible with the WCP, which we discuss further in *Section* 4.2.2. It is worth mentioning that there is no observational evidence so far which would suggest that we should impose the SCP even though the mathematical symmetries make such a principle mathematically appealing. A true test of whether this principle is applicable would be the demonstration of physically observable differences between this case and the WCP.

4.2 Dynamics of a homogeneous and irrotational Weyssenhoff fluid

The dynamical equations for an homogeneous and irrotational Weyssenhoff fluid with no peculiar acceleration are obtained by requiring the acceleration and the vorticity pseudovector to vanish,

$$\begin{aligned} a_b &= 0 \ , \\ \omega_b &= 0 \ , \end{aligned} \tag{4.19}$$

in the dynamical equations of *Chapter* 3. To study the dynamics of a homogeneous fluid, it is not necessary to solve the once-contracted Bianchi identities, which generate gravitational waves. Instead, we focus on the Ricci identities and the twice-contracted Bianchi identities, which correspond to the conservation laws.

The dynamics of an irrotational Weyssenhoff fluid with no peculiar acceleration is entirely determined by the symmetric and spin field equations, (3.48) and (3.47) respectively. The former can be used to determine the Ricci identities and the energy conservation law. The latter simply expresses spin propagation.

One important consequence of the spatial averaging of the spin density is that the stress-energy momentum tensor (3.48) reduces to an elegant expression given by

$$T^s_{ab} = \rho_s u_a u_b + p_s h_{ab} \ , \tag{4.20}$$

where the only spin contributions affecting the dynamics are the negative spin squared variance terms entering the definition of the effective energy density and pressure (3.45), as expected. These spin squared intrinsic interaction terms S^2 are a key feature that distinguishes a Weyssenhoff fluid from a perfect fluid in GR and lead to interesting properties we discuss below.

We have to be careful when performing the macroscopic spin averaging on the dynamical equations. The Ricci identities and conservation laws can be entirely determined from the stress-energy momentum tensor (4.20). As we have shown, it is perfectly legitimate to perform a macroscopic spin averaging on the stress-energy momentum tensor before obtaining explicitly the dynamical equations. However, this is not the case for the spin field equation (3.47). Performing the macroscopic spin averaging at this stage would make these field equations vanish. To be consistent, we first have to determine the dynamical equations and express them in terms of the spin density scalar before performing the spin averaging.

4.2.1 Dynamical equations

The dynamical equations for a homogenous and irrotational Weyssenhoff fluid are obtained from the dynamical relations derived in *Section* 3.5 and *Section* 3.6 by imposing the conditions (4.19) and by performing a macroscopic spin averaging (4.17). The energy conservation equation (3.76), the spin propagation equation (3.75), the Raychaudhuri equation (3.53), the generalised Friedmann equation (3.83), the momentum conservation equation (3.72) and the rate of

shear propagation equation (3.55) respectively reduce to,

$$\dot{\rho} = -\Theta\ (\rho + p)\ , \tag{4.21}$$

$$\dot{S} = -\Theta\, S\ , \tag{4.22}$$

$$\dot{\Theta} = -\tfrac{1}{3}\Theta^2 - 2\sigma^2 - \tfrac{\kappa}{2}\,(\rho_s + 3p_s)\ , \tag{4.23}$$

$${}^{(3)}\mathcal{R} = \tfrac{2}{3}\Theta^2 - 2\kappa\rho_s - 2\sigma^2\ , \tag{4.24}$$

$$D_a p_s = 0\ , \tag{4.25}$$

$$\dot{\sigma}_{\langle ab\rangle} = -\tfrac{2}{3}\Theta\,\sigma_{ab} - \sigma_{\langle a}{}^{c}\sigma_{b\rangle c} - E_{ab}\ . \tag{4.26}$$

It is worth mentioning that the spin propagation equation (4.22) implies that the spin density is inversely proportional to the volume of the fluid. Note that although the vectorial expression for the spin propagation (3.73) vanishes due to the macroscopic spin averaging (4.17), the scalar expression (4.22) still applies because it is related to the spin variance (4.18).

Note also that the momentum conservation law (4.25) expresses the homogeneity of the Weyssenhoff fluid. This is due to the fact that according to this law, the energy density, the pressure and the spin density of the fluid have to be a function of cosmic time only. Hence, the torsion tensor has also to be a function of cosmic time only, which is the homogeneity requirement (4.10). This is only the case for a Weyssenhoff fluid with no peculiar acceleration on which a macroscopic spin averaging has been performed, as otherwise the momentum conservation law (4.25) would contain additional terms.

Finally, one must take particular care when deducing the time evolution of the rate of shear from the rate of shear propagation equation (4.26). This is due to the fact that the rate of shear coupling term $\sigma_{\langle a}{}^{c}\sigma_{b\rangle c}$ and the tidal force term E_{ab} can not simply be neglected. A better route is to deduce the rate of shear evolution equation from the spatial Ricci curvature tensor ${}^{(3)}R_{ab}$ as shown explicitly by Ellis (1973) and outlined below.

In order to determine a scalar propagation equation for the rate of shear, the expression for the spatial Ricci curvature tensor (3.82) has to be contracted with the rate of shear tensor σ^{ab} according to,

$${}^{(3)}R_{ab}\sigma^{ab} = -2\sigma\,(\dot{\sigma} + \Theta\sigma)\ , \tag{4.27}$$

where we used the definition of the rate of shear scalar squared (1.16) and its time derivative,

$$\dot{\sigma}_{ab}\sigma^{ab} = 2\sigma\dot{\sigma} \ . \tag{4.28}$$

For the anisotropic Weyssenhoff fluid models, which satisfy the contracted curvature-shear condition,

$$^{(3)}R_{ab}\sigma^{ab} = 0 \ , \tag{4.29}$$

the propagation equation for the rate (4.27) of shear reduces to,

$$\dot{\sigma} = -\Theta\,\sigma \ . \tag{4.30}$$

The propagation equation of the rate of shear scalar (4.30) closes the dynamical system (4.21)-(4.23), making the rate of shear propagation equation (4.26) redundant, thus eliminating in turn the need for an evolution equation for the electric part of the Weyl tensor E_{ab}. As pointed out by Dechant *et al.* (2009), the only homogeneous Weyssenhoff fluid models which obey the rate of shear propagation equation (4.30) are those that satisfy the contracted curvature-shear condition (4.29). Note that this is a more restrictive condition than what was alleged by Brechet *et al.* (2008). Spatially-flat models like Bianchi I models, discussed notably by Stewart & Hájiček (1973), have a vanishing spatial curvature and therefore satisfy the contracted curvature-shear condition. However, the converse is not true. Anisotropic fluid models can satisfy the contracted curvature-shear condition (4.29) without necessarily having a vanishing spatial curvature. In order to show explicitly which Bianchi models satisfy the contracted curvature-shear condition (4.29), the explicit expression for the spatial Ricci tensor has to be determined using a specific metric. This is a tedious task, which we will not undertake here. However, it is worth mentioning that Dechant *et al.* (2009) undertook this task for Bianchi IX models and showed that, in this particular case, the contracted curvature-shear condition is violated. In the remainder of this chapter, we will consider only the anisotropic Weyssenhoff fluid models for which the contracted curvature-shear condition is satisfied.

4.2.2 Comparison with previous results

Let us compare our results with the conclusions reached by Lu & Cheng (1995) for an isotropic Weyssenhoff fluid without any macroscopic spin averaging as shown in *Appendix A* of their publication.

In an isotropic space-time, the dynamics of a Weyssenhoff fluid, without a macroscopic spin averaging, is greatly simplified as we now briefly explain. The projection of the effective Einstein field equations (3.44) along the worldline and on the orthogonal spatial hypersurfaces, yields the following constraint,

$$u^a h_c{}^b T^s_{ab} = 0 \ . \tag{4.31}$$

It arises from the fact that, in an isotropic case, the time-space components of the Ricci tensor vanish. From the expression for the stress-energy momentum tensor (3.48), it is clear that the constraint (4.31) implies a vanishing spin divergence,

$$D^b S_{ab} = 0 \ . \tag{4.32}$$

Moreover, the isotropy constraint implies a vanishing rate of shear (i.e. $\sigma = 0$). Thus, in this case, the effective stress energy momentum tensor without the macroscopic spin averaging (3.48) reduces to the elegant expression (4.20) obtained by performing the macroscopic spin averaging.

Hence, for a Weyssenhoff fluid and isotropic space-time, our results can be compared to those of Lu & Cheng (1995). The results of our analysis do not agree with the conclusions outlined by Lu & Cheng. First, they argue that the isotropic Friedmann equation implies that the spin density has to be a function of time only, with which we agree. Then, they claim that this stands in contradiction with the fact that the spin density has also to be a function of space in order to satisfy the projection constraint (4.31), which we dispute. The projection constraint simply implies a vanishing orthogonal projection of the spin divergence on the spatial hypersurface (4.32), which is perfectly compatible with the spin density being a function of time only. Hence, contrary to their claim, a Weyssenhoff fluid model seems to be perfectly consistent with an isotropic space-time (i.e. obeying the WCP), even without spin averaging.

4.3 Geodesic singularity analysis

For a homogeneous and irrotational Weyssenhoff fluid satisfying the macroscopic spin averaging condition, the fluid congruence is geodesic. To study the behaviour of such a fluid congruence near a singularity, we use the 1+3 covariant formalism, which applies on local as well as on global scales for a homogeneous fluid model.

In order for singularities in the timelike geodesic congruence to occur, the Raychaudhuri equation (4.23) has to satisfy the condition,

$$\dot{\Theta} + \frac{1}{3}\Theta < 0 \ , \tag{4.33}$$

near the singularity, as we now explain. Following Wald (1984), we first recast the singularity condition (4.33) in terms of the inverse expansion rate Θ^{-1} as,

$$\frac{d}{dt}\left(\Theta^{-1}\right) > \frac{1}{3} \ , \tag{4.34}$$

After integrating with respect to cosmic time t, we find,

$$\Theta^{-1}(t) > \Theta_*^{-1} + \frac{1}{3}\left(t - t_*\right) \ , \tag{4.35}$$

where $\Theta_*^{-1} \equiv \Theta^{-1}\left(t_*\right)$ and $t = t_*$ is some arbitrary cosmic time near the singularity. Thus, if $\Theta_*^{-1} > 0$ ($\Theta_*^{-1} < 0$), the model describes a fluid evolving on a spatially expanding (collapsing) hypersurface at $t = t_*$. According to the integrated singularity condition (4.35), $\Theta^{-1}\left(t\right)$ must vanish within a finite past (future) time interval $|t - t^*| < 3|\Theta_*^{-1}|$ with respect to $t = t_*$. Thus a geodesic singularity, defined by $\Theta^{-1}(\hat{t}) = 0$, occurs at $t = \hat{t}$.

The homogeneity requirement allows us to define − up to a constant factor − a generalised scale factor R according to,

$$\Theta \equiv 3\frac{\dot{R}}{R} \ . \tag{4.36}$$

In a $1 + 3$ covariant approach, R is generally a locally defined variable. If the model is homogeneous, however, R can be globally defined and interpreted as a cosmological scale factor.

The singularity condition can now be recast in terms of the scale factor R and reduces to,

$$\frac{\ddot{R}}{R} < 0 \ . \tag{4.37}$$

One must also require the scale factor to obey the consistency condition, which requires the expansion rate squared to be positively defined at all times according to,

$$\left(\frac{\dot{R}}{R}\right)^2 > 0 \ . \tag{4.38}$$

To determine explicitly these two conditions (4.37)-(4.38), the Friedmann (4.24) and Raychaudhuri (4.23) equations are recast in terms of the scale factor, using respectively the expressions for the Ricci (3.49) and stress-energy-momentum tensor (4.20) as,

$$\left(\frac{\dot{R}}{R}\right)^2 = \frac{1}{3}\left(T^s_{ab}u^a u^b + \frac{{}^{(3)}\mathcal{R}}{2} + \sigma^2\right) \ , \tag{4.39}$$

$$\frac{\ddot{R}}{R} = -\frac{1}{3}\left(R_{ab}u^a u^b + 2\sigma^2\right) \ . \tag{4.40}$$

Using the Friedmann (4.39) and the Raychaudhuri (4.40) equations, the consistency (4.38) and singularity (4.37) conditions can respectively be explicitly expressed as,

$$\frac{S^2 - \kappa^{-2}\left(\sigma^2 + \Lambda + \frac{1}{2}{}^{(3)}\mathcal{R}\right)}{\kappa^{-1}\rho} < 1 \ , \tag{4.41}$$

$$\frac{S^2 - \kappa^{-2}\left(\sigma^2 - \frac{1}{2}\Lambda\right)}{\kappa^{-1}\rho} < \frac{1+3w}{4} \ . \tag{4.42}$$

The scaling of the energy density ρ, the spin density squared S^2 and the rate of shear squared σ^2 can be deduced respectively from the energy conservation law (4.21), the spin propagation equation (4.22) and the rate of shear propagation equation (4.30) by recasting the expansion rate Θ in terms of the scale factor R (4.36) according to,

$$S^2 = \bar{S}^2\left(\frac{R}{\bar{R}}\right)^{-6} \ , \tag{4.43}$$

$$\sigma^2 = \bar{\sigma}^2\left(\frac{R}{\bar{R}}\right)^{-6} \ , \tag{4.44}$$

$$\rho = \bar{\rho}\left(\frac{R}{\bar{R}}\right)^{-3(1+w)} \ . \tag{4.45}$$

Note that the bar corresponds to an arbitrary event (defined by a cosmic time $t = \bar{t}$), subject only to the condition $\bar{R} \neq 0$.

Furthermore, the spatial Ricci scalar ${}^{(3)}\mathcal{R}$ is the Gaussian curvature of the spatial hypersurface, which scales according to,

$$ {}^{(3)}\mathcal{R} = {}^{(3)}\bar{\mathcal{R}} \left(\frac{R}{\bar{R}} \right)^{-2} , \tag{4.46} $$

and the cosmological constant Λ has by definition no scale dependence,

$$ \Lambda = \bar{\Lambda} . \tag{4.47} $$

Let us now assume the existence of singularities in the timelike geodesic congruence for a homogeneous and irrotational Weyssenhoff fluid. By comparing the scaling relations for the spatial Ricci scalar (4.46) and the cosmological constant (4.47) with those obtained for the spin density squared (4.43) and the rate of shear squared (4.44), we see that in the limit where the model tends towards a singularity (i.e. $R \to 0$), the contribution due to curvature and the cosmological constant is negligible. Hence, for a Weyssenhoff fluid with a physically reasonable equation-of-state parameter (i.e. $w < 1$), the consistency (4.41) and singularity (4.42) conditions merge into a single condition according to,

$$ \frac{S^2 - \kappa^{-2}\sigma^2}{\kappa^{-1}\rho} < 1 . \tag{4.48} $$

Moreover, we can recast this condition in terms of the scale dependence R. In the limit where the model tends towards a singularity, the condition (4.48) becomes,

$$ \lim_{R \to 0} \frac{\bar{S}^2 - \kappa^{-2}\bar{\sigma}^2}{\kappa^{-1}\bar{\rho}} \left(\frac{R}{\bar{R}} \right)^{-3(1-w)} < 1 . \tag{4.49} $$

Provided the equation-of-state parameter $w < 1$, the singularity condition (4.49) can only hold if the rate of shear squared is larger than the spin squared (i.e. $\bar{\sigma}^2 > \kappa^2 \bar{S}^2$). Hence, in the opposite case, where the macroscopic spin density squared of the Weyssenhoff fluid is larger than the fluid anisotropies according to,

$$ \kappa^2 S^2 > \sigma^2 , \tag{4.50} $$

there will be no singularity on any scale. This is a generalisation of the result established independently for a Bianchi I metric by Kopczynski (1973) and Stewart & Hájiček (1973).

Our singularity analysis is based on the assumption that the Weyssenhoff fluid flow lines are geodesics, which implies that the macroscopic fluid (i.e. with spin averaging) has to be homogeneous. A key question is whether this still holds in presence of small inhomogeneities. According to Ellis (2007), the Hawking-Penrose singularity theorems mentioned by Hawking & Ellis (1973) apply not only to homogeneous models but also to approximately homogeneous models with local pressure inhomogeneities. By analogy, if there is no singularity for geodesics fluid flow lines, singularities may still be averted provided the real fluid flow lines can be described as small perturbations around geodesics.

In following sections, we will assume that the spin-shear condition (4.50) holds, which guarantees the absence of singularities for homogeneous models.

4.4 Dynamical evolution: general considerations

For a homogeneous fluid, the Gaussian curvature ${}^{(3)}\mathcal{R}$ depends only on the scale factor according to,

$$ {}^{(3)}\mathcal{R} = -\frac{6k}{R^2} \ , \tag{4.51} $$

where $k = \{-1, 0, 1\}$ is the normalised curvature parameter.

To analyse the dynamics of a homogeneous and irrotational Weyssenhoff fluid, let us first recast explicitly the Friedmann (4.39) and Raychaudhuri (4.40) equations in terms of the physical quantities using the expression for the Gaussian curvature (4.51) according to,

$$ \left(\frac{\dot{R}}{R}\right)^2 = \frac{\kappa}{3}\left[\rho - \kappa S^2 + \frac{1}{\kappa}\left(\sigma^2 - \frac{3k}{R^2} + \Lambda\right)\right] \ , \tag{4.52} $$

$$ \frac{\ddot{R}}{R} = -\frac{\kappa}{6}\left[\rho\,(1+3w) - 4\kappa S^2 + \frac{4}{\kappa}\left(\sigma^2 - \frac{1}{2}\Lambda\right)\right] \ . \tag{4.53} $$

We will now discuss in more details the geodesic singularities presented in *Section* 4.3, drawing out more fully the geometrical and physical applications.

4.4.1 Geometric interpretation of the solutions

As outlined above, at stages of the dynamical evolution for which the scale factor $R(t)$ is small, a Weyssenhoff fluid with an equation-of-state parameter $w < 1$ is dominated by the spin density and rate of shear contributions. This follows from the scaling properties of the energy (4.45) of the spin density (4.43) and of the rate of shear (4.44). Provided the spin-shear condition (4.50) is satisfied, there can be no singularity ($R \to 0$), because the negative sign of the spin squared terms in the RHS of the Friedmann equation (4.52) would imply the existence of an imaginary rate of expansion, which is physically unacceptable ($\Theta \in \mathbb{R}$) as discussed before in *Section* 4.3. For physical consistency, the RHS of the Friedmann equation has to be positively defined at all times,

$$\rho - \kappa S^2 + \frac{1}{\kappa}\left(\sigma^2 - \frac{3k}{R^2} + \Lambda\right) \geq 0 \ , \tag{4.54}$$

which clearly excludes the presence of a singularity provided $w < 1$. The physical interpretation is that − as one goes backwards in cosmic time t from the present epoch − the spin contributions to the field equations dominate and produce a bounce, which we may take to occur at $t = 0$, that avoids an initial singularity (i.e. $R(0) > 0$). Since this model contains no initial singularity, the temporal evolution of the model, governed by the Friedmann (4.52) and Raychaudhuri (4.53) equations, extends symmetrically to the negative part of the time arrow. In order to satisfy the time symmetry requirement and avoid a kink in the time evolution of the scale factor $R(t)$ at $t = 0$, the expansion rate at the bounce has to vanish, $\dot{R}(0) = 0$, and the temporal curvature of the scale factor $\ddot{R}(0)$ has to be finite. Thus, the scale factor $R(t)$ goes through an extremum at the bounce $R(0) = R_0$ [1]. The energy density at the bounce, $\rho_0 = \rho(0)$, is determined by the limit where the consistency requirement (4.54) becomes an equality,

$$\rho_0 = \kappa S_0^2 - \frac{1}{\kappa}\left(\sigma_0^2 - \frac{3k}{R_0^2} + \Lambda\right) \ , \tag{4.55}$$

where $S_0 = S(0)$ and $\sigma_0 = \sigma(0)$ denote respectively the spin energy density and the rate of shear evaluated at the bounce. Note that this particular choice for the

[1] Note that, in this chapter, a zero subscript denotes the value of a quantity at the bounce (i.e. $t = 0$) and not at the present epoch.

energy density (4.55) at $t = 0$ has been made in order for the expansion rate to vanish at the bounce. This can be shown explicitly by evaluating the Friedmann equation (4.52) at the bounce using the expression for the energy density (4.55).

Quantitative expressions or the $R(t)$-curve in various cases are derived in *Section* 4.6 below. Before doing so, however, it is worth noting that qualitatively, the general shape of the $R(t)$-curve for a Weyssenhoff fluid is closely related to the temporal curvature of the scale factor $\ddot{R}$, which is explicitly given by the Raychaudhuri equation (4.53), and also to the range of values for $R(t)$, which is determined by the consistency condition (4.38) on the Friedmann equation (4.52).

In this section, we discuss one particular class of Weyssenhoff fluid models for which the cosmological constant Λ is small (and positively defined),

$$0 < \Lambda \ll \rho_0 \ , \tag{4.56}$$

and the curvature is also small

$$0 < \frac{3}{R_0^2} \ll \rho_0 \ . \tag{4.57}$$

The two constraints (4.56) and (4.57) on the class of models imply that the sign of the temporal curvature of the scale factor depends only on the value of the equation-of-state parameter w, which yields three different cases.

In the first case, where $w < -\frac{1}{3}$, the RHS of the Raychaudhuri equation (4.53) implies that the temporal curvature of the scale factor is positively defined at all times,

$$\ddot{R}(t) > 0 \quad \text{for} \quad t \in (-\infty, \infty) \ . \tag{4.58}$$

The positive sign of $\ddot{R}$ implies that the scale factor is minimal at the bounce and the model is perpetually inflating (for $t > 0$).

In the second case, where $w > 1$, by comparing the consistency requirement (4.54) with the Raychaudhuri equation (4.53), the temporal curvature of the scale factor is found to be negatively defined at all times,

$$\ddot{R}(t) < 0 \quad \text{for} \quad t \in (-\infty, \infty) \ . \tag{4.59}$$

Note that for a model with an equation-of-state parameter $w > 1$, we reach the same conclusion as for a fluid with an equation of state parameter $w < 1$, which

is that the model has a time-symmetric evolution and bounces at $t = 0$. The negative sign of $\ddot{R}$ implies that the scale factor is maximal at the bounce and is deflating (for $t > 0$) until it eventually collapses.

In the third case, where $-\frac{1}{3} < w < 1$, the symmetric time evolution of the scale factor can be split into five parts. Firstly, for a small cosmic time, i.e. $|t| < |t_f|$ − where the value of t_f depends on the scale parameter w − the sign of the temporal curvature of the scale factor is positive. This corresponds to the spin dominated phase. Secondly, for a specific cosmic time, i.e. $|t| = |t_f|$, the temporal curvature of the scale factor vanishes as the time evolution of the scale factor reaches an inflection point. Then, for a larger cosmic time, i.e. $|t_f| < |t| < |t_a|$, the temporal curvature of the scale factor has the opposite sign until it reaches the second inflection point $|t| = |t_a|$. This corresponds to the matter dominated phase. Finally, for large cosmic time, i.e. $|t| > |t_a|$, the sign of the temporal curvature of the scale factor becomes positive again. This corresponds to the cosmological constant dominated phase. The behaviour of $\ddot{R}(t)$ in terms of cosmic time t is summarised as follows,

$$\ddot{R}(t) > 0 \quad \text{for} \quad t \in (-t_f, t_f) \ , \tag{4.60}$$

$$\ddot{R}(t) = 0 \quad \text{for} \quad t \in \{-t_f, t_f\} \ , \tag{4.61}$$

$$\ddot{R}(t) < 0 \quad \text{for} \quad t \in (-t_a, -t_f) \cup (t_f, t_a) \ , \tag{4.62}$$

$$\ddot{R}(t) = 0 \quad \text{for} \quad t \in \{-t_a, t_a\} \ , \tag{4.63}$$

$$\ddot{R}(t) > 0 \quad \text{for} \quad t \in (-\infty, -t_a) \cup (t_a, \infty) \ . \tag{4.64}$$

In the first and second cases, the results obtained for the symmetric time evolution of the scale factor are interesting mathematical solutions, but they are inconsistent with current cosmological observations. In order to satisfy the current cosmological data, the positively defined time evolution of the model has to inflate, i.e. $\ddot{R}(t) > 0$, at early time ($t < t_f$), and produce a sufficient amount of inflation. At later time ($t > t_f$), the energy density of the fluid dominates the dynamics and acts like a brake on the expansion $\ddot{R}(t) < 0$.

During the spin-dominated phase, the contribution due to the cosmological constant can be safely neglected (4.56) and the positive temporal curvature of

the scale factor (4.60) leads to an inflation phase. The inflatability condition, $\ddot{R}(t) > 0$, may be deduced from the Raychaudhuri equation (4.53) according to,

$$\rho(1+3w) - 4\kappa S^2 + 4\kappa^{-1}\sigma^2 < 0 \ . \tag{4.65}$$

This inflation phase ends when this inequality is no longer satisfied, which corresponds to the inflection point of the temporal evolution of the scale factor, i.e. $t = t_f$. Hence, at the end of inflation the density is given by,

$$\rho_f = \frac{4\kappa}{(1+3w)}\left(S_f^2 - \kappa^{-2}\sigma_f^2\right) \ . \tag{4.66}$$

The temporal evolution of this model for a positively defined time is characterised by a maximal physical energy density $\rho = \rho_0$ coinciding with the start of an inflation phase ending when the energy density reaches the density threshold $\rho = \rho_f$. At the end of inflation, the model enters a matter dominated phase. During this stage, the Weyssenhoff fluid model reduces asymptotically to the cosmological solution obtained for a perfect fluid in GR in the limit where the cosmic time is sufficiently large $t \gg t_f$, which eventually leads to a cosmological constant dominated phase for $t \gg t_a > t_f$.

4.4.2 Amount of inflation

The amount of inflation is measured by the number N of e-folds, which is determined using the scaling of the energy density (4.45), the initial (4.55) and final (4.66) energy densities, and found to be,

$$N \equiv \ln\frac{R_f}{R_0} = -\frac{1}{3(1+w)}\ln\left[\frac{4}{1+3w}\left(\frac{\kappa^2 S_f^2 - \sigma_f^2}{\kappa^2 S_0^2 - \sigma_0^2}\right)\right] \ . \tag{4.67}$$

Using the scaling relations obtained for the spin density squared (4.43) and the rate of shear squared (4.44), the initial and final values of these quantities are found to be related by the number of e-folds according to,

$$S_0^2 = S_f^2\left(\frac{R_0}{R_f}\right)^{-6} = S_f^2 e^{6N} \ , \tag{4.68}$$

$$\sigma_0^2 = \sigma_f^2\left(\frac{R_0}{R_f}\right)^{-6} = \sigma_f^2 e^{6N} \ . \tag{4.69}$$

By recasting the initial values of the spin density squared and rate of shear squared in terms of their final values according to (4.68) and (4.69) respectively, the expression for the number of e-folds (4.67) reduces to an elegant expression,

$$N = \frac{1}{3(1-w)} \ln\left(\frac{4}{1+3w}\right) \ , \tag{4.70}$$

and is shown in *Figure* 4.1. It worth mentioning that the amount of inflation is independent of the rate of shear or the spin density of the fluid. Let us mention that Bianchi models based on a Weyssenhoff fluid have been studied previously by Lu & Cheng (1995). However, the authors did not try to estimate the amount of inflation in their analysis.

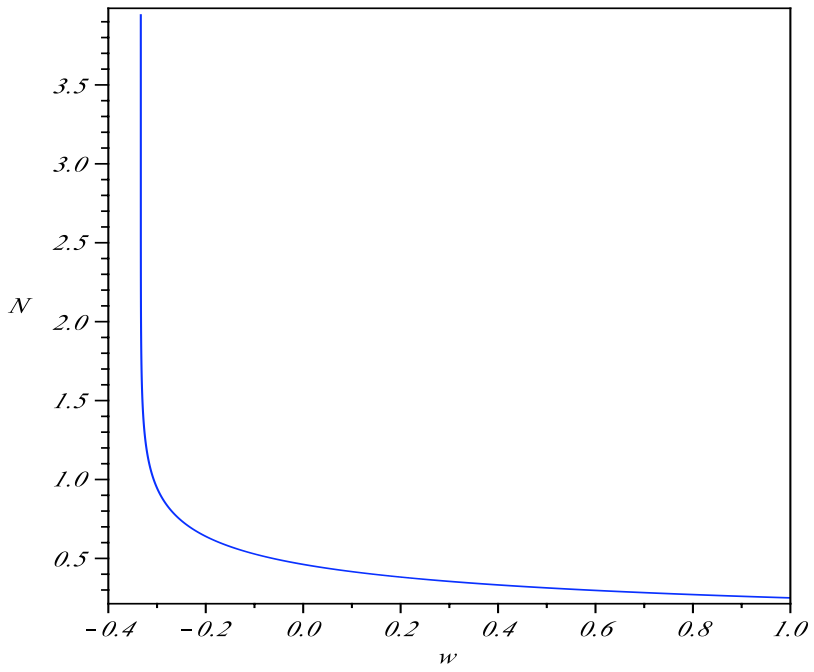

Figure 4.1: Number of e-folds N in terms of the equation-of-state parameter w. $N(w)$ has a vertical asymptote at $w = -\frac{1}{3}$.

The only way to have achieve a substantial number of e-folds is by requiring an equation of state of the form

$$w = -\frac{1}{3} + \epsilon \qquad \text{where} \qquad 0 < \epsilon \ll 1 \ , \tag{4.71}$$

which corresponds to no standard fluid and has therefore no acceptable physical basis. This conclusion has already been reached by Gasperini (1986) in the isotropic case. We have showed that the same result still holds in the anisotropic case.

It is interesting to note that a cosmic string fluid has an equation-of-state parameter $w = -\frac{1}{3}$. As mentioned by Ringeval (2001), a hybrid Weyssenhoff fluid made for example of fermionic matter cosmic strings and matter fields -- where the cosmic strings contribution dominates the dynamics at the era of interest -- has an equation-of-state parameter of the form (4.71) where the value of the fine tuning parameter ϵ depends crucially on the ratio between the cosmic string and the matter fields densities. Although such a fluid is a candidate to obtain an inflation phase at an early positively defined time (i.e. just after the bounce), it does not reduce to the cosmological standard model at later times when the spin contribution can be safely neglected. This is due to the fact that the density of the cosmic strings contribution ρ_{st} scales as $\rho_{\text{st}} \propto R^{-2}$. Hence, if the cosmic strings contribution dominates the behaviour of the cosmic fluid for an early positively defined time, it will do so at all times.

However, this problem may potentially be overcome by assuming that, at early times, the cosmic strings decay into the matter fields of the standard model leading to a reheating phase. It would be worth further investigating this possibility.

The fine tuning parameter ϵ has a magnitude that is related to the number of e-folds according to,

$$\epsilon \sim e^{-4N} \ . \tag{4.72}$$

To obtain, for example, an inflationary phase with $N = 50 - 70$ e-folds -- which is a characteristic range of values for current parameter estimations -- the equation of state has to be very fine tuned such that $\epsilon = 10^{-87} - 10^{-122}$. It is worth noting that this is a similar order of magnitude to the factor 10^{-120} relating the ratio of the cosmological constant predicted by summing the zero point energy of the Standard Model fields up to the Planck cutoff to that inferred from cosmological observations, although this is almost certainly just a numerical coincidence.

4.5 Quantitative dynamical evolution of spatially-curved models

Our general approach allows one to investigate models with non-zero spatial curvature and a cosmological constant. In general, it is not possible to find analytical solutions for the time evolution of the scale factor. However, the behaviour of the solutions can be analysed by integrating the dynamical equations numerically. The analysis and plots of the time evolution of the scale factor in spatially-curved models are presented below.

4.5.1 Solutions in presence of a cosmological constant

The dynamics of a homogeneous and anisotropic Weyssenhoff fluid in a spatially-curved model in presence of a cosmological constant relies on the Fridemann (4.52) and Raychaudhuri (4.53) equations. Using the scaling relation obtained for the energy density (4.45), for the spin density (4.43), and for rate of shear (4.44), the Friedmann (4.52) and Raychaudhuri (4.53) equations can be recast respectively as,

$$\left(\frac{\dot{R}}{R}\right)^2 = \frac{\kappa}{3}\rho_0\left(\frac{R}{R_0}\right)^{-3(1+w)} - \frac{\kappa^2}{3}\left(S_0^2 - \kappa^{-2}\sigma_0^2\right)\left(\frac{R}{R_0}\right)^{-6} - \frac{k}{R_0^2}\left(\frac{R}{R_0}\right)^{-2} + \frac{\Lambda}{3}\,, \tag{4.73}$$

$$\frac{\ddot{R}}{R} = -\frac{\kappa}{6}\rho_0\left(1+3w\right)\left(\frac{R}{R_0}\right)^{-3(1+w)} + \frac{2}{3}\kappa^2\left(S_0^2 - \kappa^{-2}\sigma_0^2\right)\left(\frac{R}{R_0}\right)^{-6} + \frac{\Lambda}{3}\,, \tag{4.74}$$

where for $t = 0$, R_0 is the scale factor, ρ_0 the energy density, S_0 the spin density and σ_0 the rate of shear.

For convenience, we introduce two dimensionless variables r, τ and four parameters δ^2, s^2, α, λ, defined as,

$$\begin{aligned} r &\equiv \frac{R}{R_0}\,, & \tau &\equiv \sqrt{\frac{\kappa\rho_0}{3}}t\,, \\ \delta^2 &\equiv \frac{\sigma_0^2}{\kappa\rho_0}\,, & s^2 &\equiv \frac{\kappa S_0^2}{\rho_0}\,, \\ \alpha &\equiv \frac{3k}{\kappa\rho_0 R_0^2}\,, & \lambda &\equiv \frac{\Lambda}{\kappa\rho_0}\,, \end{aligned} \tag{4.75}$$

which are the rescaled scale factor r, the rescaled cosmic time τ, the rate of shear squared parameter δ^2, the spin density squared parameter s^2, the curvature parameter α and the cosmological constant parameter λ. Note that r and τ depend on t, whereas δ^2, s^2, α and λ are constant, defined in terms of quantities at the bounce $t = 0$.

The consistency condition at the bounce (4.55) can be recast in terms of dimensionless parameters as,

$$s^2 - \delta^2 = 1 - \alpha + \lambda \ . \tag{4.76}$$

Using (4.76), the Friedmann (4.73) and Raychaudhuri (4.74) equations can also be recast respectively in terms of the dimensionless parameters according to,

$$r'^2 = \frac{1}{r^4}\left(r^{3(1-w)} - \alpha\left(r^4 - 1\right) - 1 + \lambda\left(r^6 - 1\right)\right) \ , \tag{4.77}$$

$$r'' = -\frac{2}{r^5}\left(\frac{1+3w}{4}r^{3(1-w)} + \alpha - 1 - \lambda\left(\frac{r^6}{2} + 1\right)\right) \ , \tag{4.78}$$

where a prime denotes a derivative with respect to the rescaled rescaled cosmic time τ. It worth emphasizing that the dynamics of a homogeneous Weyssenhoff fluid does depend on just two parameters, which were chosen to be the curvature parameter α and cosmological constant parameter λ, since they are determined by observation.

The physical interpretation of these equations is well known. The Friedmann equation corresponds to the conservation law of energy whereas the Raychaudhuri equation represents the equation of motion.

The Friedmann equation (4.77) can be recast as follows,

$$\frac{1}{2}r'^2 + U_{\text{eff}}(r) = -\frac{\alpha}{2} \ , \tag{4.79}$$

where the effective potential is given by

$$U_{\text{eff}}(r) = -\frac{1}{2r^4}\left(r^{3(1-w)} + \alpha - 1 + \lambda\left(r^6 - 1\right)\right) \ . \tag{4.80}$$

The parameters present in the Friedmann and Raychaudhuri equations are respectively,

- w: relativistic pressure (SR: continuous parameter),

- α: curvature (GR: continuous parameter),
- -1: spin (EC: discrete parameter),
- λ: cosmological constant.

From the expression for the effective potential (4.80), we see that the spin contribution has a positive sign, which means that it behaves like a potential barrier. In other words, the spin-spin interaction leads to repulsive centrifugal forces opposing the attractive effect of gravity, thus preventing collapse. Note that this is also the case for a positive cosmological constant.

In the absence of relativistic pressure (i.e. $w = 0$), curvature (i.e. $\alpha = 0$), spin (i.e. the -1 factor vanishes), and cosmological constant (i.e. $\lambda = 0$) the Friedmann and the Raychaudhuri equations reduce respectively to the energy conservation law for a particle in a gravitational field with a vanishing total energy ($E_{\text{tot}} = 0$), and Newton's second law of motion.

The mathematical solutions for the time evolution of rescaled scale factor depend on the whole real range of the parameters (i.e. $w, \alpha, \lambda \in \mathbb{R}$). But for physical consistency, we have to restrict the value of these parameters. Firstly, the Weyssenhoff fluid cannot violate causality (i.e. $c_s < c$), which sets an upper bound on the equation-of-state parameter w,

$$w < 1 \ . \tag{4.81}$$

Secondly, the spin-shear condition (4.50) and the consistency condition at the bounce (4.76) restrict the range of the cosmological and curvature parameters according to,

$$\lambda > \alpha - 1 \ . \tag{4.82}$$

In general, it is not possible to find analytic solutions for the Friedmann (4.77) and Raychaudhuri (4.78) equations. However, it is possible to deduce the behaviour of the solutions by studying the asymptotic behaviour of the expansion rate parameter r' and its derivative r''.

In the limit where $r \to 1$, the temporal curvature of the rescaled scale factor behaves like,

$$\lim_{r\to 1} r'' = -3\left(\tfrac{2}{3}\alpha + \tfrac{1}{2}(w-1) - \lambda\right) \ , \tag{4.83}$$

and the expansion rate parameter r' has to vanish,

$$\lim_{r\to 1} r' = 0 \ , \tag{4.84}$$

to satisfy the consistency condition at the bounce (4.76). Hence, we find three types of solutions, which depend on the respective value of the parameters:

1. $\lim_{r\to 1} r'' > 0$, which implies that the solution $r(\tau)$ is found within the range

$$1 \leq r < \infty \ , \tag{4.85}$$

provided the parameters w and α satisfy

$$\lambda > \tfrac{2}{3}\alpha + \tfrac{1}{2}(w-1) \ . \tag{4.86}$$

2. $\lim_{r\to 1} r'' = 0$, which implies that the solution $r(\tau)$ is static

$$r = 1 \ , \tag{4.87}$$

when the parameters w and α satisfy

$$\lambda = \tfrac{2}{3}\alpha + \tfrac{1}{2}(w-1) \ . \tag{4.88}$$

3. $\lim_{r\to 1} r'' < 0$, which implies that the solution $r(\tau)$ is found within the range

$$0 \leq r \leq 1 \ , \tag{4.89}$$

provided the parameters w and α satisfy

$$\lambda < \tfrac{2}{3}\alpha + \tfrac{1}{2}(w-1) \ . \tag{4.90}$$

Moreover, the limit, $\lim_{r\to 0} r'^2 = -\infty < 0$, clearly does not exist. Hence, the solutions always satisfy $r > 0$, which means that there cannot be any singularity. Thus, for a negative temporal curvature $r'' < 0$, the rescaled scale factor r reaches a minimum value r^* found within the range $0 < r^* < 1$.

The behaviour of the solutions for the rescaled scale factor $r(\tau)$ is summarised in *Table* 4.1 below. Explicit numerical solutions in presence of a cosmological constant for particular values of the curvature parameter $\alpha = \{-\frac{1}{2}, 0, \frac{1}{2}\}$ and equation-of-state parameter $w = \{-1, -\frac{1}{3}, 0, \frac{1}{3}\}$ are displayed in *Figure* 4.2 - *Figure* 4.13.

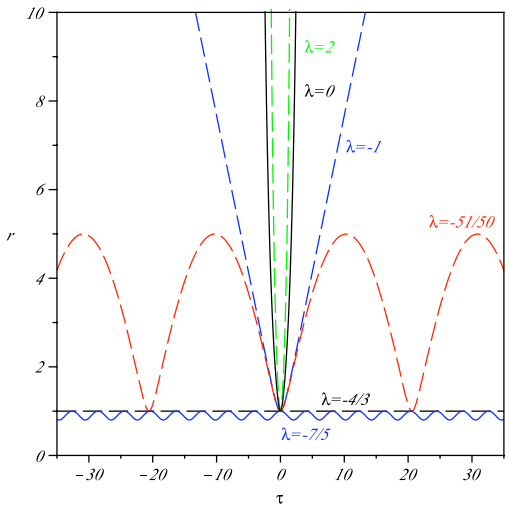

Figure 4.2: $\left(w=-1, \alpha=-\frac{1}{2}\right)$: $r(\tau)$ curves for $\lambda=\{-\frac{7}{5}, -\frac{4}{3}, -\frac{51}{50}, -1, 0, 2\}$

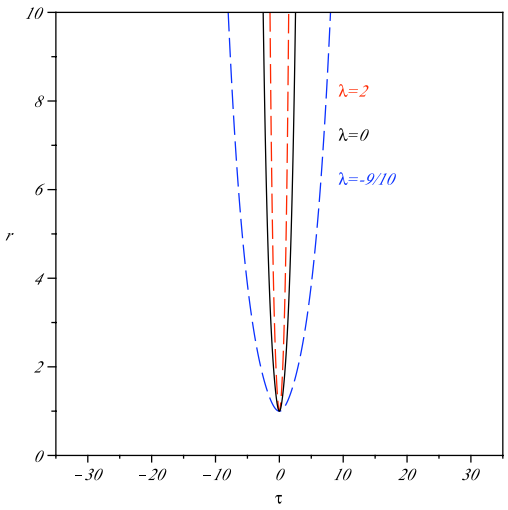

Figure 4.3: $(w=-1, \alpha=0)$: $r(\tau)$ curves for $\lambda=\{-\frac{9}{10}, 0, 2\}$

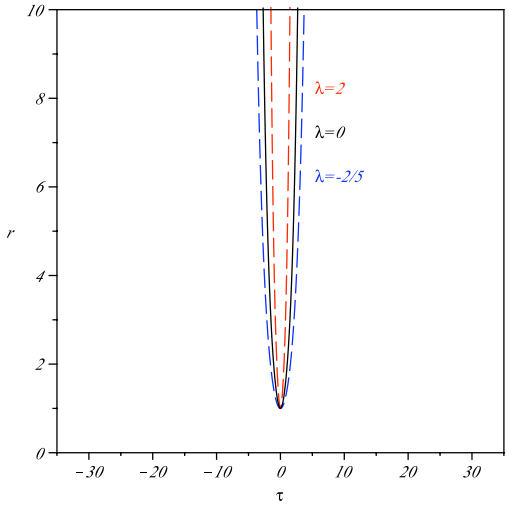

Figure 4.4: $\left(w=-1, \alpha=\frac{1}{2}\right)$: $r(\tau)$ curves for $\lambda=\{-\frac{2}{5}, 0, 2\}$

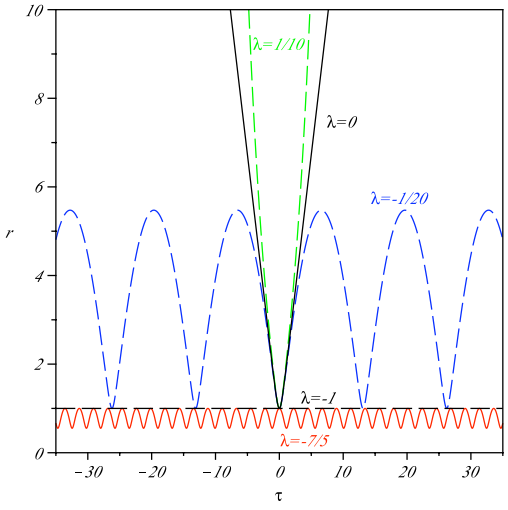

Figure 4.5: $\left(w=-\frac{1}{3}, \alpha=-\frac{1}{2}\right)$: $r(\tau)$ curves for $\lambda=\{-\frac{7}{5}, -1, -\frac{1}{20}, 0, \frac{1}{10}\}$

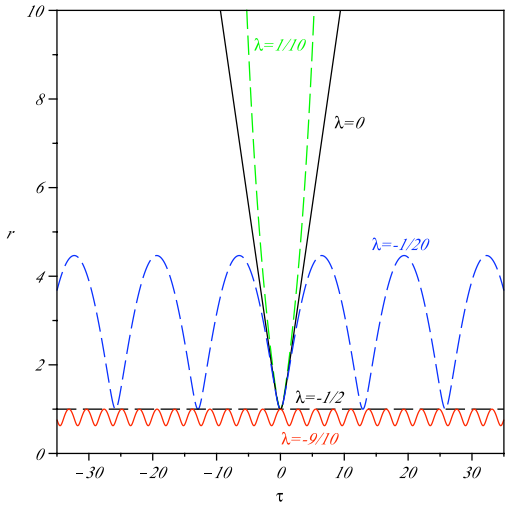

Figure 4.6: $\left(w=-\frac{1}{3}, \alpha=0\right)$: $r(\tau)$ curves for $\lambda=\{-\frac{9}{10}, -\frac{1}{2}, -\frac{1}{20}, 0, \frac{1}{10}\}$

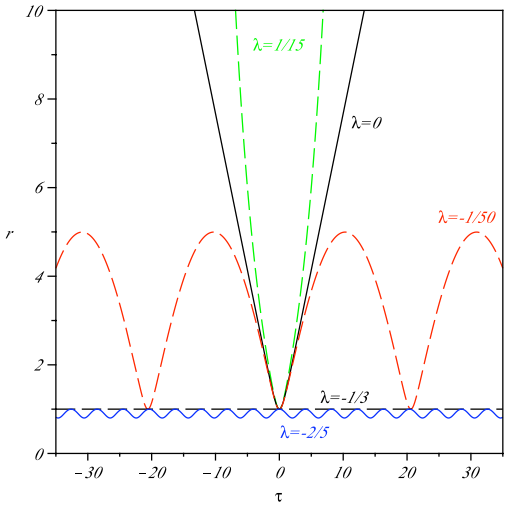

Figure 4.7: $\left(w=-\frac{1}{3}, \alpha=\frac{1}{2}\right)$: $r(\tau)$ curves for $\lambda=\{-\frac{2}{5}, -\frac{1}{3}, -\frac{1}{50}, 0, \frac{1}{15}\}$

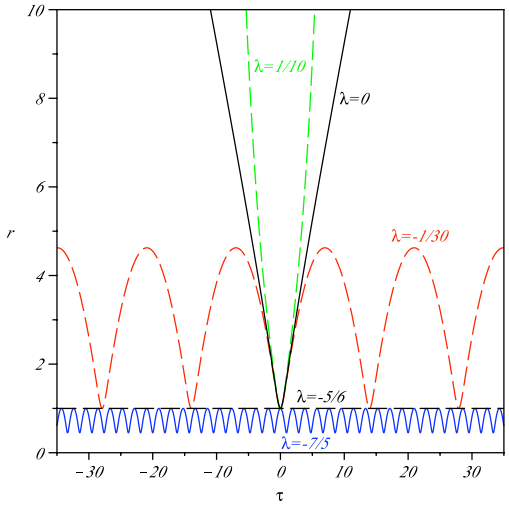

Figure 4.8: $\left(w=0, \alpha=-\frac{1}{2}\right)$: $r(\tau)$ curves for $\lambda=\{-\frac{7}{5}, -\frac{5}{6}, -\frac{1}{30}, 0, \frac{1}{10}\}$

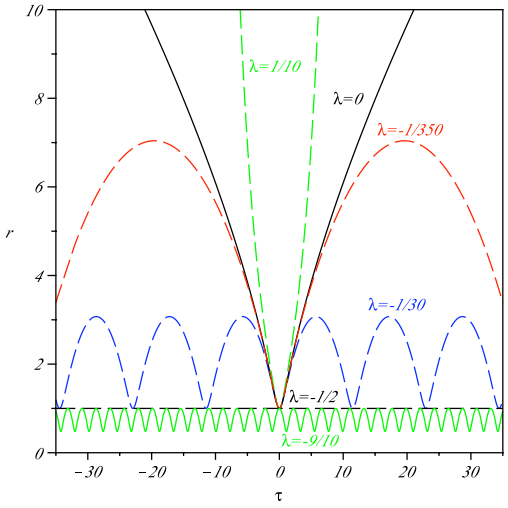

Figure 4.9: $(w=0, \alpha=0)$: $r(\tau)$ curves for $\lambda=\{-\frac{9}{10}, -\frac{1}{2}, -\frac{1}{30}, -\frac{1}{350}, 0, \frac{1}{10}\}$

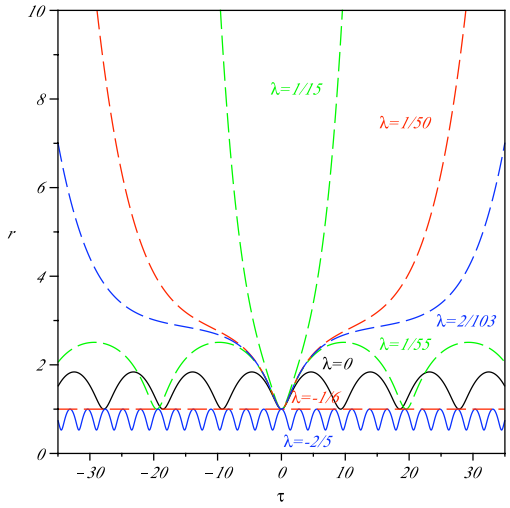

Figure 4.10: $\left(w=0, \alpha=\frac{1}{2}\right)$: $r(\tau)$ curves for $\lambda=\{-\frac{2}{5}, -\frac{1}{6}, 0, \frac{1}{55}, \frac{2}{103}, \frac{1}{50}, \frac{1}{15}\}$

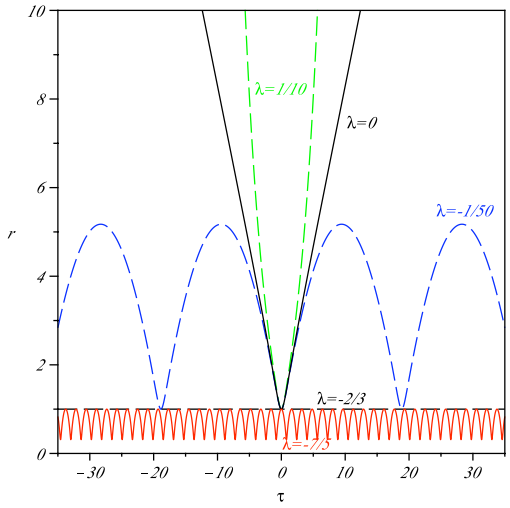

Figure 4.11: $\left(w=\frac{1}{3}, \alpha=-\frac{1}{2}\right)$: $r(\tau)$ curves for $\lambda=\{-\frac{7}{5}, -\frac{2}{3}, -\frac{1}{50}, 0, \frac{1}{10}\}$

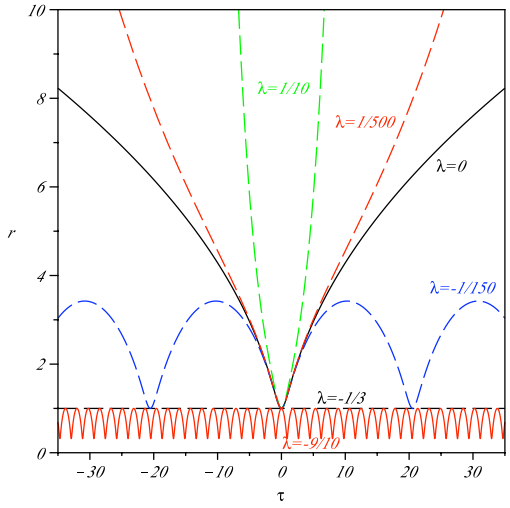

Figure 4.12: $\left(w=\frac{1}{3}, \alpha=0\right)$: $r(\tau)$ curves for $\lambda=\{-\frac{9}{10}, -\frac{1}{3}, -\frac{1}{150}, 0, \frac{1}{500}, \frac{1}{10}\}$

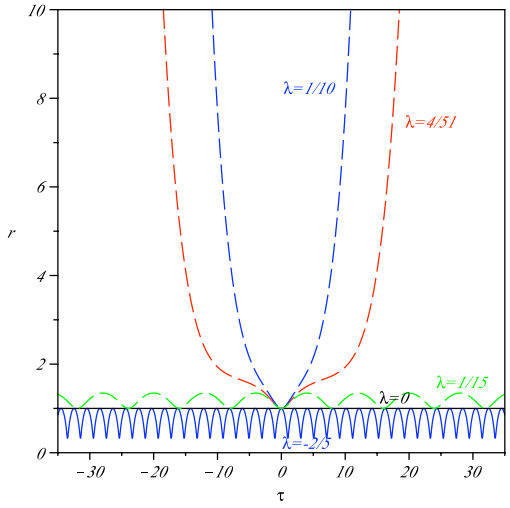

Figure 4.13: $\left(w=\frac{1}{3}, \alpha=\frac{1}{2}\right)$: $r(\tau)$ curves for $\lambda=\{-\frac{2}{5}, 0, \frac{1}{15}, \frac{4}{51}, \frac{1}{10}\}$

Table 4.1: Behaviour of the solutions $r(w, \alpha, \lambda)$

λ	r
$\lambda > \frac{2}{3}\alpha + \frac{1}{2}(w-1)$	$1 \leq r \leq \infty$
$\lambda = \frac{2}{3}\alpha + \frac{1}{2}(w-1)$	$r = 1$
$\lambda < \frac{2}{3}\alpha + \frac{1}{2}(w-1)$	$0 < r^* \leq r \leq 1$

4.5.2 Solutions in the absence of a cosmological constant

In the absence of a cosmological constant, the consistency condition at the bounce (4.76) reduces to,

$$s^2 - \delta^2 = 1 - \alpha \ . \tag{4.91}$$

Using the consistency condition (4.91), the Friedmann (4.77) and Raychaudhuri (4.78) respectively reduce to,

$$r'^2 = \frac{1}{r^4}\left(r^{3(1-w)} - \alpha\left(r^4 - 1\right) - 1\right) \ , \tag{4.92}$$

$$r'' = -\frac{1}{r^5}\left(\frac{1+3w}{2}r^{3(1-w)} + 2\left(\alpha - 1\right)\right) \ . \tag{4.93}$$

As in the presence of a cosmological constant, the behaviour of the solutions can be deduced from the asymptotic behaviour of the expansion rate parameter r' and its derivative r''. The corresponding results concerning limiting values of r' and r'' are obtained by setting $\lambda = 0$ in (4.83), (4.86), (4.88) and (4.90). In this simpler case, let us now consider the behaviour of the expansion rate parameter r' in the limit where $r \to \infty$ and $r \to 0$.

1. $w \leq -\frac{1}{3}$

$$\lim_{r\to\infty} r'^2 = \infty \geq 0 \ , \tag{4.94}$$

which implies that the solutions for the rescaled scale factor $r(\tau)$ diverge independently of the value of α.

2. $-\frac{1}{3} \leq w \leq 1$

$$\lim_{r\to\infty} r'^2 = -\alpha \geq 0 \ , \tag{4.95}$$

which implies that the solutions for the rescaled scale factor $r(\tau)$ diverge only for a non-closed spatial geometry (i.e. $\alpha \leq 0$). Hence for a weakly closed spatial geometry (i.e $r'' > 0$ and $0 < \alpha < \frac{3}{4}(1-w)$), the rescaled scale factor oscillates between a minimum value $r = 1$ and a maximum value r^* defined by $\lim_{r\to r^*} r' = 0$ according to,

$$1 \leq r \leq r^* \tag{4.96}$$

3. $w < 1$,

$$\lim_{r\to 0} r'^2 = -\infty < 0 \ , \tag{4.97}$$

which does clearly not exist. Hence, the solutions always satisfies $r > 0$, which means that there cannot be any singularity. For a strongly closed spatial geometry (i.e $r'' < 0$ and $0 < \frac{3}{4}(1-w) < \alpha < 1$), the rescaled scale factor oscillates between a maximum value $r = 1$ and a minimum value r^* defined by $\lim_{r\to r^*} r' = 0$ according to,

$$0 < r^* \leq r \leq 1 \tag{4.98}$$

The behaviour of the solutions for the rescaled scale factor $r(\tau)$ is summarised in *Table* 4.2 below. Explicit numerical solutions in presence of curvature (i.e. $\alpha \neq 0$) for $w = \{-1, -\frac{1}{3}, 0, \frac{1}{3}\}$ are displayed in *Figure* 4.14-*Figure* 4.17.

Table 4.2: Behaviour of the solutions $r(w, \alpha)$ for $\lambda = 0$

w	α	r
$w \leq -\frac{1}{3}$	$\alpha < 1$	$1 \leq r \leq \infty$
$-\frac{1}{3} < w < 1$	$\alpha \leq 0$	$1 \leq r \leq \infty$
	$0 < \alpha < \frac{3}{4}(1-w) < 1$	$1 \leq r \leq r^*$
	$0 < \alpha = \frac{3}{4}(1-w) < 1$	$r = 1$
	$0 < \frac{3}{4}(1-w) < \alpha < 1$	$0 < r^* \leq r \leq 1$

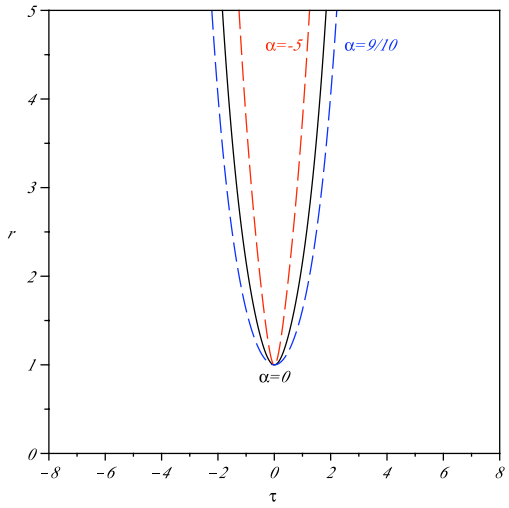

Figure 4.14: $(w = -1)$: $r(\tau)$ curves for $\alpha = \{-5, 0, \frac{9}{10}\}$

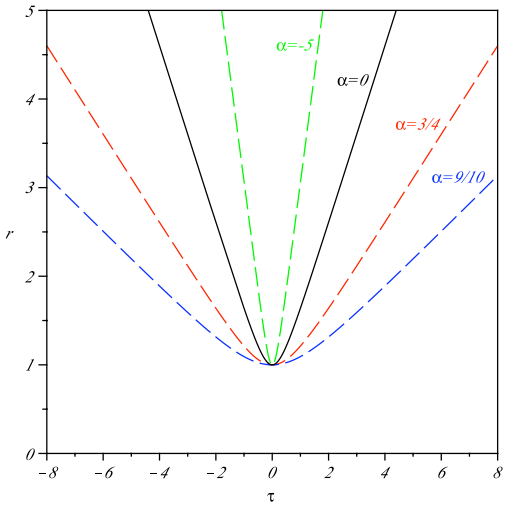

Figure 4.15: $\left(w = -\frac{1}{3}\right)$: $r(\tau)$ curves for $\alpha = \{-5, 0, \frac{3}{4}, \frac{9}{10}\}$

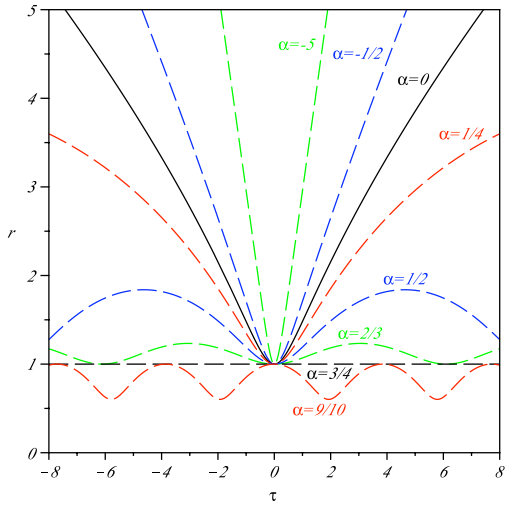

Figure 4.16: $(w = 0)$: $r(\tau)$ curves for $\alpha = \{-5, -\frac{1}{2}, 0, \frac{1}{4}, \frac{1}{2}, \frac{2}{3}, \frac{3}{4}, \frac{9}{10}\}$

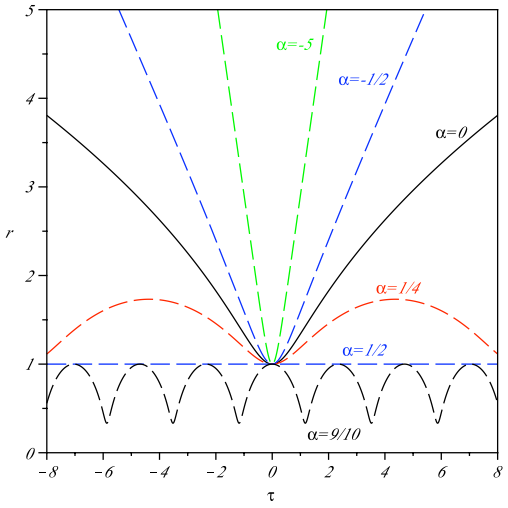

Figure 4.17: $\left(w = \frac{1}{3}\right)$: $r(\tau)$ curves for $\alpha = \{-5, -\frac{1}{2}, 0, \frac{1}{4}, \frac{1}{2}, \frac{9}{10}\}$

4.6 Dynamical evolution of spatially-flat models with zero cosmological constant

In this section, we restrict our study to models with a vanishing spatial curvature and cosmological constant (i.e. ${}^{(3)}\mathcal{R} = \Lambda = 0$) and find explicit solutions for the time evolution of the rescaled scale factor. The reason for choosing this particular class of models is because they admit analytical solutions. The dynamics of a homogeneous and anisotropic Weyssenhoff fluid in a spatially-flat model in the absence of a cosmological constant can be solved explicitly by determining the asymptotic behaviour of the time evolution of the rescaled scale factor for particular values of the equation of state parameter.

It is worth mentioning that exact bouncing solutions for spatially-flat cosmological models based on metric affine gravity theories (MAG), which include the solutions for the class of models based on a Weyssenhoff fluid, have previously been discussed by Stachowiak & Szydłowski (2007).

In the absence of curvature and a cosmological constant, the consistency condition at the bounce (4.76) reduces to,

$$s^2 - \delta^2 = 1 \ . \tag{4.99}$$

Using the consistency condition at the bounce (4.99) the Friedmann (4.77) and Raychaudhuri (4.78) equations can be rewritten in terms of the dimensionless parameters according to,

$$\left(\frac{r'}{r}\right)^2 = r^{-3(1+w)} - r^{-6} \ , \tag{4.100}$$

$$\frac{r''}{r} = -\frac{1+3w}{2} r^{-3(1+w)} + 2r^{-6} \ . \tag{4.101}$$

To obtain the explicit time evolution for the rescaled scale factor r, the Friedmann (4.100) or Raychaudhuri (4.101) equations have to be integrated. In order to obtain an analytical result, it is easier to integrate the Friedmann equation (4.100) according to,

$$\int \frac{r^2 dr}{\sqrt{r^{3(1-w)} - 1}} = \int d|\tau| \ . \tag{4.102}$$

The solution of this integral relation depends critically on the value of the equation of state parameter w. We will consider six special cases given respectively by $w = \{-1, -\frac{1}{3}, 0, \frac{1}{3}, 1, 2\}$, which all admit analytical solutions to (4.102). The last two solutions (i.e. $w = 1, 2$) are physically unacceptable (4.81) but mathematically interesting solutions.

We first note, however, that in the limit where the model approaches the bounce ($r \to 1$), the asymptotic solution for the rescaled scale factor has the quadratic form,

$$r(\tau) = \left(1 + \frac{3}{4}(1-w)\tau^2\right) \ , \tag{4.103}$$

for any equation-of-state parameter w.

Moreover, in the limit where the model is sufficiently far away from the bounce ($r \gg 1$), the asymptotic solution for the rescaled scale factor is given by,

$$r(\tau) = \ \exp\left(|\tau|\right) \ , \tag{4.104}$$

for an equation-of-state parameter $w = -1$, and evolves according to,

$$r(\tau) = \left(\frac{3}{2}\left(1+w\right)\tau\right)^{\frac{2}{3(1+w)}} \ , \tag{4.105}$$

for an equation-of-state parameter w satisfying $-1 < w < 1$. Hence, for a positively defined rescaled cosmic time ($\tau > 0$), the asymptotic solutions for the rescaled scale factor at late times, ($r \gg 1$), have the same time dependence as the solutions found within a GR framework. This is due to the fact that the spin contributions can be neglected at late times, which implies that the evolution of an effective Weyssenhoff fluid asymptotically reduces to a perfect fluid in GR at late times.

4.6.1 $w = -1$ case

A fluid with an equation-of-state parameter $w = -1$ behaves like a cosmological constant. By solving the integrated Friedmann equation (4.102) for such an equation-of-state parameter, the symmetric evolution of the rescaled scale factor with respect to the rescaled cosmic time is found to be,

$$r = \left(\cosh\left(3\tau\right)\right)^{1/3} \ . \tag{4.106}$$

For a Weyssenhoff fluid satisfying such an equation-of-state parameter, the symmetric temporal curvature of the rescaled scale factor $\ddot{r}(\tau)$ is positively defined at all times. Hence, for a positively defined rescaled cosmic time ($\tau > 0$), the model inflates perpetually. It starts with a power law inflation phase (4.103) and tends towards an exponentially inflating solution at late times (4.104).

4.6.2 $w = -\frac{1}{3}$ case

A fluid with $w = -\frac{1}{3}$ behaves like a macroscopic fluid made of cosmic strings. This result has been established by Vilenkin (1981) by performing a spatial averaging over a chaotic distribution of linear strings made of matter fields. For such an equation-of-state parameter, an implicit relation for the symmetric time evolution of the rescaled scale factor is found according to,

$$|\tau| = \frac{1}{r}\sqrt{r^4 - 1} + \mathfrak{Re}\left(\frac{1}{\sqrt{2}}\mathrm{F}\left(\arccos\left(\frac{1}{r}\right), \frac{1}{\sqrt{2}}\right) - \sqrt{2}\mathrm{E}\left(\arccos\left(\frac{1}{r}\right), \frac{1}{\sqrt{2}}\right)\right) , \tag{4.107}$$

where $F(\phi, k)$ and $E(\phi, k)$ are the elliptic integral of the first and second kind respectively. As in the previous case, the symmetric temporal curvature of the rescaled scale factor $\ddot{r}(\tau)$ is positively defined at all times. For a positively defined rescaled cosmic time ($\tau > 0$), the rescaled scale factor $r(\tau)$ tends asymptotically towards a constant rate of expansion (i.e. $\lim_{\tau \to \infty} \ddot{r}(\tau) = 0$) in this limiting case.

4.6.3 $w = 0$ case

A fluid with $w = 0$ behaves like dust. The non-singular behaviour of dust with spin was first investigated by Trautman (1973) and extended by Kuchowicz (1978). The integrated Friedmann equation (4.102) for an isotropic Weyssenhoff dust can be solved exactly. The symmetric evolution of the rescaled scale factor with respect to the rescaled cosmic time is given by,

$$r = \left(1 + \frac{9}{4}\tau^2\right)^{1/3} , \tag{4.108}$$

which agrees with the result established by Trautman.

4.6.4 $w = \frac{1}{3}$ case

A fluid with $w = \frac{1}{3}$ behaves like radiation. For such an equation-of-state parameter, an implicit relation for the symmetric time evolution of the rescaled scale factor is found according to,

$$|\tau| = \frac{1}{2}\left(r\sqrt{r^2-1} + \operatorname{arccosh}(r)\right) \ . \tag{4.109}$$

As in the anisotropic case, the isotropic solution of the rescaled scale factor for a relativistic fluid with spin (4.109) has a clear physical meaning. It is an interpolation between two limiting solutions, which describe an inflationary (4.103) and a radiation dominated (4.105) era respectively.

4.6.5 $w = 1$ case

A fluid with $w = 1$ behaves like stiff matter. For such an equation-of-state parameter, the derivative of the integrated Friedmann equation (4.102) with respect to the cosmic parameter yields a vanishing rate of expansion,

$$r' = 0 \ . \tag{4.110}$$

The value of the rescaled scale factor at the bounce is given by $r(0) = 1$. Hence, the trivial solution for the evolution of the rescaled scale factor with respect to the rescaled cosmic time is found according to,

$$r = 1 \ . \tag{4.111}$$

4.6.6 $w = 2$ case

Finally, a fluid with $w = 2$ behaves like ultra stiff matter. A fluid with an equation-of-state parameter $w > 1$ is physically unreasonable given that for such a fluid the speed of sound exceeds the speed of light ($c_s > c$). However, such a solution is mathematically interesting because it leads to the presence of singularities. By solving the integrated Friedmann equation (4.102) for an equation-of-state parameter $w = 2$, an implicit relation for the symmetric time evolution of the rescaled scale factor is found according to,

$$|\tau| = \frac{1}{3}\left(\sqrt{r^3\left(1-r^3\right)} + \arctan\sqrt{r^{-3}-1}\right) \ . \tag{4.112}$$

For a Weyssenhoff fluid with an equation-of-state parameter $w = 2$, the time-symmetric temporal curvature of the rescaled scale factor $\ddot{r}(\tau)$ is negatively defined at all times (4.59). To ensure the continuity of the expansion rate Θ at the bounce, the energy density at the bounce ρ_0 has to satisfy (4.55) even if the cosmological solution leads to the presence of singularities. As the absolute value of the rescaled cosmic time $|\tau|$ increases, the value of the rescaled scale factor decreases before eventually collapsing. From the implicit dynamical relation (4.112), the rescaled cosmic time $|\tau_c|$ at the collapse − defined by a vanishing rescaled scale factor $r(|\tau_c|) = 0$ − is found to be,

$$|\tau_c| = \frac{\pi}{6} \ . \tag{4.113}$$

The collapse of the scale factor $R \to 0$ is equivalent to the divergence of the expansion rate $\Theta \to \infty$. For an equation of state parameter $w = 2$, the collapse of the scale factor represents a mathematical singularity for the evolution of the scale factor with respect to the rescaled cosmic time given that the rate of expansion diverges at that point, $\Theta(\tau_c) = -\infty$.

4.6.7 Graphic solutions

The cosmological constant ($w = -1$), cosmic strings ($w = -\frac{1}{3}$), dust ($w = 0$), radiation ($w = \frac{1}{3}$), stiff matter ($w = 1$) and ultra stiff matter ($w = 2$) solutions for the evolution of the rescaled scale factor with respect the rescaled cosmic time $r(\tau)$ are shown in *Figure* 4.18. For a positively defined rescaled cosmic time ($\tau > 0$), the inflection point on the graph of $r(\tau)$ − for the dust and radiation solutions − corresponds to the end of inflation. The coordinates of this point are $(1.28, 1.41)$ for the radiation case and $(1.15, 1.59)$ for the dust case.

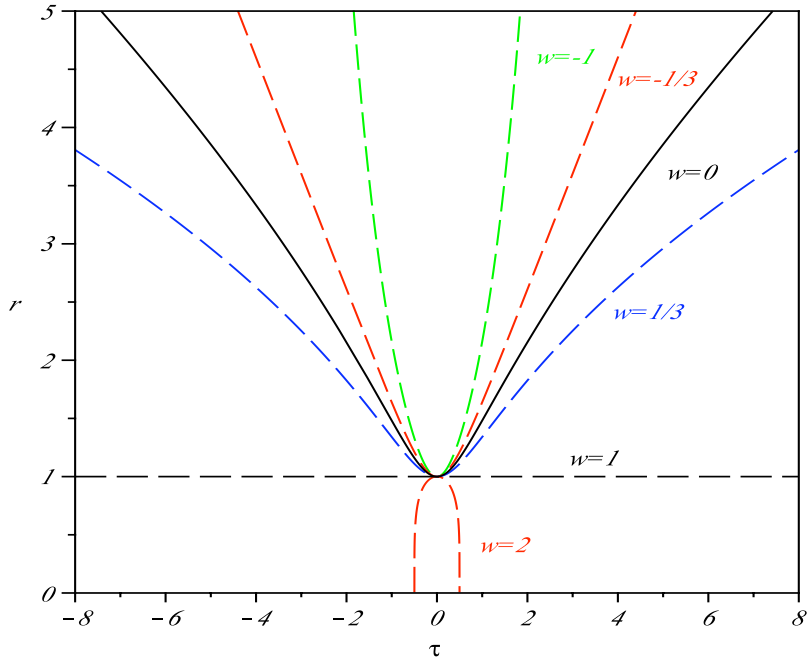

Figure 4.18: ($\alpha = \lambda = 0$): $r(\tau)$ curves for $w = \{-1, -\frac{1}{3}, 0, \frac{1}{3}, 1, 2\}$

Chapter 5

Classical initial conditions for the background evolution of inflation models

Cosmological inflation was first introduced by Guth (1981) and then extended by Linde (1982), to solve long standing problems with the paradigm of Big Bang cosmology. In addition to solving the monopole, flatness and horizon problems, inflation provides a mechanism for generating super-horizon scale cosmological perturbations from quantum fluctuations of the inflaton field (see, for example, Mukhanov *et al.* (1992)). Inflation thus predicts that large scale structures in the universe are the result of quantum-mechanical fluctuations occurring during the inflationary epoch. Inflationary perturbations of this type are consistent with the anisotropy power spectrum of the CMB as mentioned by Hinshaw *et al.* (2003).

In this chapter, we focus primarily on the background dynamics of inflationary models. This cosmological evolution can generally only be determined numerically, which implies that initial conditions for the numerical integration have first to be obtained. Although inflationary dynamics requires a rigorous quantum treatment, it is possible to adopt a classical phenomenological approach to setting the initial conditions. In particular, we consider two different inflationary models proposed by Boyanovsky *et al.* (2006b) (BVS), and by Lasenby & Doran (2005) (LD), which have followed such an approach. We then develop a new

method that is inspired by the LD approach, but relies only on a kinetic dominated regime which describes the dynamics of the inflaton field immediately after the model emerges from the initial singularity.

The structure of this chapter is as follows. In *Section* 5.1, we will briefly introduce the dynamics of inflationary models based on a scalar field. In *Section* 5.2 and *Section* 5.3 we will discuss how the initial conditions are obtained respectively in the BVS model and the LD model. In *Section* 5.4 and *Section* 5.5, we will examine how the initial conditions are determined in the kinetically dominated regime for a chaotic and a new inflation potential respectively. Finally, we will briefly discuss the scalar perturbations of inflationary models with a chaotic and a new inflation potentials in *Section* 5.6.

5.1 Scalar field inflation models

The simplest way to create a homogeneous and isotropic cosmological background model which undergoes an inflation phase is by assuming a real, time-dependent and homogeneous scalar field as the matter source.

For a scalar field ϕ with a potential $V(\phi)$, the evolution equations, i.e. the Raychaudhuri equation and the equation of motion for the scalar field, are respectively given by,

$$\dot{H} + H^2 = -\frac{\kappa}{3}\left(\dot{\phi}^2 - V(\phi)\right) \ , \tag{5.1}$$

$$\ddot{\phi} + 3H\dot{\phi} + \frac{d}{d\phi}V(\phi) = 0 \ , \tag{5.2}$$

where $\kappa = 8\pi$, H is the Hubble parameter and a dot denotes a derivative with respect to cosmic time. The energy conservation of the scalar field is expressed by the Friedmann equation,

$$H^2 = \frac{\kappa}{3}\left(\frac{1}{2}\dot{\phi}^2 + V(\phi)\right) - \frac{k}{R^2} \ , \tag{5.3}$$

where R is the scale factor, k the curvature parameter and $H = \dot{R}/R$.

The onset of inflation is defined as $\ddot{R} = 0$, or equivalently as $\dot{H}+H^2 = 0$, which can be recast in terms of the scalar field using the Raychaudhuri equation (5.1)

as,

$$\dot{\phi}^2 = V(\phi) \ . \tag{5.4}$$

The slow roll inflation regime satisfies,

$$\dot{\phi}^2 \ll V(\phi) \ . \tag{5.5}$$

The amount of inflation is measured by the number of e-folds N, which is related to the Hubble parameter H by,

$$\dot{N} = H \ . \tag{5.6}$$

For a generic potential $V(\phi)$, there is no analytic solution for the dynamics of a scalar field inflation model. Hence, the evolution equations (5.1) and (5.2) have to be integrated numerically using suitable initial conditions on H, ϕ and $\dot{\phi}$. In the following sections, three different ways of determining the initial conditions are discussed. The inflationary model of Boyanovsky, de Vega and Sanchez (BVS) is compared to the model of Lasenby and Doran (LD) and the latter is used as the basis for our new method based on the kinetic domination of the scalar field energy at early times.

5.2 Boyanovsky, de Vega and Sanchez (BVS) initial conditions for inflation

BVS assume a spatially-flat model and an inflaton potential typical of new inflation. One of the main features of the BVS model, is that the initial conditions are set via energy equipartition,

$$\frac{1}{2}\dot{\phi}_{\rm eq}^2 = V(\phi_{\rm eq}) \ , \tag{5.7}$$

where the eq-suffix denotes quantities evaluated at equipartition $t = t_{\rm eq}$ which, from (5.4), is prior to the onset of inflation. At the onset of inflation (5.4), the inflaton ϕ does not enter the slow-roll regime (5.5) straight away. Before reaching the slow-roll regime, the inflaton loses most of its kinetic energy in the so-called "fast-roll" regime, defined by Linde (2001), which is very brief compared to the slow-roll phase.

It is worth mentioning, even if this is not the main purpose of this work, that the existence of a fast-roll period has important consequences for behaviour of the inflationary perturbations. The fast-roll regime behaves like an attractive potential in the wave equations for the mode functions of curvature and tensor perturbations. This potential leads then to the suppression of the primordial power spectra on large scales. Hence, it might be able to account for the suppression of the quadrupole of the CMB in agreement with observational data as suggested by Boyanovsky *et al.* (2006a).

For convenience, we introduce a dimensionless parameter h defined as,

$$h \equiv \frac{H}{H_i} \ , \tag{5.8}$$

where H_i is the Hubble parameter at the onset $t = t_i$ of slow-roll inflation, and is nearly constant during the slow-roll inflation regime (i.e. $H \simeq H_i$). To recover the results of BVS, it is also useful to recast the evolution equations in terms of the number of e-folds. Using (5.6), we deduce that an arbitrary functional $f(N(t))$ has to satisfy,

$$\dot{f} = H f' \ , \tag{5.9}$$

where the prime denotes a derivative with respect to the number of e-folds. Using this change of variables (5.9), the evolution equations (5.1) and (5.2) are respectively recast as,

$$h h' + h^2 = -\frac{\kappa}{3}\left(h^2 \phi'^2 - \frac{1}{H_i^2} V(\phi)\right) \ , \tag{5.10}$$

$$h^2 \phi'' + 3h^2 \phi' + \frac{1}{H_i^2}\frac{d}{d\phi} V(\phi) = 0 \ . \tag{5.11}$$

In order to have no explicit dependence on H_i in their model, BVS studied a new inflation potential of the form,

$$V(\phi) = \frac{3H_i^2}{\kappa}\left(1 - \mu\kappa\phi^2\right)^2 \ , \tag{5.12}$$

displayed in *Figure* 5.1, where $\mu \propto m^{-2}$ is a constant, and m is the mass of the scalar field. We note that, rather curiously, the amplitude of the potential is set by the Hubble parameter during the slow-roll inflation period that results from this same potential, which appears as a rather circular methodology.

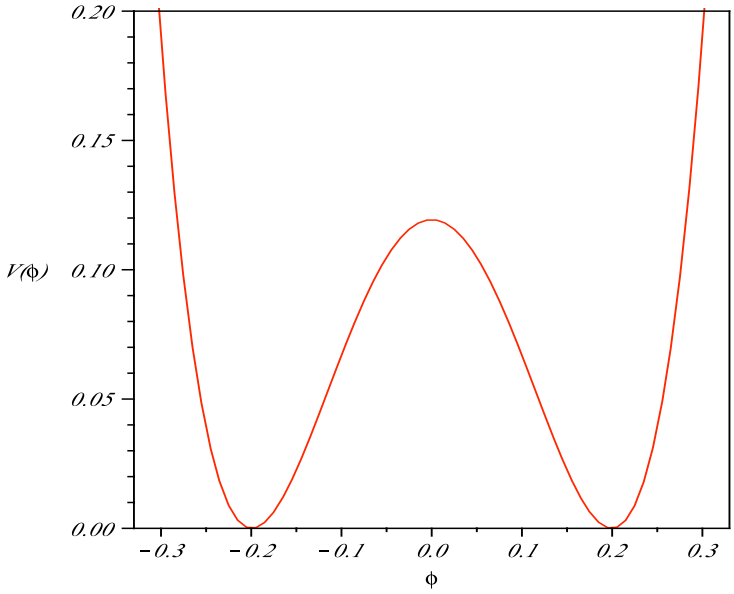

Figure 5.1: New inflation potential $V(\phi)$ with $\mu = 1$ and $H_i = 1$.

The evolution equations (5.10) and (5.11) can then be recast as,

$$hh' + h^2 = -\frac{\kappa}{3}\left(h^2\phi'^2 - \frac{3}{\kappa}\left(1 - \mu\kappa\phi^2\right)^2\right) \ , \tag{5.13}$$

$$h^2\phi'' + 3h^2\phi' - 12\mu\phi\left(1 - \mu\kappa\phi^2\right) = 0 \ . \tag{5.14}$$

During the slow-roll phase defined by (5.5), the kinetic term ϕ'^2 can be neglected, whilst the Hubble parameter $H \simeq H_i$ and the inflaton field $\phi \simeq \phi_i$ are nearly constant. The Friedmann equation (5.3) in a spatially-flat case ($k = 0$) and the expression for the potential (5.12) in the slow-roll regime imply that,

$$H_i^2 \simeq \frac{\kappa}{3}V(\phi_i) = H_i^2\left(1 - \mu\kappa\phi_i^2\right)^2 \ , \tag{5.15}$$

This expression sets a constraint on the scalar field during the slow-roll phase according to,

$$\mu\kappa\phi_i^2 \ll 1 \ . \tag{5.16}$$

To set up the initial value of the scalar field $\phi_{\rm eq}$, BVS assumed that the inflaton ϕ was initially at the local maximum of the potential $V(\phi)$, i.e.

$$\phi_{\rm eq} = 0 \ . \tag{5.17}$$

Using the initial condition for the scalar field (5.17) and the constraint on the scalar field during the slow roll phase (5.16), the potential $V_{\rm eq}$ at $t = t_{\rm eq}$ and the potential V_i at the onset of slow-roll inflation $t = t_i$ are simply related as follows,

$$V_{\rm eq} \simeq V_i \ . \tag{5.18}$$

Using (5.18) and the equipartition of energy relation (5.7) to evaluate the Friedmann equation at equipartition (i.e. $t = t_{\rm eq}$) and comparing this result to the Friedmann equation during slow roll (i.e. $t = t_i$), the initial value of the parameter $h_{\rm eq}$ is found to be,

$$h_{\rm eq} = \sqrt{2} \ . \tag{5.19}$$

By substituting the expression for the potential (5.12) into the initial equipartition of energy relation (5.7) and using the initial condition for the dimensionless Hubble parameter (5.19), $\phi'_{\rm eq}$ is found to be,

$$\phi'_{\rm eq} = \sqrt{\frac{3}{\kappa}} \ . \tag{5.20}$$

The last parameter which needs to be set is μ. BVS made the arbitrary choice $\mu = 0.008$, as mentioned in their publication.

Using the initial conditions (5.17), (5.19) and (5.20), and numerically integrating the evolution equations (5.13) and (5.14), we studied the behaviour of the $h(N)$-curves for different values of μ as shown in *Figure* 5.2. Note that the middle curve corresponds to the result found by BVS and displayed by Boyanovsky *et al.* (2006b).

Figure 5.2 shows that the BVS model is highly fine-tuned given that a change by factor of 10 in the value of the parameter μ changes the number of e-folds by an order of magnitude. Hence, the arbitrary $\mu = 0.008$ seems to be carefully chosen in order to lead to an amount of inflation in agreement with current observations. For $\mu = 0.05$, the numerical value of $\kappa\mu\phi_i^2 \approx 0.03$, which implies that the constraint on the potential (5.16) is satisfied. For smaller values of μ, the inequality (5.16) is even better satisfied.

It is worth mentioning that although the BVS procedure enables numerical solutions to be obtained for a new inflation like potential, it cannot be applied for a chaotic potential. In the latter case, the initial value of the scalar field

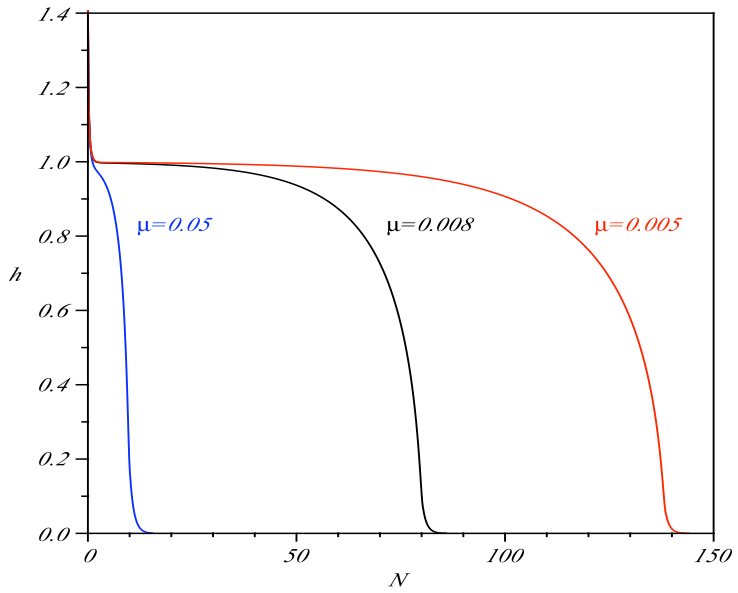

Figure 5.2: Hubble parameter h in terms of the number of e-folds N for $\mu = \{0.005, 0.008, 0.05\}$.

cannot be zero because otherwise it would already be at the global minimum of the potential and could certainly not inflate.

5.3 Lasenby, Doran (LD) initial conditions for inflation

LD assume a spatially-closed model with a natural boundary on the total conformal time and a chaotic inflation potential. To compare this model with the BVS model, however, we will restrict our analysis to a spatially-flat limit. One important feature of the model is that it shows quite generally how the Hubble parameter H and the scalar field ϕ admit a series expansion about the initial singularity at $t = 0$. These series expansions enable one to set initial conditions very shortly after the big bang singularity, as set out below.

We first briefly explain how these series expansions can be constructed follow-

ing the procedure of LD. The LD-model is based on a chaotic potential,

$$V(\phi) = \frac{1}{2}m^2\phi^2 \ . \tag{5.21}$$

Using this expression, the evolution equations (5.1) and (5.2) are respectively recast as,

$$\dot{H} + H^2 = -\frac{\kappa}{3}\left(\dot{\phi}^2 - \frac{1}{2}m^2\phi^2\right) \ , \tag{5.22}$$

$$\ddot{\phi} + 3H\dot{\phi} + m^2\phi = 0 \ . \tag{5.23}$$

The Friedmann (5.3) equation becomes,

$$H^2 = \frac{\kappa}{3}\left(\frac{1}{2}\dot{\phi}^2 + \frac{1}{2}m^2\phi^2\right) \ . \tag{5.24}$$

The solutions of the evolution equations (5.22) and (5.23) satisfy a classical scaling property which relates two solutions in a family of solutions determined respectively at t and $\tilde{t} = \sigma^{-1}t$ by a constant scaling factor σ,

$$\begin{aligned} \tilde{H}(\tilde{t}) &= \sigma H(t) \ , \\ \tilde{\phi}(\tilde{t}) &= \phi(t) \ , \\ \tilde{m} &= \sigma m \ , \end{aligned} \tag{5.25}$$

where a tilde denotes rescaled solutions. Note that this scaling property is useful for numerical integration but does not survive quantisation. By changing the mass of the scalar field, the solutions are not qualitatively but only quantitatively changed given that the physical variables are rescaled. Without loss of generality, we will from now on consider the case where $m = m_p = 1$.

Coming out of the initial singularity, the dynamics of the inflationary model is kinetically dominated ($\dot{\phi}^2 \gg V(\phi)$), which means that the Hubble parameter $H \propto t^{-1}$. The Raychaudhuri equation (5.22) implies that the scalar field ϕ must contain a term going as $\ln(t)$. But this then implies that the Hubble parameter H must also contain a term in $t\ln(t)$ in order to satisfy the equation of motion of the scalar field (5.23). By iterating this process, we conclude that a series expansion in terms of $\ln(t)$ is required to describe the behaviour around the singularity. To

perform the series expansion, it is convenient to introduce the dimensionless time variable,

$$\tau = \frac{t}{t_p} \ , \tag{5.26}$$

where t_p is the Planck time, which is used for dimensional reasons only, given that in Planck units $t_p = 1$. The series expansion about the initial singularity can now be written as,

$$H(\tau) = \frac{1}{t_p} \sum_{n=0}^{\infty} H_n(\tau) \ln^n(\tau) \ , \tag{5.27}$$

$$\phi(\tau) = \frac{1}{l_p} \sum_{n=0}^{\infty} \phi_n(\tau) \ln^n(\tau) \ , \tag{5.28}$$

where $l_p = 1$ is the Planck length. Note that all the coefficients in the expansion, i.e. H_n and ϕ_n, are dimensionless. Since we are working in Planck units, i.e. $t = \tau$, we will use only the dimensional cosmic time t from now on.

By substituting the series expansions for H and ϕ into the evolution equations (5.22) and (5.23), LD showed that the series are controlled by only one arbitrary constant, b_0, which determines the number of e-folds. To second order, the series expansions for $H(t)$ and $\phi(t)$ are respectively,

$$\begin{aligned} H_{\text{exp}}(t) = \frac{1}{3t} &+ \left(\frac{2}{81} + \frac{4}{9}\sqrt{\frac{\pi}{3}} b_0 + \frac{4\pi}{3} b_0^2 \right) m^2 t \\ &- \left(\frac{2}{27} t + \frac{4}{3}\sqrt{\frac{\pi}{3}} b_0 t \right) m^2 \ln(t) \\ &+ \left(\frac{1}{9} t \right) m^2 \ln^2(t) + \mathcal{O}(3) \ , \end{aligned} \tag{5.29}$$

$$\begin{aligned} \phi_{\text{exp}}(t) = b_0 &- \left(\frac{11}{1296}\sqrt{\frac{3}{\pi}} + \frac{1}{36} b_0 - \frac{1}{2}\sqrt{\frac{\pi}{3}} b_0^2 \right) m^2 t^2 \\ &- \left(\frac{1}{6}\sqrt{\frac{3}{\pi}} - \left(\frac{1}{216}\sqrt{\frac{3}{\pi}} - \frac{1}{6} b_0 \right) m^2 t^2 \right) \ln(t) \\ &+ \left(\frac{1}{72}\sqrt{\frac{3}{\pi}} t^2 \right) m^2 \ln^2(t) + \mathcal{O}(3) \ , \end{aligned} \tag{5.30}$$

where we reintroduced explicitly the mass variable $m = 1$ to compare the expanded solution with the massless case.

In principle, the series expansions $H_{\rm exp}(t)$ and $\phi_{\rm exp}(t)$ enable us to determine suitable 'initial' conditions, at some arbitrary time $t = t_0$ prior to inflation, for the subsequent numerical integration of the evolution equations (5.22) and (5.23) by simply setting,

$$\begin{aligned} H(t_0) &= H_{\rm exp}(t_0) \ , \\ \phi(t_0) &= \phi_{\rm exp}(t_0) \ , \\ \dot{\phi}(t_0) &= \dot{\phi}_{\rm exp}(t_0) \ . \end{aligned} \tag{5.31}$$

In practice, expanding series to some order to set initial conditions for numerical integration means that the initial integration time $t = t_0$ must lie within the domain in which these series, i.e. (5.29) and (5.30), provide a good approximation. The analysis of the range of validity of the series expansions is given in *Appendix* C.1.

The analytic expressions for the series expansions depend on an undetermined parameter b_0, which we arbitrarily set to $b_0 = 2.48$ in the previous discussion. The physical role of this parameter can be inferred from *Figure* 5.3. A variation of the series expansion parameter b_0 translates the $H(N)$-curves thus directly affecting the number of e-folds as shown in *Figure* 5.3. This is in line with the analysis of LD who showed that b_0 is related to the number of e-folds. Note that, similarly to the BVS model, the LD model is also fine tuned given that a factor 5 variation in the numerical value of b_0 results in an order of magnitude change in the number of e-folds N as illustrated in *Figure* 5.3.

5.4 Kinetic initial conditions for a chaotic inflation potential

As the universe emerges from the initial singularity, the kinetic energy dominates, i.e. $\dot{\phi}^2 \gg V(\phi)$, which is the main feature of our new procedure to set the initial conditions for the pre-inflationary dynamics. In the singularity limit, where potential $V(\phi)$ can be neglected, the evolution equations (5.1)-(5.3) reduce

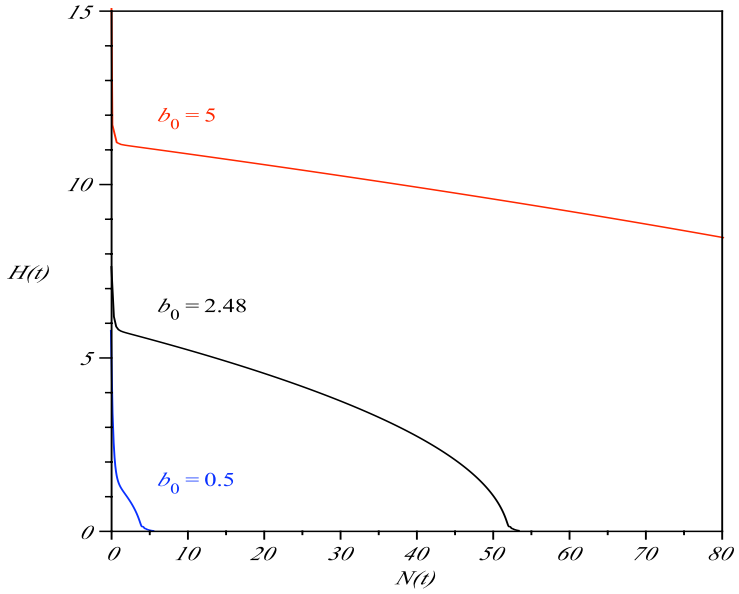

Figure 5.3: $H(N)$ for different values of $b_0 = \{0.5, 2.48, 5\}$.

respectively to,

$$\dot{H}_{\rm kin} + H^2_{\rm kin} = -\frac{\kappa}{3}\dot{\phi}^2_{\rm kin} \ , \tag{5.32}$$

$$H^2_{\rm kin} = \frac{\kappa}{6}\dot{\phi}^2_{\rm kin} - \frac{k}{R^2_{\rm kin}} \ , \tag{5.33}$$

$$\ddot{\phi}_{\rm kin} + 3H_{\rm kin}\dot{\phi}_{\rm kin} = 0 \ , \tag{5.34}$$

where the subscript $_{\rm kin}$ refers to a kinetically dominated model. By integrating the equation of motion for the (effectively massless) scalar field (5.34), the kinetic energy term is found to scale like $\dot{\phi}^2_{\rm kin} \propto R^{-6}_{\rm kin}$. Thus, in the singularity limit, i.e. $R_{\rm kin} \to 0$, the kinetic energy dominates the curvature term $\frac{k}{R^2_{\rm kin}}$ and the Friedmann equation (5.33) can be recast as,

$$H^2_{\rm kin} = \frac{\kappa}{6}\dot{\phi}^2_{\rm kin} \ , \tag{5.35}$$

By integrating the Raychaudhuri (5.32) and Friedmann (5.35) equations, the expression for the Hubble parameter $H_{\rm kin}(t)$ and scalar field $\phi_{\rm kin}(t)$ are found to

be,

$$H_{\rm kin}(t) = \frac{1}{3t} \ , \tag{5.36}$$

$$\phi_{\rm kin}(t) = \lambda - \sqrt{\frac{2}{3\kappa}}\,\ln(t) \ , \tag{5.37}$$

where λ is an integration constant. Note that with the parameter identification $\lambda = b_0$, the kinetically dominated quantities (5.36) and (5.37) represent the leading order terms of the LD series expansions, which are (5.29) and (5.30) respectively. The kinetically dominated solutions simply correspond to the dynamics obtained for a massless scalar field. Hence, by switching off the potential in the LD model, we recover the solutions of our kinetic model.

For spatially open or flat models, the curvature term in (5.3) will not be negative, which implies that $H^2 > 0$ at all times from the initial singularity to the end of the inflationary epoch. However, for spatially closed models, this is not necessarily the case, since the negative curvature term may cause a bounce. In order to avoid a bounce, a singularity condition has to be imposed on spatially closed models. At the onset of inflation, i.e. $\dot{\phi}_b^2 = V(\phi_b)$, the kinetic energy term scales like a curvature term, i.e. $\dot{\phi}_b^2 \propto R^{-2}$, where the suffix b denotes the beginning of inflation. The scaling of the kinetic energy term before and after the onset of inflation is determined by (5.2) according to,

$$\begin{aligned} \dot{\phi}^2(t) &\propto R^{-2-\epsilon} \qquad \text{if} \quad t < t_b \\ \dot{\phi}^2(t) &\propto R^{-2+\epsilon} \qquad \text{if} \quad t > t_b \ , \end{aligned} \tag{5.38}$$

where $\epsilon > 0$. Since any potential is defined up to a constant (without loss of generality), we only consider a positive potential, i.e. $V(\phi) > 0$, in the following discussion. If the total energy of the scalar field at the onset of inflation is larger than the curvature term

$$H_b^2 = \frac{\kappa}{3}\left(\frac{1}{2}\dot{\phi}_b^2 + V(\phi_b)\right) - \frac{1}{R_b^2} > 0 \ , \tag{5.39}$$

then it will be so at all times, thereby ensuring the presence of an initial singularity. Hence, the condition (5.39), which a spatially-closed model has to satisfy

in order to avoid a bounce, depends explicitly on the potential at the onset of inflation (5.4) and is given by,

$$V(\phi_b) > \frac{2}{\kappa R_b^2} \ . \tag{5.40}$$

To sum up, we have shown that all homogeneous and isotropic inflation models which do not have a bounce, go through a kinetically dominated regime as they emerge from the initial singularity where the dynamics is independent of the potential and the curvature.

The analysis of the range of validity of the kinetically dominated regime for a chaotic inflation potential is given in *Appendix* C.2. In a kinetically dominated regime, $H_{\rm kin}(t)$ and $\phi_{\rm kin}(t)$ are respectively determined by (5.36) and (5.37) and thus satisfy,

$$\frac{d\ln(H_{\rm kin})}{d\ln(t)} = -1 \ , \tag{5.41}$$

$$\frac{d\phi_{\rm kin}}{d\ln(t)} = -\sqrt{\frac{2}{3\kappa}} \approx -0.16 \ . \tag{5.42}$$

On a logarithmic scale, the estimated time range within which the solutions are kinetically dominated is $\ln(t_0) \lesssim -6$, which is well before the onset of inflation occurring at $\ln(t_i) = -2.74$. The logarithmic curves displayed in *Figure* 5.4 and *Figure* 5.5 show that for a time range $\ln(t) \lesssim -4$ the behaviour of the numerically integrated solutions $H_{\rm int}(t)$ and $\phi_{\rm int}(t)$ is virtually indistinguishable from the behaviour of the solutions $H_{\rm kin}(t)$ and $\phi_{\rm kin}(t)$ obtained in a kinetically dominated regime. This corroborates the fact that we are entirely justified in considering the solutions to be kinematically dominated for a time range $t \leq 10^{-3}$.

5.5 Kinetic initial conditions for a new inflation potential

Since the kinetic dominated approach can be applied at early times to models with arbitrary inflation potential, as shown in *Section* 5.4, we discuss now the kinetic initial conditions for an inflation model with a new inflation potential. Kinetic

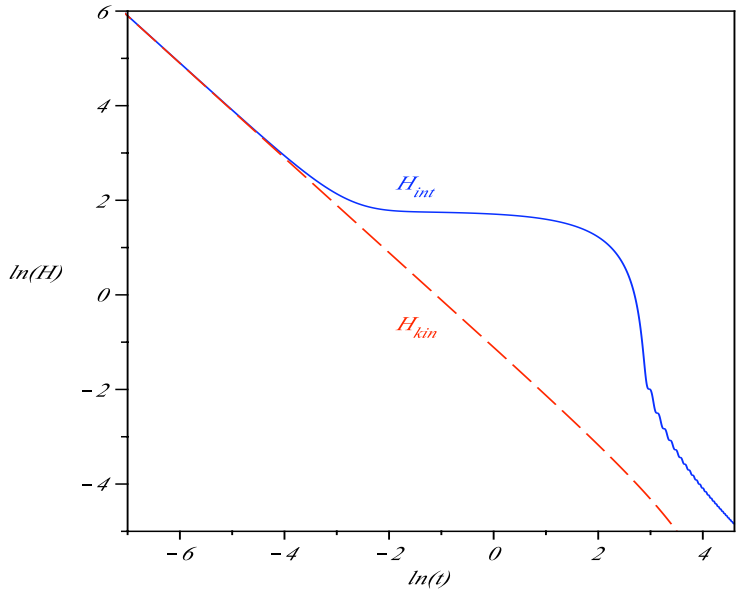

Figure 5.4: Comparison between $\ln(H_{\rm int})$ and $\ln(H_{\rm kin})$ as a function of $\ln(t)$ for a chaotic inflation potential

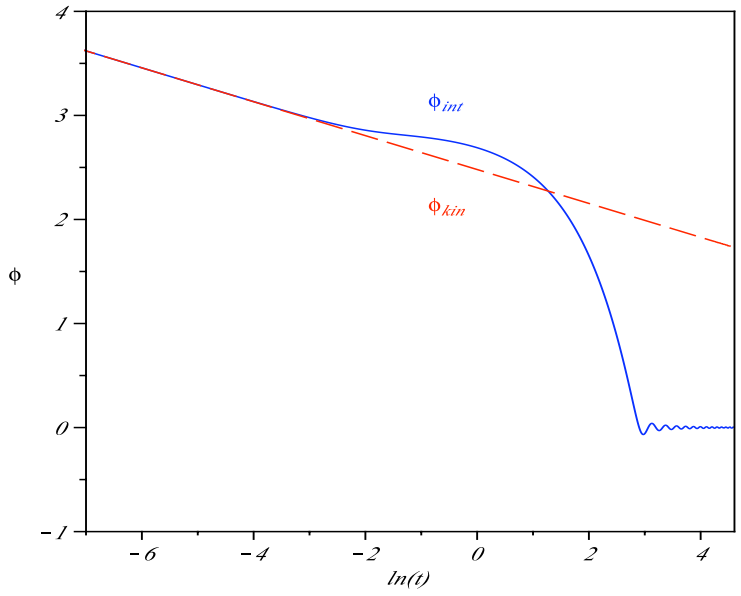

Figure 5.5: Comparison between $\phi_{\rm int}$ and $\phi_{\rm kin}$ as a function of $\ln(t)$ for a chaotic inflation potential

initial conditions for inflation are not generally incompatible with a generic new inflation potential. However, they are incompatible with the specific new inflation model proposed by BVS, as we now briefly show. Energy conservation in the BVS model implies that,

$$\tfrac{1}{2}\dot{\phi}_0^2 + V(\phi_0) = 2V(\phi_{\rm eq}) \ . \tag{5.43}$$

The BVS model also requires the inflaton field to vanish at the equipartition of energy, $\phi_{\rm eq} = 0$. Using the expression for the potential (5.12), and the constraint on the inflaton at the equipartition of energy (5.17), the energy conservation relation (5.43) and the kinetically dominated constraint on the initial conditions $\dot{\phi}_0^2 \gg V(\phi_0)$ respectively become,

$$\left(1 - \mu\kappa\phi_0^2\right)^2 = 2 - \frac{3\kappa}{2H_i^2}\dot{\phi}_0^2 \ , \tag{5.44}$$

$$\left(1 - \mu\kappa\phi_0^2\right)^2 \ll \frac{3\kappa}{H_i^2}\dot{\phi}_0^2 \ . \tag{5.45}$$

The energy conservation (5.44) and the kinetic constraint on the initial conditions (5.45) require the initial value of the inflaton field ϕ_0 and its first derivative $\dot{\phi}_0$ to satisfy respectively,

$$\left(1 - \mu\kappa\phi_0^2\right)^2 \ll \frac{4}{3} \ . \tag{5.46}$$

$$\dot{\phi}_0^2 \gg \frac{4H_i^2}{9\kappa} \ , \tag{5.47}$$

Using the energy conservation relation (5.44) and the constraint on the initial inflaton field (5.46), the initial value of its first derivative is found to be,

$$\dot{\phi}_0^2 \approx \frac{4H_i^2}{3\kappa} \ , \tag{5.48}$$

which contradicts the constraint (5.47). Thus, the kinetic initial conditions are incompatible with the constraint imposed by the BVS model, which requires the inflaton field (5.17) to vanish at the equipartition of energy. There is no theoretical reason or physical argument to justify this assumption, whereas the kinetic initial conditions do have a physical justification: as the universe comes out of the initial singularity, the kinetic energy of the inflaton dominates over the potential energy, which can safely be neglected. In order to use the kinetic

dominated approach, we therefore relax the requirement in the BVS model for the inflaton to vanish at the equipartition of energy. Moreover, we slightly modify the new inflation potential used in the BVS potential (5.12), according to,

$$V(\phi) = \frac{3A^2}{\kappa}\left(1 - \mu\kappa\phi^2\right)^2 \ , \tag{5.49}$$

where A is a time independent parameter fixing the amplitude of the potential. The modified new inflation potential (5.49) does not depend on the numerical value of the Hubble parameter H_i during the 'slow-roll' inflation phase. There is a theoretical justification for this. In the BVS model, H_i is determined by numerically integrating the dynamical equations, which in turn depend on H_i. Hence, the potential determining the dynamics is defined in terms of the resulting evolution. This is a circular methodology. On a conceptual level, the potential can only be defined in terms of parameters which are independent of the solution of the dynamical equations.

It is useful to mention that for a new inflation potential of the type (5.49), the evolution equations remain qualitatively unchanged under the scaling properties the scaling properties,

$$\begin{aligned} \tilde{A} &= \sigma A \ , \\ \tilde{\mu} &= \mu \ . \end{aligned} \tag{5.50}$$

where σ is the scaling constant.

In order to obtain a similar amount of inflation as for the chaotic potential and use the numerical value $\mu = 0.008$ as in the BVS model, we set $\lambda = 5.1$, which determines the kinetic initial conditions (5.36) and (5.37). In order for the model with a new inflation potential to enter the inflation phase with a similar numerical value of H as the model with a chaotic inflation potential, we set $A = 1.2$ in (5.49).

The analysis of the range of validity of the kinetically dominated regime for a new inflation potential is given in *Appendix* C.3. On a logarithmic scale, the estimated time range within which the solutions are kinetically dominated is $\ln(t_0) \lesssim -6$, which is well before the onset of inflation occurring at $\ln(t_i) = -2.75$. The logarithmic curves displayed in *Figure* 5.6 and *Figure* 5.7 show that for a time range $\ln(t) \lesssim -4$ the behaviour of the numerically integrated solutions $H_{\rm int}(t)$ and

$\phi_{\rm int}(t)$ is virtually indistinguishable from the behaviour of the solutions $H_{\rm kin}(t)$ and $\phi_{\rm kin}(t)$ obtained in a kinetically dominated regime. This corroborates the fact that we are entirely justified in considering the solutions to be kinematically dominated for a time range $t \leq 10^{-3}$.

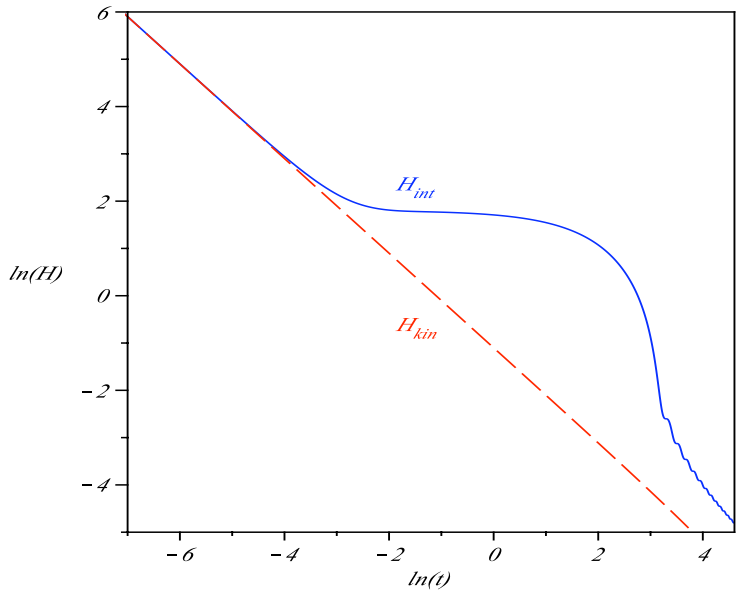

Figure 5.6: Comparison between $\ln(H_{\rm int})$ and $\ln(H_{\rm kin})$ as a function of $\ln(t)$ for a new inflation potential

5.6 Scalar perturbations for chaotic and new inflation potentials

Having discussed the time evolution of the background of inflation models, we now briefly examine the scalar perturbations. BVS and LD both reach the conclusion that their model leads to a damping of the power spectrum at low values of k compared to what would be expected from a straightforward power law as predicted by Starobinsky (1996). Given that an inflation model based on a chaotic potential with kinetic initial conditions corresponds to the LD model to leading order, our perturbation analysis is expected to emulate the one obtained

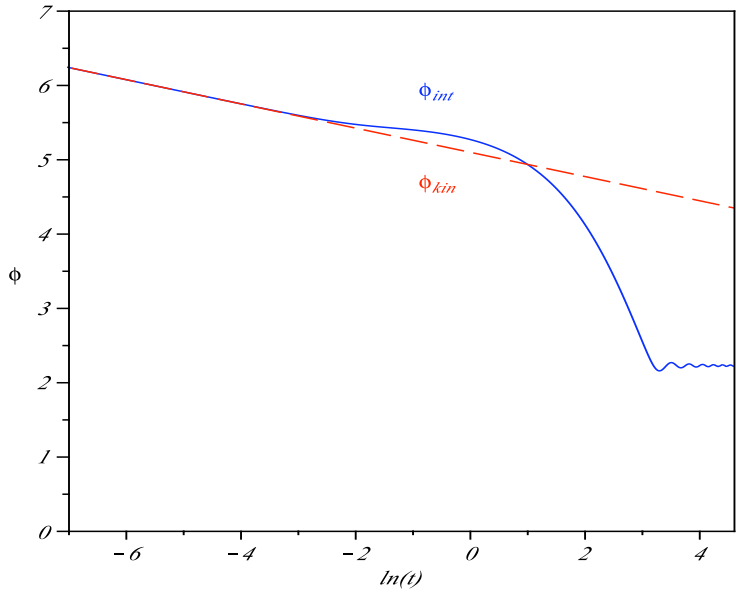

Figure 5.7: Comparison between $\phi_{\rm int}$ and $\phi_{\rm kin}$ as a function of $\ln(t)$ for a new inflation potential

by Lasenby & Doran (2005) for a suitably small initial integration time. Similarly, an inflation model based on the new inflation potential (5.49) is expected to lead to a similar perturbation analysis as that obtained by Boyanovsky *et al.* (2006b) for a suitably small initial integration time.

In order to generate scalar perturbations for a chaotic potential, which are consistent with current observations, the mass of the scalar field m is of the order $10^{-6}m_p$, as mentioned by Lasenby & Doran (2005). Hence, the solutions for a chaotic potential have to be rescaled with $\sigma = 10^{-6}$. Similarly, the solutions for a new inflation potential have to be rescaled by the same factor σ. Using the scaling properties (5.25), the numerical threshold for the range of applicability of the kinetically dominated initial conditions becomes $t_0 \leq 10^3 t_p$. Hence, the kinetic initial conditions are set three orders of magnitude above the Planck scale and more than one order of magnitude below the onset of inflation which occurs at $t_i \leq 3 \times 10^4 t_p$. There is no need to advocate transplanckian physics here, as we are well within the classical regime.

As shown by Liddle & Lyth (2000), the curvature power spectrum of the scalar

perturbations $\mathcal{P}_{\mathcal{R}}(k)$ is given by

$$\mathcal{P}_{\mathcal{R}}(k) = \left(\frac{H^2}{2\pi\dot{\phi}}\right)^2 , \tag{5.51}$$

and is governed by the ratio

$$\chi = -\frac{H^2}{\dot{\phi}} \tag{5.52}$$

which represents the magnitude of the curvature perturbation obtained by numerical integration using kinetic initial conditions as displayed in *Figure* 5.8.

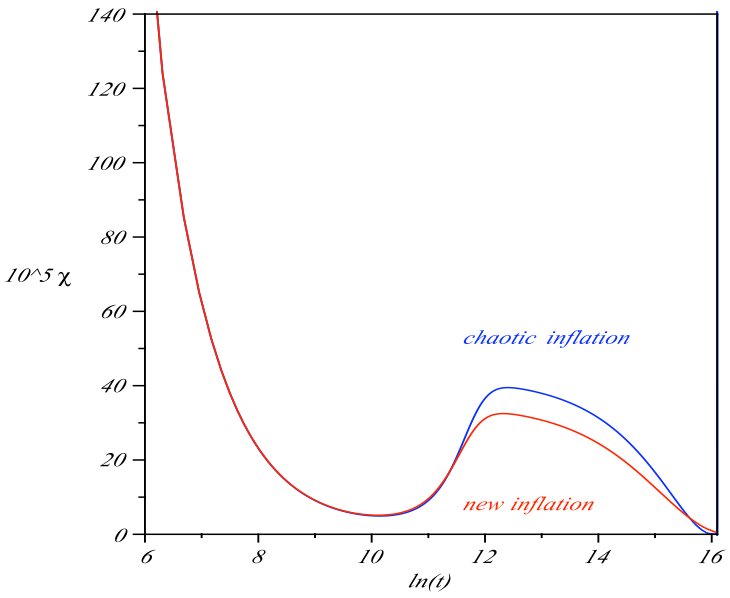

Figure 5.8: Curvature perturbation magnitude $10^5\chi$ as a function of $\ln(t)$.

The $\chi(\ln(t))$-curves in *Figure* 5.8 have the same shape as the corresponding curve obtained by LD. As explained by Lasenby & Doran (2005), the turnover of the $\chi(\ln(t))$-curves at around $\ln(t) = 12$, which coincides with the onset of inflation and suggests that the spectrum will contain less power at low-k values as would be expected from a power law behaviour. This is an important result since it shows that the falloff in the matter spectrum at low values of k is not related to the spatial geometry or to the shape of the inflationary potential of the model but is simply a generic feature which comes from the fact that the initial integration conditions have been chosen during the kinetically dominated regime.

Finally the primordial spectra of the curvature perturbation $\mathcal{P}_R(k)$ for the chaotic and the new inflation potential is plotted as a function of $\ln(k)$ in *Figure* 5.9, where $k = RH$. The shape of the power spectra corresponds to the shape of the power spectrum obtained by LD although the $\ln(k)$ is shifted since it is defined up to a constant. From *Figure* 5.9, we deduce that the power spectrum for the model with a chaotic inflation potential contains more power that the power spectrum for the model with a new inflation potential on all scales.

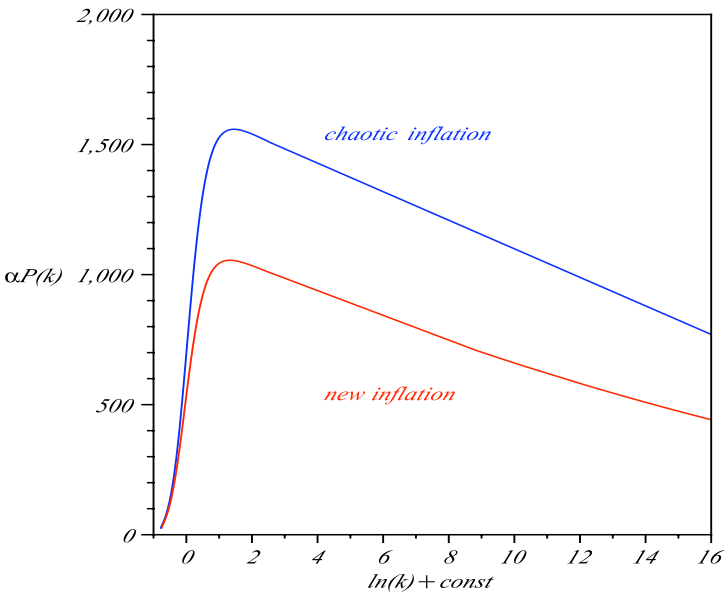

Figure 5.9: $\alpha\mathcal{P}_R(k)$ as a function of $\ln(k)$+ const, where $\alpha = 10^{10}$

Chapter 6

Conclusions

In *Chapter* 2, we performed a perturbation analysis of an adiabatic perfect fluid to first order using the $1+3$ covariant and gauge-invariant formalism and identified the analog of the Mukhanov-Sasaki variable and the Grishchuk variables needed to quantise the scalar and tensor perturbations respectively about a spatially-curved FLRW background space-time. We also determined the dynamics of the vector perturbations, which does not lead to a second order wave-equation, unlike the scalar and tensor perturbation, but to a first order equation involving the vorticity. In an expanding universe, the vorticity decays provided the sound speed squared satisfies $c_s^2 < \frac{2}{3}$ and the vector perturbations can therefore be neglected in the analysis.

In cosmological perturbation theory, there are in general six degrees of freedom: two scalars, two vectors and two tensors as mentioned by R. Schaeffer, J. Silk, M. Spiro, & J. Zinn-Justin (1996). However, in the perfect fluid case, the two Bardeen potential are related by $\Phi_A = -\Phi_H$, and thus there is only one remaining scalar degree of freedom. To sum up, to first-order, there is one degree of freedom associated with the scalar analog of the Mukhanov-Sasaki variable v, two degrees of freedom associated with the divergence-free vorticity covector ω_a and two degrees of freedom related to the two Grishchuk variables h^+ and $h^\times$ representing the scalar amplitudes of the tensor perturbations. Hence, to first-order, the dynamics of the adiabatic perturbations of a perfect fluid are described by five parameters, as expected.

It would be of interest to extend the first-order perturbation analysis of a perfect fluid using the $1+3$ covariant and gauge-invariant formalism by considering the isocurvature perturbations. Ellis & Bruni (1989) defined the isocurvature perturbations as the perturbations obtained by requiring the curvature perturbation to vanish (i.e. $\zeta = 0$) and showed that they decayed in an expanding universe. Such a definition should be distinguished from the one given by Mukhanov *et al.* (1992) and typically found in the literature, where the term isocurvature usually means distortions in multi-component systems with zero perturbation in the total energy-density initially. By analogy with the 'background based' approach, it would therefore be worth investigating the isocurvature perturbations generated by multi-component fluid using a $1+3$ covariant and gauge-invariant approach, which has been investigated by Dunsby (1991), Dunsby *et al.* (1992) and Tsagas *et al.* (2008). For such an endeavour, the equation-of-state of the fluid would have to be modified since the entropy of the different components would play a crucial role and could not simply be neglected. This would be quite an ambitious enterprise, which would be worth pursuing.

In *Chapter* 3, Brechet *et al.* (2007) have used the $1+3$ covariant approach to determine the dynamics of an effective Weyssenhoff fluid in a non-perturbative and hence completely general manner. This procedure leads to a consistent set of seven propagation and six constraint equations. These give respectively the time and spatial covariant derivative of the set of dynamical variables (ρ, Θ, σ, ω, E, B, S). Compared to the dynamics of a perfect fluid in GR, there is one additional propagation equation which is the spin density propagation equation. Note that the spin constraint is included in the shear constraint. We also verified these equations for the special case of irrotational flow with zero peculiar acceleration by evolving the constraints.

In *Chapter* 4, Brechet *et al.* (2008) performed a dynamical analysis of an effective homogeneous and irrotational Weyssenhoff fluid using the $1+3$ covariant and gauge-invariant approach. Contrary to the case of a perfect fluid in GR, the effective spin contributions to the fluid dynamics act like centrifugal forces preventing the formation of singularities for isotropic and anisotropic models satisfying the spin-shear constraint (4.50). The temporal evolution of the models is symmetric with respect to $t = 0$. In a cosmological context, the energy density

at the bounce state ρ_0 has to be sufficiently dense in order to seed large scale structures from primordial quantum fluctuations. For cosmological parameters which are consistent with current cosmological data (4.56) and (4.57), the temporal curvature of scale factor of a Weyssenhoff fluid is positively defined near the bounce (4.60). However such a fluid is not a suitable candidate for inflation given that the only way to include an inflation phase of about $50 - 70$ e-folds, is by considering a fluid with a very fine-tuned equation-of-state (4.71), which does not reduce to the standard cosmological fluid at later times. It is worth emphasizing that the time evolution of the scale factor of a homogeneous and irrotational Weyssenhoff fluid exhibits eternal oscillations, without any singularities. By contrast, the corresponding solutions obtained for a perfect fluid in GR are cycloids, which do exhibit singularities. Hence, the absence of singularities for a specific range of parameters is a genuinely new feature of cosmological models based on a Weyssenhoff fluid. Such singularity free bouncing cosmological model exhibits a similar behaviour to the ekpyrotic and cyclic models developed by Steinhardt & Turok (2002). Note that cosmological model based on a Weyssenhoff fluid also predict the existence of stable static solutions, which do not diverge under perturbations.

Weyssenhoff cosmological models have a positive temporal curvature of the scale factor around the bounce for a broad range of parameters, which leads to an inflation phase after the bounce. In order to be in agreement with current observational data, the model has to generate enough inflation, which is only possible for a very fine-tuned equation of state. Alternatively, a bouncing model might offer an unexpected way to bypass inflation as Gasperini *et al.* (2004) explain:"Technically speaking, the pre-bounce phase can replace the inflationary phase of standard slow-roll inflation since it allows the cosmologically interesting scales we observe today to start well inside the Hubble radius, and thus to have time to homogenize through causal microphysics". It is currently agreed that inflation is required for quantum fluctuations on subhorizon scales to exit the horizon. For an accelerated expansion, as occurring during the inflationary phase, a mode can exit the horizon if it is stretched at a faster rate than the Hubble radius. Conversely, as shown by Steinhardt & Turok (2002) for a decelerated

contraction occurring during an ekpyrotic or pre-bounce phase, a mode can enter the horizon if it shrinks at a faster rate than the Hubble radius.

Therefore, it is of great interest to investigate how perturbations behave as they pass through a bounce. Large scale structures might be seeded by density perturbations occurring before the bounce, which naturally rises the question of how perturbations modes can be matched at the bounce. This is particularly relevant for a wide range of bouncing models such as braneworld models discussed by Davis & Brechet (2005). The matching of pre- and post-bounce perturbations has been addressed by Gordon & Turok (2003) for a spatially-closed bouncing model with a scalar field in GR, but also by Gratton *et al.* (2004) for the cyclic model with a scalar field. To extend their work, it would be valuable to investigate the evolution of density perturbations of a Weyssenhoff fluid through a bounce on a classical and quantum level. This is quite an extensive task, which will probably take a few years to be fully completed.

It is useful to carry the analysis out classically first using the $1+3$ covariant approach. This choice is motivated by the clear physical meaning and gauge invariance of the variables. The scalar perturbations have to satisfy the Mukhanov-Sasaki equation. In presence of an initial singularity, the time dependent frequency varies very quickly with respect to cosmic time as the model emerges from the Big Bang whereas in a bouncing model the time dependent frequency is slowly varying around the bounce given that the Hubble parameter is vanishing. This enables us to use the WKB method in an iterative way around the bounce in order to find classical analytic solutions for the perturbation modes.

In the first stage of the perturbation analysis, the pre-bounce phase can be ignored and thus we set the initial conditions or conditions for physical quantities at the bounce, which is a state of finite energy density. These bouncing conditions for the classical and positively defined time evolution of the perturbations as determined by a quantum description of cosmological perturbations. The quantisation of matter fields in an expanding model leads in general to particle production, unlike in a Minkowskian space-time, because the quantum modes are not uniquely defined and related by the Bogolubov transformations. However, in the deflationary and inflationary periods on either of the bounce, space-time obeys a De Sitter geometry. By approaching the bounce, the expansion rate falls

smoothly to zero and the particle creation rate as well, thereby asymptotically recovering the well defined Minkowski modes, as shown by Birrell & Davies (1982). Note that this would clearly not be the case for Big Bang cosmological models in GR given that the expansion rate diverges as the model emerges form the initial singularity. Hence, a bounce seems to be more suited to set "initial conditions on perturbations".

Once the conditions for physical quantities at the bounce have been set on a quantum level, the behaviour of the perturbations during the pre-bounce phase can then be investigated. During the contraction or ekpyrotic phase, the perturbation modes exit successively the horizon. At the bounce, only small scale perturbations will still be oscillating within the horizon. The quantum modes of those pre-bounce perturbations will then have to be matched with the quantum modes of the post-bounce perturbations in order to understand the entire history of the density perturbations.

This investigation will enable us to understand better the impact of pre-bounce perturbations on the post-bounce perturbation spectrum based on an effective GR perturbation analysis. It will also predict how scale invariance is affected by pre-bounce perturbations. This perturbation analysis will be performed for different types of fields including spinors, which will yield deeper insight for the evolution of perturbation through a bounce.

In *Chapter* 5, we investigated the methods used to find suitable classical initial conditions to start the numerical integration of the equations of motion for the background dynamics of general inflationary models. The method proposed by BVS and LD are suited only to their specific choice of inflationary potential. The procedure followed by BVS requires a potential which scales like $V(\phi) \propto H_i^2$ since then the evolution equations can be recast in terms of the dimensionless parameter h. Their procedure is unsatisfactory because it leaves the scaling factors H_i and ϕ_i undetermined and chooses the value of H and ϕ at equipartition as initial conditions for numerical integration. The procedure adopted by LD requires a quadratic potential for the series expansion in power of $\ln(t)$. It is conceptually more satisfying since the initial conditions are set in a more natural way as the model emerges from the initial singularity. Since the model is kinetically dominated just after the Big Bang, an analytic solution can be found for all the

physical quantities of interest, the Hubble parameter $H_{\rm kin}$ and the inflaton $\phi_{\rm kin}$. These results can be used to set classical initial conditions at $t \simeq t_0$ for any type of potential provided that $t \gg t_p$, irrespective of the curvature of the underlying space-time, provided that the model does not have a bounce. This seems to be the simplest way to find suitable classical initial conditions for numerical integration. By initiating the numerical integration during the kinetic dominated era, the matter perturbation spectrum exhibits a falloff at low-k. Such a feature might possibly provide an explanation for the low-ℓ falloff in the CMB power spectrum observed by WMAP for any type of inflationary potential.

Appendix A

Transformation of physical quantities in the $1+3$ formalism under a signature change

The signature convention $(-,+,+,+)$ we have used throughout this paper is the opposite of the one $(+,-,-,-)$ adopted by many authors. To facilitate the comparison between results obtained using different conventions, the explicit transformations for physical quantities evaluated within the effective field theory are given below.

The metrics, the Levi-Civita tensors and the derivatives transform as,

$$g_{ab} \to -g_{ab} \ , \qquad h_{ab} \to -h_{ab} \ , \qquad \varepsilon_{abcd} \to \varepsilon_{abcd} \ , \qquad \varepsilon_{abc} \to \varepsilon_{abc} \ ,$$
$$\partial_a \to \partial_a \ , \qquad \nabla_a \to \nabla_a \ , \qquad D_a \to D_a \ .$$

The kinematical quantities transform as,

$$u^a \to u^a \ , \qquad u_a \to -u_a \ , \qquad a^b \to a^b \ , \qquad a_b \to -a_b \ ,$$
$$\sigma_{ab} \to -\sigma_{ab} \ , \qquad \omega_{ab} \to -\omega_{ab} \ , \qquad \omega^a \to \omega^a \ , \qquad \omega_a \to -\omega_a \ .$$

The dynamical quantities transform as,

$$
\begin{array}{lll}
R_{abcd} \to -R_{abcd} \ , & R_{ab} \to R_{ab} \ , & R \to -R \ , \\
C_{abcd} \to -C_{abcd} \ , & E_{ab} \to -E_{ab} \ , & H_{ab} \to -H_{ab} \ , \\
T_{ab} \to T_{ab} \ , & S_{ab} \to S_{ab} \ , & S^a \to -S^a \ .
\end{array}
$$

Appendix B

Covariant identities for an irrotational Weyssenhoff fluid with no peculiar acceleration

It is straightforward to show that the derivatives of the induced metric h_{ab} and the Levi-Civita tensor ε_{abc} vanish,

$$D_c h_{ab} = 0 \ , \qquad {}^{(3)}(h_{ab})^{\cdot} = 0 \ , \tag{B.1}$$

$$D_d \varepsilon_{abc} = 0 \ , \qquad {}^{(3)}(\varepsilon_{abc})^{\cdot} = 0 \ . \tag{B.2}$$

In this appendix, we consider an irrotational Weyssenhoff fluid ($\omega_{ab} = 0$) with no peculiar acceleration ($a^b = 0$). The covariant identities are defined in terms of a scalar field S, a vector field V_a and three tensor fields, A_{ab}, B_{ab} and C_{ab} satisfying the following properties

$$V_a u^a = 0 \ , \qquad A_{ab} u^a = A_{ab} u^b = 0 \ ,$$

$$B_{ab} = B_{\langle ab \rangle} \ , \qquad C_{ab} = C_{\langle ab \rangle} \ .$$

Using the kinematical decomposition (1.11), the identities involving the deriva-

tives of the scalar field S are found to be,

$$D_{[a}D_{b]}S = 0 \ , \tag{B.3}$$

$$^{(3)}(D_aS)^{\cdot} = D_a\dot{S} - \tfrac{1}{3}\Theta D_aS - \sigma_a{}^bD_bS \ . \tag{B.4}$$

Using the Ricci identities (2.27), the identities involving the derivatives of the vector field V_{ab} and tensor field A_{ab} are given by,

$$^{(3)}(D_aV_b)^{\cdot} = D_a\dot{V}_b - \tfrac{1}{3}\Theta D_aV_b - \sigma_{ac}D^cV_b + \varepsilon_{bcd}V^cH_a{}^d + \kappa h_{a[b}V^cD^dS_{c]d} \ , \tag{B.5}$$

$$^{(3)}(D^aV_a)^{\cdot} = D^a\dot{V}_a - \tfrac{1}{3}\Theta D^aV_a - \sigma_{ab}D^aV^b + \kappa V^aD^bS_{ab} \ , \tag{B.6}$$

$$\begin{aligned} ^{(3)}(D_cA_{ab})^{\cdot} = {} & D_c\dot{A}_{ab} - \tfrac{1}{3}\Theta D_cA_{ab} - \sigma_{cd}D^dA_{ab} - \left(\varepsilon_{ade}A^d{}_b + \varepsilon_{bde}A_a{}^d\right)H_c{}^e \\ & + \kappa\left(A^d{}_bh_{c[a} + A_a{}^dh_{c[b}\right)D^eS_{d]e} \ , \end{aligned} \tag{B.7}$$

$$\begin{aligned} ^{(3)}(D^bA_{ab})^{\cdot} = {} & D^b\dot{A}_{ab} - \tfrac{1}{3}\Theta D^bA_{ab} - \sigma_{bc}D^bA_a{}^c - \varepsilon_{abc}A^b{}_dH^{cd} \\ & + \tfrac{\kappa}{2}\left(A^b{}_a + 2A_a{}^b\right)D^cS_{bc} \ . \end{aligned} \tag{B.8}$$

Using the definition of the curl (1.10) and the spatial Ricci identities (2.28),the identities involving the derivatives of the symmetric trace-free tensor fields B_{ab} and C_{ab} yield,

$$\varepsilon_{abc}C^b{}_d\,(\mathrm{curl}B)^{cd} = 2C^{bc}D_{[a}B_{b]c} - \tfrac{1}{2}C_{ab}D_cB^{bc} \ , \tag{B.9}$$

$$\begin{aligned} D^b\,\mathrm{curl}\,B_{ab} = {} & \tfrac{1}{2}\varepsilon_{abc}D^b\left(D_dB^{cd}\right) + \varepsilon_{abc}B^b{}_d\left(\tfrac{1}{3}\Theta\sigma^{cd} - E^{cd}\right) \\ & - \varepsilon_{bcd}\sigma^b{}_a\sigma^c{}_eB^{de} + \tfrac{3}{2}\kappa\varepsilon_{abc}\sigma^{\langle b}{}_dS^{e\rangle d}B_e{}^c \ . \end{aligned} \tag{B.10}$$

$$\begin{aligned} ^{(3)}(\,\mathrm{curl}\,B)^{\cdot}_{ab} = {} & \mathrm{curl}\,\dot{B}_{ab} - \tfrac{1}{3}\Theta\,\mathrm{curl}\,B_{ab} - \sigma_c{}^d\varepsilon_{de\langle a}D^cB_{b\rangle}{}^e \\ & + 3H_{\langle a}{}^cB_{b\rangle c} + \tfrac{\kappa}{2}\varepsilon_{cd\langle a}B_{b\rangle}{}^cD_eS^{de} \ . \end{aligned} \tag{B.11}$$

Note that for a vanishing spin density tensor (i.e. $S_{ab} = 0$), these identities reduce to the identities established by Maartens (1997) for a perfect fluid in GR.

Appendix C

Range of validity of the initial conditions of dynamical quantities for inflationary models

C.1 Range of validity of the series expansions of dynamical quantities in the LD model

To analyse the range of validity of the series expansions of dynamical quantities in the LD model, we begin by setting the initial conditions at a very early time $t_0 = 10^{-7}$ using (5.31), with the RHS evaluated to second-order, and integrating numerically to obtain the results $H_{\text{int}}(t)$ and $\phi_{\text{int}}(t)$. These are then compared with $H_{\text{exp}}(t)$ and $\phi_{\text{exp}}(t)$ evaluated to first and second order (i.e. $\mathcal{O}(1)$ and $\mathcal{O}(2)$). The choice of $t_0 = 10^{-7}$ is arbitrary, but is intended to be sufficiently small to provide an accurate description of inflationary dynamics and sufficiently large to avoid computational errors. In order for the dynamics to produce an amount of inflation compatible with current observations, we set $b_0 = 2.48$, as we will show below. The qualitative behaviour of the $H(t)$-curves is shown in *Figure* C.1 and

relevant numerical results are given in *Table* C.1.

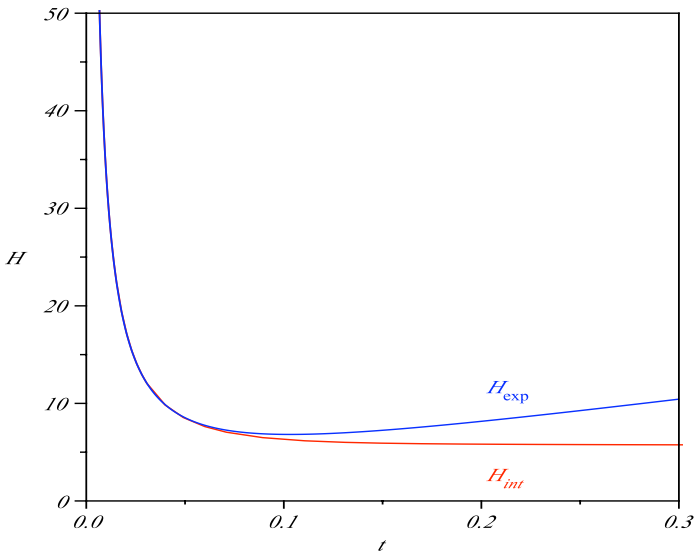

Figure C.1: Comparison between the series expansion $H_{\exp}$ (to second-order) and the numerically integrated solution H_{int}.

The numerical solution for the time evolution of the Hubble parameter $H_{\text{int}}(t)$ decreases monotically before reaching the slow-roll plateau whereas the series expansion $H_{\exp}(t)$ reaches a minimum at $t_{\min} = 0.103$, as illustrated in *Figure* C.1. For the series expansion of the inflaton $\phi_{\exp}(t)$, the minimum value occurs at a time $t^*_{\min} > t_{\min}$ as illustrated in *Figure* C.2. Qualitatively, $t_{\min}$ represents an upper bound on the numerical value for the initial integration time t_0. However, since we are interested in determining the inflationary dynamics, the initial integration time must also be chosen before the onset of inflation, which occurs at $t_i = 0.0649$. This imposes the further practical constraint $t < t_i$ on the domain of applicability of the series expansions. Quantitatively, for a time $t \leq 10^{-2}$ the difference between the series expansions to first and second order and the numerically integrated solutions are less than 0.1% for $H(t)$ and less than 0.01% for $\phi(t)$, as shown in *Table* C.1. Hence, it seems reasonable to claim that in the time range $t \leq 10^{-2}$ the series expansions to first or second order can be considered as

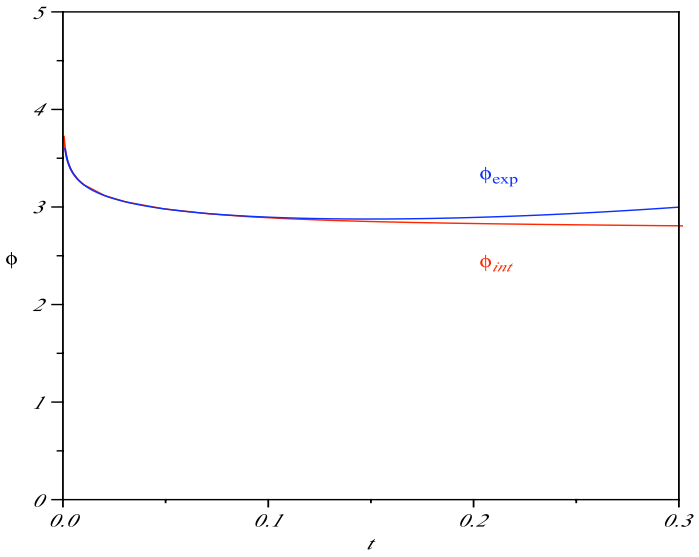

Figure C.2: Comparison between the series expansion ϕ_{exp} (to second-order) and the numerically integrated solution ϕ_{int}.

well within their domain of validity, which is why we did not consider any further expansion order.

From *Figure* C.3, we see that the $H(N)$-curves converge as the initial integration time t_0 approaches the singularity ($t_0 \to 0$). For a time range $t_0 \leq 10^{-2}$, the $H(N)$-curves are virtually indistinguishable, thus corroborating the fact that the initial integration time $t_0 = 10^{-2}$ can be considered as a numerical threshold for the range of applicability of the series expansions.

Table C.1: Behaviour of $H_{\rm exp}$ and $\phi_{\rm exp}$ compared to $H_{\rm int}$ and $\phi_{\rm int}$

t	$H_{\rm exp}$ $\mathcal{O}(1)$	$H_{\rm exp}$ $\mathcal{O}(2)$	$H_{\rm int}$	$\phi_{\rm exp}$ $\mathcal{O}(1)$	$\phi_{\rm exp}$ $\mathcal{O}(2)$	$\phi_{\rm int}$
10^{-1}	6.87	6.82	6.28	2.8959	2.8951	2.8878
10^{-2}	33.79	33.76	33.76	3.2306	3.2305	3.2305
10^{-3}	333.39	333.38	333.38	3.6051	3.6051	3.6051
10^{-4}	3333.33	3333.33	3333.33	3.9801	3.9801	3.9801

C.2 Range of validity of the kinematically dominated regime for a chaotic inflation potential

To determine the time range for which the kinetically dominated regime provides a good approximation to the pre-inflationary dynamics, we follow the same procedure used in *Appendix* C.1. For comparison, we consider a spatially-flat model with a chaotic potential and set $\lambda = 2.48$. As in the LD model, we set the initial conditions at very early time $t_0 = 10^{-7}$, but using the kinetic solutions (5.36) and (5.37) and integrate numerically to obtain $H_{\rm int}(t)$ and $\phi_{\rm int}(t)$, which we then compare with $H_{\rm kin}(t)$ and $\phi_{\rm kin}(t)$. The qualitative behaviour of the $H(t)$-curves and $\phi(t)$-curves are shown respectively in *Figure* C.4 and in *Figure* C.5, and relevant numerical results are given in *Table* C.2.

The qualitative difference between the solutions for the Hubble scale factor obtained in the kinetically dominated regime $H_{\rm kin}(t)$ and by numerical integration $H_{\rm int}(t)$ are displayed in *Figure* C.4. For a time range $t \leq 10^{-3}$, the quantitative difference between the kinetically dominated solutions, i.e. $H_{\rm kin}(t)$ and $\phi_{\rm kin}(t)$, and the numerically integrated ones, i.e. $H_{\rm int}(t)$ and $\phi_{\rm int}(t)$, is respectively less than 0.015% and less than 0.003% as shown in *Table* C.2. For such a time range, the $H(t)$-curves and the $\phi(t)$-curves displayed respectively in *Figure* C.4 and

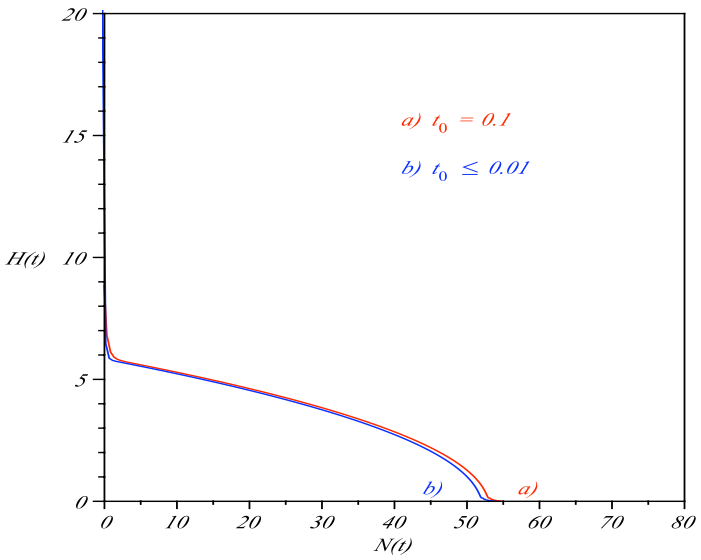

Figure C.3: $H_{int}(N)$ for different initial integration times $\{t_0 = 0.1, t_0 \leq 0.01\}$.

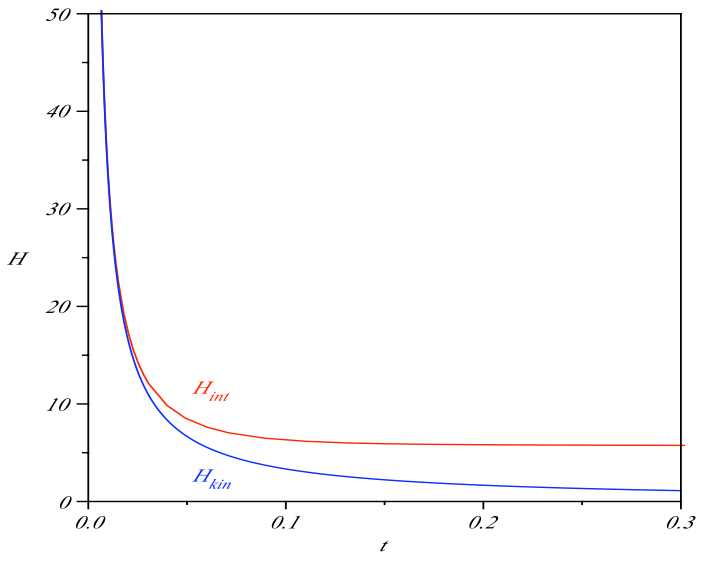

Figure C.4: Comparison between the kinetically dominated Hubble scale factor $H_{\rm kin}$ and the numerically integrated solution $H_{\rm int}$ for a chaotic inflation potential.

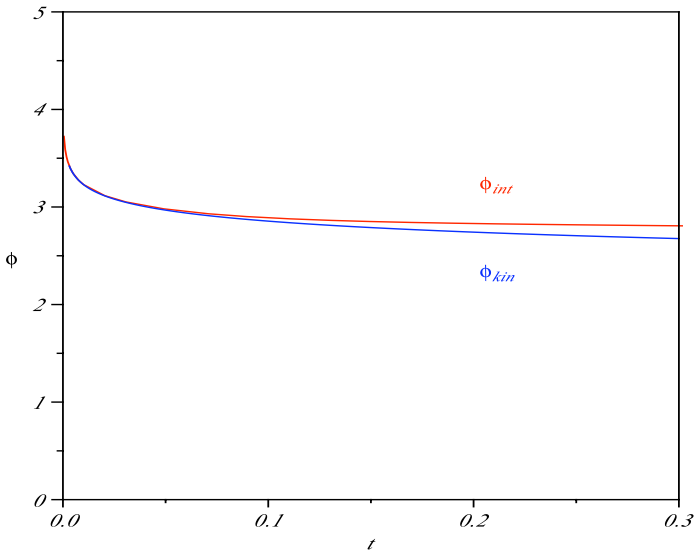

Figure C.5: Comparison between the kinetically dominated inflaton $\phi_{\rm kin}$ and the numerically integrated solution $\phi_{\rm int}$ for a chaotic inflation potential.

Figure C.5 are clearly indistinguishable. Hence, for a time range $t \leq 10^{-3}$, the pre-inflationary model can be reasonably considered as kinetically dominated.

As for the LD model, we see from *Figure* C.6 that the $H(N)$-curves converge as the initial integration time t_0 approaches the singularity. For a time range $t_0 \leq 10^{-3}$, the $H(N)$-curves are virtually indistinguishable, thus corroborating the fact that the initial integration time $t_0 = 10^{-3}$ can be considered as a numerical threshold for the validity of the kinematically dominated regime.

Note that there is an order of magnitude difference between the range of applicability of the LD series expansions and the domain in which the kinematically dominated quantities can be used to set the initial conditions. For a chaotic potential, the LD series expansions are by definition a better approximation to the pre-inflationary dynamics than the kinetically dominated model, given that they take into account the effect of the potential. However, for a sufficiently small time range, the two models agree up to a very high precision and we are entirely justified in considering the dynamics of the model as kinetically dominated. One should recall, however, that the kinetic dominated approach can be applied at

Table C.2: Behaviour of H_{kin} and ϕ_{kin} compared to H_{int} and ϕ_{int} for a chaotic inflation potential

t	H_{kin}	H_{int}	ϕ_{kin}	ϕ_{int}
10^{-1}	3.33	6.28	2.8550	2.8878
10^{-2}	33.33	33.76	3.2300	3.2305
10^{-3}	333.33	333.38	3.6050	3.6051
10^{-4}	3333.33	3333.33	3.9801	3.9801

very early times to models with arbitrary spatial curvature and any inflation potential.

C.3 Range of validity of the kinematically dominated regime for a new inflation potential

To determine the time range for which the kinetically dominated regime provides a good approximation to the pre-inflationary dynamics, we follow the same procedure used in *Appendix* C.1 and *Appendix* C.2. We set the initial conditions at very early time $t_0 = 10^{-7}$, but using the kinetic solutions (5.36) and (5.37) and integrate numerically to obtain $H_{\text{int}}(t)$ and $\phi_{\text{int}}(t)$, which we then compare with $H_{\text{kin}}(t)$ and $\phi_{\text{kin}}(t)$. The qualitative behaviour of the $H(t)$-curves and $\phi(t)$-curves are shown respectively in *Figure* C.7 and in *Figure* C.8, and relevant numerical results are given in *Table* C.3.

The qualitative difference between the solutions for the Hubble scale factor obtained in the kinetically dominated regime $H_{\text{kin}}(t)$ and by numerical integration $H_{\text{int}}(t)$ are displayed in *Figure* C.7. For a time range $t \leq 10^{-3}$, the quantitative difference between the kinetically dominated solutions, i.e. $H_{\text{kin}}(t)$ and $\phi_{\text{kin}}(t)$, and the numerically integrated ones, i.e. $H_{\text{int}}(t)$ and $\phi_{\text{int}}(t)$, is respectively less

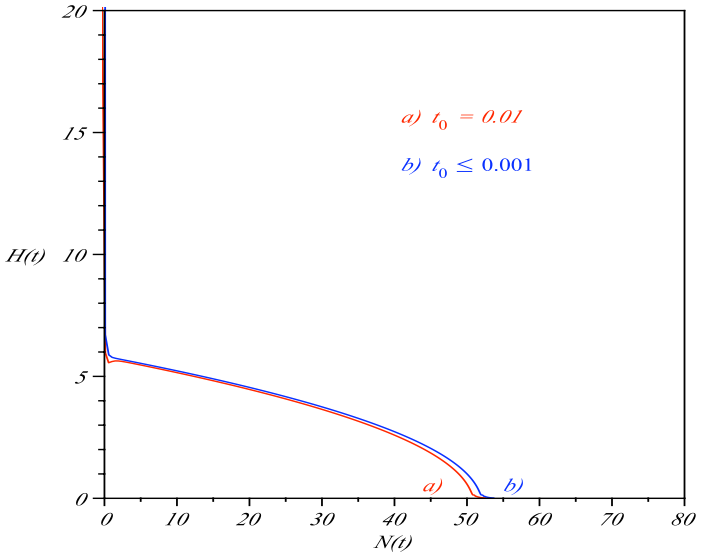

Figure C.6: $H_{int}(N)$ for a chaotic potential with different initial integration times $\{t_0 = 10^{-2}, t_0 \leq 10^{-3}\}$.

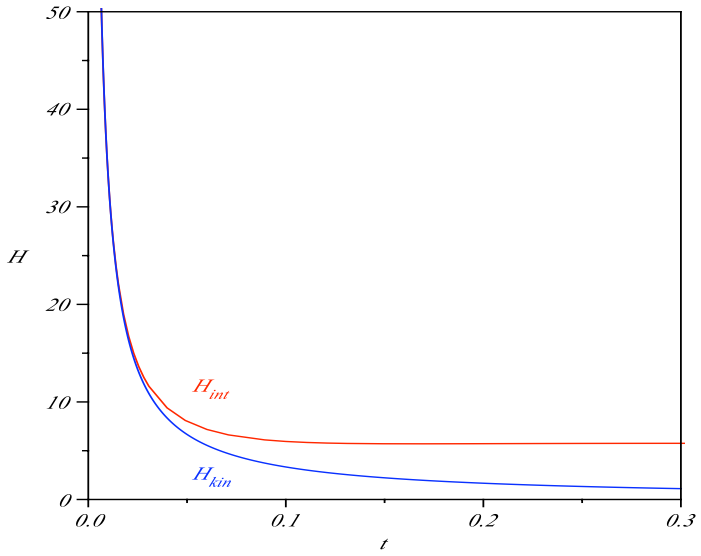

Figure C.7: Comparison between the kinetically dominated Hubble scale factor $H_{\rm kin}$ and the numerically integrated solution $H_{\rm int}$ for a new inflation potential.

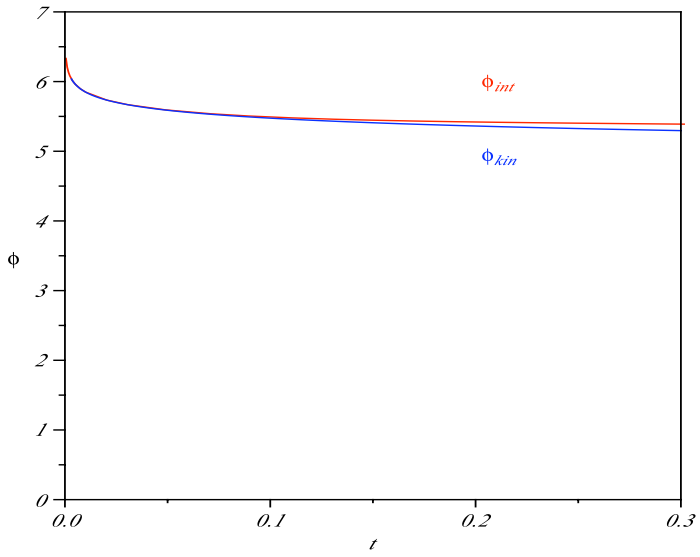

Figure C.8: Comparison between the kinetically dominated inflaton ϕ_{kin} and the numerically integrated solution ϕ_{int} for a new inflation potential.

than 0.020% and less than 0.001% as shown in *Table* C.3. For such a time range, the $H(t)$-curves and the $\phi(t)$-curves displayed respectively in *Figure* C.7 and *Figure* C.8 are clearly indistinguishable. Hence, for a time range $t \leq 10^{-3}$, the pre-inflationary model can be reasonably considered as kinetically dominated.

As for the inflation model with a chaotic potential, we see from *Figure* C.9 that the $H(N)$-curves converge as the initial integration time t_0 approaches the singularity. For a time range $t_0 \leq 10^{-3}$, the $H(N)$-curves are virtually indistinguishable, so the initial integration time $t_0 = 10^{-3}$ can be considered as a numerical threshold for the validity of the kinematically dominated regime. The $H(N)$-curves obtained for the new inflation potential (5.49) do not undergo a period of slow-roll inflation since $H'(N) \neq 0$ as (C.9) clearly shows. It is worth emphasising that an inflation model does not have to undergo a period of slow-roll in order to produce enough inflation, which does not discredit the new inflation potential. However, the absence of a slow-roll inflation period, corroborates the fact that an inflation potential defined explicitly in terms of the Hubble parameter during the slow-roll phase H_i is inconsistent.

Table C.3: Behaviour of H_{kin} and ϕ_{kin} compared to H_{int} and ϕ_{int} for a new inflation potential

t	H_{kin}	H_{int}	ϕ_{kin}	ϕ_{int}
10^{-1}	3.33	6.48	5.4750	5.5092
10^{-2}	33.33	33.82	5.8500	5.8505
10^{-3}	333.33	333.39	6.2250	6.2250
10^{-4}	3333.33	3333.34	6.6000	6.6000

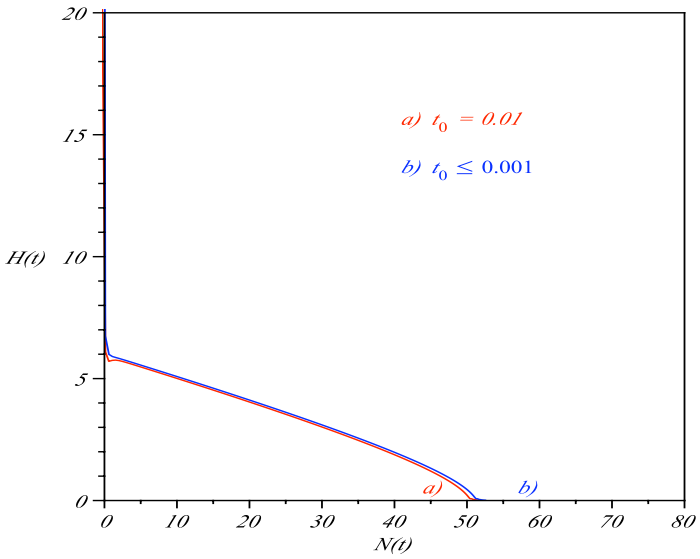

Figure C.9: $H_{int}(N)$ for a new inflation potential with different initial integration times $\{t_0 = 10^{-2}, t_0 \leq 10^{-3}\}$.

References

Alpher, R.A., Bethe, H. & Gamow, G. (1948). The Origin of Chemical Elements. *Physical Review*, **73**, 803–804. 1

Andersson, N. & Comer, G.L. (2007). Relativistic Fluid Dynamics: Physics for Many Different Scales. *Living Reviews in Relativity*, **10**, 1, arXiv:gr-qc/0605010. 12

Bardeen, J.M. (1980). Gauge-invariant cosmological perturbations. *Phys. Rev. D.*, **22**, 1882–1905. 2, 24

Birrell, N.D. & Davies, P.C.W. (1982). *Quantum fields in curved space*. Cambridge University Press. 12, 129

Boehmer, C.G. & Bronowski, P. (2006). The homogeneous and isotropic Weyssenhoff fluid. *ArXiv General Relativity and Quantum Cosmology e-prints*, arXiv:gr-qc/0601089. 72

Boyanovsky, D., de Vega, H.J. & Sanchez, N.G. (2006a). CMB quadrupole suppression. I. Initial conditions of inflationary perturbations. *Phys. Rev. D.*, **74**, 123006–123021, arXiv:astro-ph/0607508. 108

Boyanovsky, D., de Vega, H.J. & Sanchez, N.G. (2006b). CMB quadrupole suppression. II. The early fast roll stage. *Phys. Rev. D.*, **74**, 123007–123021, arXiv:astro-ph/0607487. 105, 110, 122

Brechet, S.D., Hobson, M.P. & Lasenby, A.N. (2007). Weyssenhoff fluid dynamics in general relativity using a 1 + 3 covariant approach. *Classical and Quantum Gravity*, **24**, 6329–6348, 0706.2367. v, 3, 8, 19, 69, 126

Brechet, S.D., Hobson, M.P. & Lasenby, A.N. (2008). Classical big-bounce cosmology: dynamical analysis of a homogeneous and irrotational Weyssenhoff fluid. *Classical and Quantum Gravity*, **25**, 245016, 0807.2523. v, 8, 77, 126

Bridges, M., Lasenby, A.N. & Hobson, M.P. (2006). A Bayesian analysis of the primordial power spectrum. *Mon. Not. R. Ast. Soc.*, **369**, 1123–1130, arXiv:astro-ph/0511573. 69

Bruni, M., Dunsby, P.K.S. & Ellis, G.F.R. (1992a). Cosmological perturbations and the physical meaning of gauge-invariant variables. *Astrophys. J.*, **395**, 34–53. 2, 3, 11, 12, 22, 24, 26

Bruni, M., Ellis, G.F.R. & Dunsby, P.K.S. (1992b). Gauge-invariant perturbations in a scalar field dominated universe. *Classical and Quantum Gravity*, **9**, 921–945. 29

Capozziello, S. & Stornaiolo, C. (1998). Scalar perturbations in a cosmological model with torsion. *Nuovo Cimento B Serie*, **113**, 879–886. 43

Cartan, E. (1922). Sur une généralisation de la notion de courbure de riemann et les espaces à torsion. *Comptes Rendus de l'Académie des Sciences*, **174**, 593–607. 39, 45

Challinor, A. (2000). Microwave background anisotropies from gravitational waves: the 1 + 3 covariant approach. *Classical and Quantum Gravity*, **17**, 871–889, arXiv:astro-ph/9906474. 3, 10, 32, 33

Davis, S.C. & Brechet, S.D. (2005). Vacuum decay on a brane world. *Phys. Rev. D.*, **71**, 104023–104027, arXiv:hep-ph/0503243. 128

Dechant, P.P., Lasenby, A.N. & Hobson, M.P. (2009). Anisotropic, non-singular early universe model leading to a realistic cosmology. *Phys. Rev. D.*, **79**, 043524–043540, 0809.4335. 77

Dunsby, P.K.S. (1991). Gauge invariant perturbations in multi-component fluid cosmologies. *Classical and Quantum Gravity*, **8**, 1785–1806. 126

Dunsby, P.K.S., Bruni, M. & Ellis, G.F.R. (1992). Covariant perturbations in a multifluid cosmological medium. , **395**, 54–74. 126

Durrer, R. (2008). *The Coscmic Microwave Background*. Cambridge University Press. 25, 28, 29, 35

Ehlers, J. (1961). Beiträge zur relativistischen Mechanik kontinuierlicher Medien. *Mainz Akademie Wissenschaften Mathematisch Naturwissenschaftliche Klasse*, **11**, 792–837. 3

Einstein, A. (1905). On the Electrodynamics of Moving Bodies. *Annalen der Physik*, **17**, 891–921. 1

Einstein, A. (1916). The Foundation of the General Theory of Relativity. *Annalen der Physik*, **49**, 769–822. 1

Einstein, A. (1917). Cosmological Considerations on the General Theory of Relativity. *Siztungsberichte der Preussischen Akademie der Wissenschaften*, **1**, 142–152. 1

Ellis, G.F.R. (1971). Relativistic Cosmology. In *General Relativity and Cosmology*, 104–182. 69

Ellis, G.F.R. (1973). Relativistic Cosmology. In E. Schatzman, ed., *Cargese Lectures in Physics*, vol. 6 of *Cargese Lectures in Physics*, 1. 76

Ellis, G.F.R. (2007). On the Raychaudhuri equation. *Pramana*, **69**, 15–22. 82

Ellis, G.F.R. & Bruni, M. (1989). Covariant and gauge-invariant approach to cosmological density fluctuations. *Phys. Rev. D.*, **40**, 1804–1818. 3, 126

Ellis, G.F.R. & van Elst, H. (1999). Cosmological Models (Cargèse lectures 1998). In *NATO ASIC Proc. 541: Theoretical and Observational Cosmology*, 1–116. 3, 7, 13, 60, 69

Ellis, G.F.R., Hwang, J. & Bruni, M. (1989). Covariant and gauge-independent perfect-fluid Robertson-Walker perturbations. *Phys. Rev. D.*, **40**, 1819–1826. 2, 7

Ellis, G.F.R., Bruni, M. & Hwang, J. (1990). Density-gradient-vorticity relation in perfect-fluid Robertson-Walker perturbations. *Phys. Rev. D.*, **42**, 1035–1046. 7

Ellis, G.F.R., van Elst, H. & Maartens, R. (2001). General relativistic analysis of peculiar velocities. *Classical and Quantum Gravity*, **18**, 5115–5123, arXiv:gr-qc/0105083. 13

Friedman, A. (1922). On the curvature of space. *Zeitschrift für Physik*, **10**, 377–386. 1

Friedman, A. (1924). On the possibility of a world with constant negative curvature of space. *Zeitschrift für Physik*, **A**, 326–332. 2

Fulling, S.A. (1989). *Aspects of Quantum Field Theory in Curved Spacetime*. Cambridge University Press. 12

Gasperini, M. (1986). Spin-dominated inflation in the Einstein-Cartan theory. *Physical Review Letters*, **56**, 2873–2876. 68, 69, 73, 88

Gasperini, M., Giovannini, M. & Veneziano, G. (2004). Cosmological perturbations across a curvature bounce. *Nuclear Physics B*, **694**, 206–238, arXiv:hep-th/0401112. 127

Goode, S.W. (1989). Analysis of spatially inhomogeneous perturbations of the FRW cosmologies. , **39**, 2882–2892. 11

Gordon, C. & Turok, N. (2003). Cosmological perturbations through a general relativistic bounce. *Phys. Rev. D.*, **67**, 123508–123518, arXiv:hep-th/0206138. 128

Gratton, S., Khoury, J., Steinhardt, P.J. & Turok, N. (2004). Conditions for generating scale-invariant density perturbations. *Phys. Rev. D.*, **69**, 103505–103511, arXiv:astro-ph/0301395. 128

Grishchuk, L.P. (1974). Amplification of gravitational waves in an isotropic universe. *Soviet Journal of Experimental and Theoretical Physics*, **40**, 409–+. 2, 33

Guth, A.H. (1981). Inflationary universe: A possible solution to the horizon and flatness problems. *Phys. Rev. D.*, **23**, 347–356. 29, 105

Hammond, R.T. (2002). Torsion gravity. *Reports on Progress in Physics*, **65**, 599–649. 41

Hawking, S.W. (1966). Perturbations of an Expanding Universe. *Astrophys. J.*, **145**, 544–554. 3, 13, 16, 17, 31

Hawking, S.W. & Ellis, G.F.R. (1973). *The large scale structure of space-time*. Cambridge University Press. 82

Heckmann, O. & Schücking, E. (1955). Bemerkungen zur Newtonschen Kosmologie. I. Mit 3 Textabbildungen in 8 Einzeldarstellungen. *Zeitschrift fur Astrophysik*, **38**, 95–109. 3

Hehl, F.W. (1974). Spin and torsion in general relativity II: Geometry and field equations. *General Relativity and Gravitation*, **5**, 491–516. 64

Hehl, F.W., von der Heyde, P., Kerlick, G.D. & Nester, J.M. (1976). General relativity with spin and torsion: Foundations and prospects. *Reviews of Modern Physics*, **48**, 393–416. 38, 39, 43

Hinshaw, G., Spergel, D.N., Verde, L., Hill, R.S., Meyer, S.S., Barnes, C., Bennett, C.L., Halpern, M., Jarosik, N., Kogut, A., Komatsu, E., Limon, M., Page, L., Tucker, G.S., Weiland, J.L., Wollack, E. & Wright, E.L. (2003). First-Year Wilkinson Microwave Anisotropy Probe (WMAP) Observations: The Angular Power Spectrum. *Astrophys. J. Suppl. Series*, **148**, 135–159, arXiv:astro-ph/0302217. 105

Hubble, E. (1929). A relation between distance and radial velocity among extra-galactic nebulae. *Proc. Natl. Acad. Sci. USA*, **15**, 168–173. 1

Kodama, H. & Sasaki, M. (1984). Cosmological Perturbation Theory. *Progress of Theoretical Physics Supplement*, **78**, 1–166. 2

Kopczynski, W. (1973). An anisotropic universe with torsion. *Physics Letters A*, **43**, 63–64. 69, 82

Krawiec, A., Szydlowski, M. & Godlowski, W. (2005). Complementary constraints on non-standard cosmological models from CMB and BBN. *Physics Letters B*, **619**, 219–225, arXiv:astro-ph/0502412. 69

Kuchowicz, B. (1978). Friedmann-like cosmological models without singularity. *General Relativity and Gravitation*, **9**, 511–517. 101

Langlois, D. & Vernizzi, F. (2005). Conserved nonlinear quantities in cosmology. *Phy. Rev. D.*, **72**, 103501–103510, arXiv:astro-ph/0509078. 11

Langlois, D. & Vernizzi, F. (2007). Non-linear perturbations of cosmological scalar fields. *Journal of Cosmology and Astro-Particle Physics*, **2**, 17–+, arXiv:astro-ph/0610064. 29

Lasenby, A. & Doran, C. (2005). Closed universes, de Sitter space, and inflation. *Phys. Rev. D.*, **71**, 063502–063522, arXiv:astro-ph/0307311. 105, 122, 123

Lemaitre, G. (1927). A homogeneous universe of constant mass and increasing radius accounting for the radial velocity of extra-galactic nebulæ. *Annales de la Société Scientifique de Bruxelles*, **A**, 49–56. 1, 2

Liddle, A.R. & Lyth, D.H. (2000). *Cosmological Inflation and Large-Scale Structure*. Cambridge University Press. 122

Lifschitz, E.M. (1947). On the gravitational stability of the expanding universe. *J. Phys. USSR*, **10**, 116–128. 2

Lifshitz, E.M. & Khalatnikov, I.M. (1963). Investigations in relativistic cosmology. *Advances in Physics*, **12**, 185–249. 2

Linde, A. (2001). Fast-Roll Inflation. *Journal of High Energy Physics*, **11**, 52–73, arXiv:hep-th/0110195. 107

Linde, A.D. (1982). Scalar field fluctuations in the expanding universe and the new inflationary universe scenario. *Physics Letters B*, **116**, 335–339. 29, 105

Lu, H.Q. & Cheng, K.S. (1995). A Bianchi type-V cosmological model with spin matter. *Classical and Quantum Gravity*, **12**, 2755–2765. 78, 87

Lyth, D.H. & Woszczyna, A. (1995). Large scale perturbations in the open universe. , **52**, 3338–3357, arXiv:astro-ph/9501044. 12, 28

Maartens, R. (1997). Linearization instability of gravity waves? *Phys. Rev. D.*, **55**, 463–467, arXiv:astro-ph/9609198. 60, 63, 134

Mather, J.C., Smoot, G.F., Boggess, N.W., Weiss, R., Bennett, C.L., Cheng, E.S., Dwek, E., Gulkis, S., Hauser, M.G., Janssen, M.A., Kelsall, T., Meyer, S.S., Moseley, S.H., Murdock, T.L., Shafer, R.A., Silverberg, R.F., Wilkinson, D.T. & Wright, E.L. (1992). The COBE mission - Its design and performance two years after launch. *Astrophys. J.*, **397**, 420–429. 1

Mukhanov, V. (2005). *Physical foundations of cosmology*. Cambridge University Press. 25

Mukhanov, V.F., Feldman, H.A. & Brandenberger, R.H. (1992). Theory of cosmological perturbations. *Phys. Rep.*, **215**, 203–333. 2, 10, 22, 27, 105, 126

Obukhov, Y.N. & Korotky, V.A. (1987). The Weyssenhoff fluid in Einstein-Cartan theory. *Classical and Quantum Gravity*, **4**, 1633–1657. 3, 39, 40, 41, 45, 48, 49, 50, 62, 63

Olson, D.W. (1976). Density perturbations in cosmological models. *Phys. Rev. D.*, **14**, 327–331. 3

Palle, D. (1999). On primordial cosmological density fluctuations in the Einstein-Cartan gravity and COBE data. *Nuovo Cimento B Serie*, **114**, 853–860, arXiv:astro-ph/9811408. 40, 63, 64, 69

Palle, D. (2007). Comment on the paper "Weyssenhoff fluid dynamics in a 1+3 covariant approach" (arXiv:0706.2367). 64, 65

Penzias, A.A. & Wilson, R.W. (1970). Microwave Noise from Rainstorms. *Science*, **169**, 583–584. 1

Pitrou, C. & Uzan, J.P. (2007). Quantization of perturbations during inflation in the 1+3 covariant formalism. *Phys. Rev. D.*, **75**, 087302–087305, arXiv:gr-qc/0701121. 11

Puetzfeld, D. & Chen, X. (2004). Testing non-standard cosmological models with supernovae. *Classical and Quantum Gravity*, **21**, 2703–2722, arXiv:gr-qc/0402026. 39

R. Schaeffer, J. Silk, M. Spiro, & J. Zinn-Justin, ed. (1996). *Cosmology and large scale structure*. 125

Raychaudhuri, A. (1957). Relativistic and Newtonian Cosmology. *Zeitschrift fur Astrophysik*, **43**, 161–164. 3

Ringeval, C. (2001). Equation of state of cosmic strings with fermionic current carriers. *Phys. Rev. D.*, **63**, 063508–063531, arXiv:hep-ph/0007015. 88

Robertson, H.P. (1935). Kinematics and world structure. *Astrophys. J.*, **82**, 248–301. 2

Sachs, R.K. & Wolfe, A.M. (1967). Perturbations of a Cosmological Model and Angular Variations of the Microwave Background. *Astrophys. J.*, **147**, 73–90. 2

Schouten, J.A. (1954). *Ricci-Calculus: An introduction to tensor analysis and its geometrical applications*. Springer Verlag (Berlin). 41

Sciama, D.W. (1962). *On the analogy between charge and spin in general relativity*, 415. 39, 45

Smirnov-Rueda, R. (2005). On two complementary types of total time derivative in classical field theories and maxwell's equations. *Foundations of Physics*, **35**, 10. 12

Stachowiak, T. & Szydłowski, M. (2007). Exact solutions in bouncing cosmology. *Physics Letters B*, **646**, 209–214, arXiv:gr-qc/0610121. 99

Starobinsky, A.A. (1996). Spectrum of initial perturbations in open and closed inflationary models. In M.Y. Klopov, ed., *3rd Paris Cosmology Colloquium*, 43. 121

Steinhardt, P.J. & Turok, N. (2002). A Cyclic Model of the Universe. *Science*, **296**, 1436–1439, arXiv:hep-th/0111030. 127

Stewart, J. & Hájiček, P. (1973). Can spin avert singularities? *Nature Phys. Sc.*, **244**, 96–98. 69, 77, 82

Stewart, J.M. (1990). Perturbations of Friedmann-Robertson-Walker cosmological models. *Classical and Quantum Gravity*, **7**, 1169–1180. 2

Stewart, J.M. & Walker, M. (1974). Perturbations of space-times in general relativity. *Royal Society of London Proceedings Series A*, **341**, 49–74. 7

Szydłowski, M. & Krawiec, A. (2004). Cosmological model with macroscopic spin fluid. *Phy. Rev. D.*, **70**, 043510–043521, arXiv:astro-ph/0305364. 69

Thiffeault, J.L. (2001). Covariant time derivatives for dynamical systems. *Journal of Physics A Mathematical General*, **34**, 5875–5885, arXiv:nlin/0102038. 11

Trautman, A. (1973). Cosmology-Model with torsion of a universe filled with spinning dust. *Nature Phys. Sc.*, **242**, 7–9. 68, 69, 101

Tsagas, C.G., Challinor, A. & Maartens, R. (2008). Relativistic cosmology and large-scale structure. *Phys. Rep.*, **465**, 61–147, 0705.4397. 3, 28, 30, 31, 32, 126

Tsamparlis, M. (1979). Cosmological principle and torsion. *Physics Letters A*, **75**, 27–28. 72, 73

Uhlenbeck, G.E. & Goudsmit, S. (1925). Replacement of the hypothesis of nonmechanical connection by an internal degree of freedom of the electron. *Naturw. 13*, **13**, 953. 45

van Elst, H. (1996). *Extensions and applications of 1+3 decomposition methods in general relativistic cosmological modelling*. Ph.D. thesis, University of London, Queen Mary and Westfield College, London, United Kingdom. 63

Vilenkin, A. (1981). Cosmic strings. *Phys. Rev. D.*, **24**, 2082–2089. 101

Wald, R.M. (1984). *General relativity*. The University of Chicago Press. 79

Walker, A.G. (1937). On Milne's theory of world-structure. *Proceedings of the London Mathematical Society*, **42**, 90–127. 2

Weinberg, S. (1972). *Gravitation and Cosmology: Principles and Applications of the General Theory of Relativity*. 34, 71

Weinberg, S. (2008). *Cosmology*. Oxford University Press. 29

Weyssenhoff, J. & Raabe, A. (1947). Relativistic dynamics of spin-fluids and spin-particules. *Acta Phys. Polon.*, **9**, 7–20. 39

Woszczyna, A. & Kulak, A. (1989). Cosmological perturbations - Extension of Olson's gauge-invariant method. *Classical and Quantum Gravity*, **6**, 1665–1671. 11, 12, 22, 24